THE COENZYME M BIOSYNTHETIC PATHWAY IN PROTEOBACTERIUM *XANTHOBACTER AUTOTROPHICUS* PY2

by

Sarah Eve Partovi

A dissertation submitted in partial fulfillment
of the requirements for the degree

of

Doctor of Philosophy

in

Biochemistry

MONTANA STATE UNIVERSITY
Bozeman, Montana

January 2018

DEDICATION

I dedicate this dissertation to my family, without whom none of this would have been possible. My husband Ky has been a part of the graduate school experience since day one, and I am forever grateful for his support. My wonderful family; Iraj, Homa, Cameron, Shireen, Kevin, Lin, Felix, Toby, Molly, Noise, Dooda, and Baby have all been constant sources of encouragement.

ACKNOWLEDGEMENTS

First, I would like to acknowledge Dr. John Peters for his mentorship, scientific insight, and for helping me gain confidence as a scientist even during the most challenging aspects of this work. I also thank Dr. Jennifer DuBois for her insightful discussions and excellent scientific advice, and my other committee members Dr. Brian Bothner and Dr. Matthew Fields for their intellectual contributions throughout the course of the project. Drs. George Gauss and Florence Mus have contributed greatly to my laboratory technique and growth as a scientist, and have always been wonderful resources during my time in the lab. Members of the Peters Lab past and present have all played an important role during my time, including Dr. Oleg Zadvornyy, Dr. Jacob Artz, and future Drs. Gregory Prussia, Natasha Pence, and Alex Alleman. Undergraduate researchers/REU students including Hunter Martinez, Andrew Gutknecht and Leah Connor have worked under my guidance, and I thank them for their dedication to performing laboratory assistance. Dr. Bernd Markus Lange of Washington State University has been instrumental in helping us collect mass spectrometry data, and Dr. Brian Tripet assisted in collecting exciting time-resolved ^{1}H-NMR data. Many other people in the Department of Chemistry and Biochemistry have contributed through stimulating conversation despite being involved in disciplines other than biochemistry, including Drs. Ky Mickelsen, Colin Miller, Ryan Latterman, David Skowron, Ashley Beckstead, Christine Gobrogge, Anna Michel, Amanda Mattson, and Doreen Brown. Finally, I would like to thank the DOE for their ongoing support.

TABLE OF CONTENTS

TABLE OF CONTENTS CONTINUED

TABLE OF CONTENTS CONTINUED

LIST OF TABLES

LIST OF FIGURES

Figure Page

LIST OF FIGURES CONTINUED

Figure Page

LIST OF FIGURES CONTINUED

Figure Page

LIST OF FIGURES CONTINUED

LIST OF SCHEMES

Scheme Page

GLOSSARY

CoM – coenzyme M
PEP - phosphoenolpyruvate
PLP- pyridoxal 5'-phosphate
AMO – alkene monooxygenase
ECP – epoxide carboxylation pathway
AMP – adenosine monophosphate
NADH – nicotinamide adenine dinucleotide
EaCoMT – epoxyalkane: coenzyme M transferase
R-HPCDH – (*R*)-hydroxypropyl-CoM-dehydrogenase
S-HPCDH – (*S*)- hydroxypropyl-CoM-dehydrogenase
2-KPCC – 2-ketopropyl-CoM-oxidoreductase/carboxylase
2-KPC – 2-ketopropyl-CoM
XcbB1 – Product of *xcbB1*, homologous to phosphosulfolactate synthase (ComA)
XcbC1 – Product of *xcbC1*, homologous to argininosuccinate lyases
XcbD1 – Product of *xcbD1*, homologous to adenylosuccinate lyases
XcbE1 – Product of *xcbE1*, homologous to D-cysteine desulfhdyrases
ACCD – 1-aminocyclopropane-1-carboxylate deaminase
AFS – aspartase/fumarase superfamily
ASL – argininosuccinate lyase
ADL – adenylosuccinate lyase

ABSTRACT

The metabolically versatile bacterium *Xanthobacter autotrophicus* Py2 has been the focus of many studies within the field of bioenergy sciences, as it contains two unique CO_2 fixing enzymes, and can utilize unconventional substrates such as propylene and acetone as the sole supplemented carbon source while fixing CO_2 in the process. Unexpectedly, coenzyme M (CoM) was found to play a crucial role as a C_3 carrier in the pathway for propylene metabolism in the late 1990s. Previously, CoM was thought to be present solely as a C_1 carrier in methanogenic archaea for nearly 30 years. Though CoM biosynthesis has been characterized in methanogenic archaea, bacterial CoM biosynthesis remained uncharacterized. In *X. autotrophicus* Py2, four putative CoM biosynthetic enzymes encoded by *xcbB1*, *C1*, *D1*, and *E1* have been identified through informatics and proteomic approaches. XcbB1 is homologous to the archaeal ComA which catalyzes the addition of sulfite to phosphoenolpyruvate, and forms the initial intermediate, phosphosulfolactate, in one of the methanogen CoM biosynthetic pathways. The remaining genes do not encode homologues of any of the previously characterized enzymes in methanogen CoM biosynthesis, suggesting bacteria have a unique pathway. The production of phosphosulfolactate by ComA homolog XcbB1 was verified, indicating that bacterial CoM biosynthesis is initiated in an analogous fashion to the PEP-dependent methanogenic archaeal CoM biosynthesis pathway. XcbC1 and D1 are members of the aspartase/fumarase superfamily (AFS), and XcbE1 is a pyridoxal 5'-phosphate-containing enzyme with homology to D-cysteine desulfhydrases. Direct demonstration of activities for XcbB1 and C1 strengthens their hypothetical assignment to a CoM biosynthetic pathway, and puts firm contraints on our proposed functions for XcbD1 and E1. Known AFS members catalyze β-elimination reactions of succinyl-containing substrates, yielding fumarate as the common unsaturated elimination product. We demonstrate herein that XcbC1 catalyzes a β-elimination reaction on the substrate phosphosulfolactate to yield sulfoacrylic acid and inorganic phosphate. To our knowledge, β-elimination reactions releasing phosphate is unprecedented among the AFS, indicating XcbC1 is a unique phosphatase. This work will serve as the framework for future studies aimed at uncovering the final stages of the biosynthetic pathway. By elucidating the XcbB1 and XcbC1 reactions, we have made significant strides towards understanding bacterial CoM biosynthesis which evaded characterization in previous years.

CHAPTER ONE

INTRODUCTION

Introduction to Coenzyme M

In 1971, a cofactor for methyl transfer was discovered in the cell extracts of methanogenic archaea by McBride and Wolfe[1]. The most notable characteristic exhibited by this cofactor was its crucial role in the penultimate step of methane formation. Using IR and UV spectroscopy, as well as ^{1}H-NMR, the structure of this cofactor was revealed to be 2,2'-dithiodiethanesulfonic acid, with additional evidence indicating that the active form of the cofactor is 2-mercaptoethanesulfonic acid, otherwise known as coenzyme M (CoM) [2]. Containing a sulfonic acid moiety separated from a thiol moiety by an ethyl group, CoM is acidic and strongly nucleophilic, and contains a remarkably high concentration of sulfur (45% of molecular weight) for its small size[1-3] (Fig 1.1).

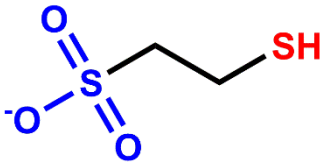

Figure 1.1. Structure for CoM is depicted with the acidic sulfonic acid moiety colored in blue and nucleophilic thiol moiety colored in red.

Along with required energy and carbon sources, CoM is essential to the growth of *Methanobacterium ruminantium* strain M1, implicating the importance of this small cofactor among methanogens[4,5]. R.S. Wolfe et al. attempted to determine the distribution of CoM in other organisms, and the results of their extensive tissue bioassay indicated it was not present in eukaryotic or other prokaryotic cells, suggesting that CoM was unique

to the methanoarchaea[6]. For nearly 30 years, it was thought that CoM functions solely as a C_1 carrier in the terminal stages of methanogenesis, but during the late 1990s, CoM was discovered as a key C_3 carrier in the pathway for bacterial propylene metabolism in *Xanthobacter autotrophicus* Py2. Analysis of available crystal structures from enzymes involved methanogenesis and propylene metabolism have revealed a unique role for CoM as a handle for properly orienting respective substrates during catalysis[12].

A Role for CoM in Methanogenesis

In methanogenic archaea, CoM is essential during the terminal stages of methanogenesis[7]. CO_2 and H_2 are utilized in a cyclic reaction that is responsible for the production of 400 million tons of methane every year[8]. Methanogens can also use other substrates to form methane, including acetate and/or other C1 compounds like methanol, methylthiols, and methylamines[7]. Initially, the molybdopterin and iron-sulfur cluster-containing formylmethanofuran dehydrogenase fixes CO_2 onto a C_1 carrier, followed by reduction to produce formyl-methanofuran (formyl-MF) as the first stable product of the pathway (Fig 1.2)[9]. Formyl-MF transfers the formyl group to a second C_1 carrier, tetrahydromethanopterin (THMP), forming formyltetrahydromethanopterin (Formyl-THMP), catalyzed by formylmethanofuran-THMP-formyltransferase[7]. Formyl THMP undergoes conversion to N^5-N^{10}-methenyl-THMP catalyzed by methenyl-THMP-cyclohydrolase.

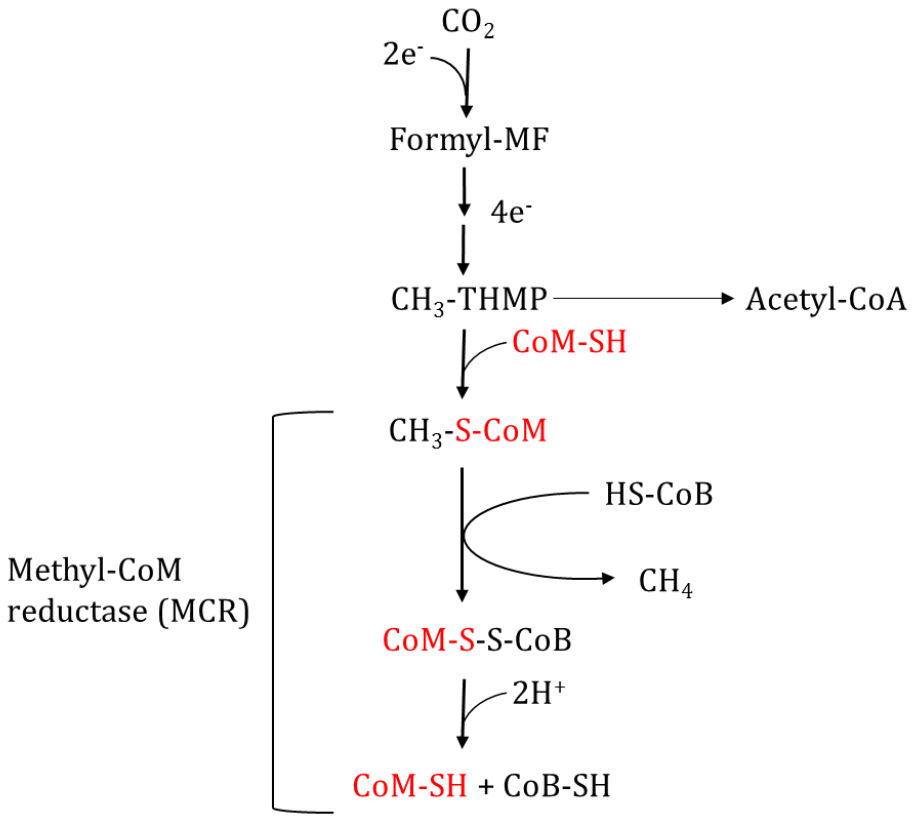

Figure 1.2. Simplified depiction of the methanogenesis pathway, where all steps between the formation of Formyl-MF and CH_3-THMP are collapsed.

Methenyl-THMP undergoes reduction by an F_{420}-dependent or independent methylene-THMP-dehydrogenase to yield N^5-N^{10}-methylene-THMP, which then undergoes an F_{420}-dependent reduction catalyzed by methylene-THMP-reductase to form methyl-THMP (CH_3-THMP). This substrate can proceed with methanogenesis or go towards acetyl CoA formation. The methyl group from CH_3-THMP is transferred to the third C_1 carrier of the pathway, CoM, by a zinc or cobalt and methylcob(III)alamin -dependent CoM methyltransferase to form the methylated CoM (CH_3-S-CoM), which serves as a substrate for methyl CoM reductase (MCR), a two-component enzyme. The Ni^I-F_{430} containing methyl-reductase utilizes the electron donor coenzyme B (CoB) to

reduce CH_3-S-CoM to CH_4 and CoM-S-S-CoB[10,11]. The second component consists of a heterodisulfide reductase that is responsible for reducing CoM-S-S-CoB to CoM-SH and CoB-SH.

Analysis of substrate-bound MCR indicates that the enzyme recognizes CoM through direct interactions with the CoM sulfonate moiety, through a salt bridge with Arg120 and hydrogen bonds to the Tyr444 backbone nitrogen[10,12]. Thauer and coworkers have proposed that CoM plays an analogous role in anaerobic oxidation of methane (AOM) in ANME-archaea, in which the reverse reaction catalyzed by an MCR homolog converts methane to methyl-CoM (Fig 1.3)[13,14]. Oxidation of methane to HCO^{3-} by ANME-archaea occurs in close association with sulfate-reducing bacteria, per the equation: $CH_4 + SO_4^{2-} \rightarrow HCO_3^- + HS^- + H_2O$.

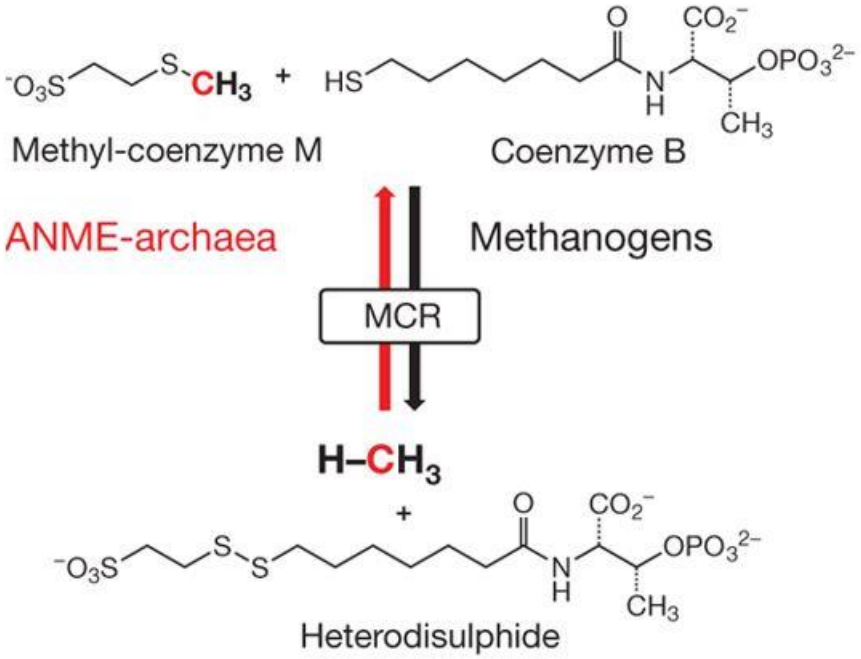

Figure 1.3. CoM-dependent reactions for the forward (methanogens) and reverse (ANME-archaea) MCR reaction[13]. Methane is converted to methyl-CoM in the reverse reaction.

Introduction to *Xanthobacter autotrophicus* Py2

Interest in organisms containing unique metabolic pathways with bioenergy or bioremediation potential has led to the discovery of novel carboxylation reactions. The bacterium *X. autotrophicus* Py2 has been the focus of several studies, as it contains two unique carboxylating enzymes; an acetone carboxylase as well as a 2-ketopropyl-CoM oxidoreductase /carboxylase (2-KPCC)[15-20]. *X. autotrophicus* is a gram-negative, aerobic α-proteobacterium that has also been a microorganism of interest due to its unique metabolic flexibility, including nitrogen fixation, acetone metabolism, metabolism of short chain alkenes and some aromatic compounds, in addition to CO_2 fixation[15,21-24]. This versatile, yellow-pigmented bacterium was isolated on propylene and 1-butene as growth substrates in the wake of several studies focusing on the production of epoxyalkanes from alkenes in multiple organisms[21]. While investigating multiple pathways for consumption of short chain alkenes and epoxides, a similar metabolic strategy emerged which involved CO_2 fixation to yield β-ketoacids[22,23].

Each year, over 200 million tons of alkene gasses are released into the environment as a result of either biological or industrial processes[25]. Aliphatic alkenes can serve as substrates for oxygenases (*e.g.* cytochrome P450s) with wide ranges of specificity, leading to the formation of epoxides with potential mutagenic or carcinogenic properties[26-28]. The electrophilic epoxides exhibit high reactivity with cellular nucleophiles such as DNA or proteins, forming covalent adducts that contribute to the toxicity of these compounds[23,26]. Some organisms have developed means for using these potentially harmful compounds as growth supporting substrates, and in particular, *X.*

autotrophicus Py2 has been shown to utilize unconventional substrates such as propylene, propylene oxide, acetone, and isopropyl alcohol as the sole supplemented carbon source in pathways that also fix CO_2[15,16,22,29].

Methods for Identifying CoM as a C3 Carrier

By the late 90's, the progression of the pathway for propylene metabolism was understood, but the identity of the intermediates and formal enzyme assignments were still under study (Fig 1.4). Through previous biochemical work, the general structural characteristics of the intermediates were understood, and it was also established that an unidentified thiol (R-SH) was acting as a C3 carrier for the pathway. S.A. Ensign and coworkers utilized ^{1}H-NMR and ^{13}C-NMR to provide evidence that the C3 carrier was CoM[25]. It was already established that Enzyme I yields (*R*)-and (*S*)-β-hydroxythioether conjugates, so the natural product of this reaction was isolated and analyzed via ^{1}H-NMR (Fig 1.5A). Enzyme I was then inactivated and incubated with [^{14}C]-epoxypropane, followed by screening the enzyme with multiple commercially available thiols. Out of all thiols tested, only CoM returned activity to the enzyme. The product of [^{14}C]-epoxypropane and CoM catalyzed by Enzyme I was isolated and analyzed via ^{1}H-NMR (Fig 1.5B), resulting in a spectrum that matched the natural product spectrum. Synthetic 2-hydroxypropyl-CoM, or the product of an epoxypropane and CoM adduct, was analyzed to confirm the identity of the two products isolated from the enzymes (Fig 1.5C), again resulting in a matching spectrum. Thus, CoM was confirmed as a C3 carrier for at least the first step.

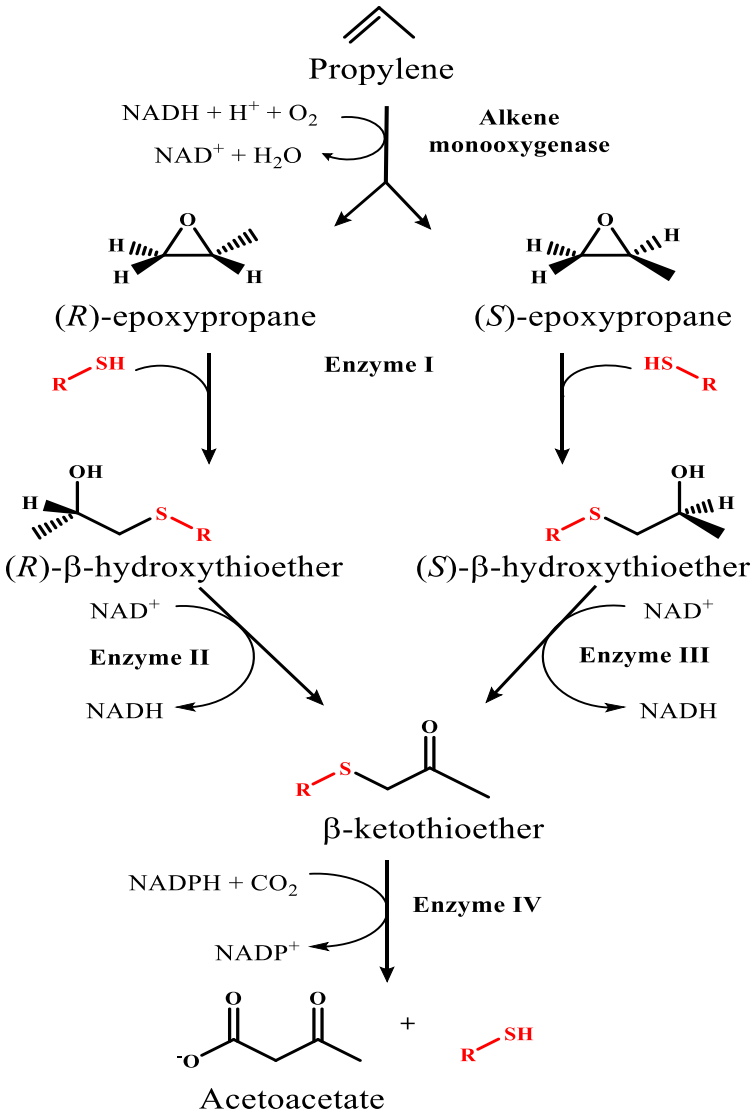

Figure 1.4. The progression of the propylene metabolism pathway during the late nineties was understood, but the enzyme assignments and identity of the intermediates were still under study. The identity of the thiol that acted as a C3 carrier in the pathway was the subject of study in J.R. Allen et al. (1999)[25].

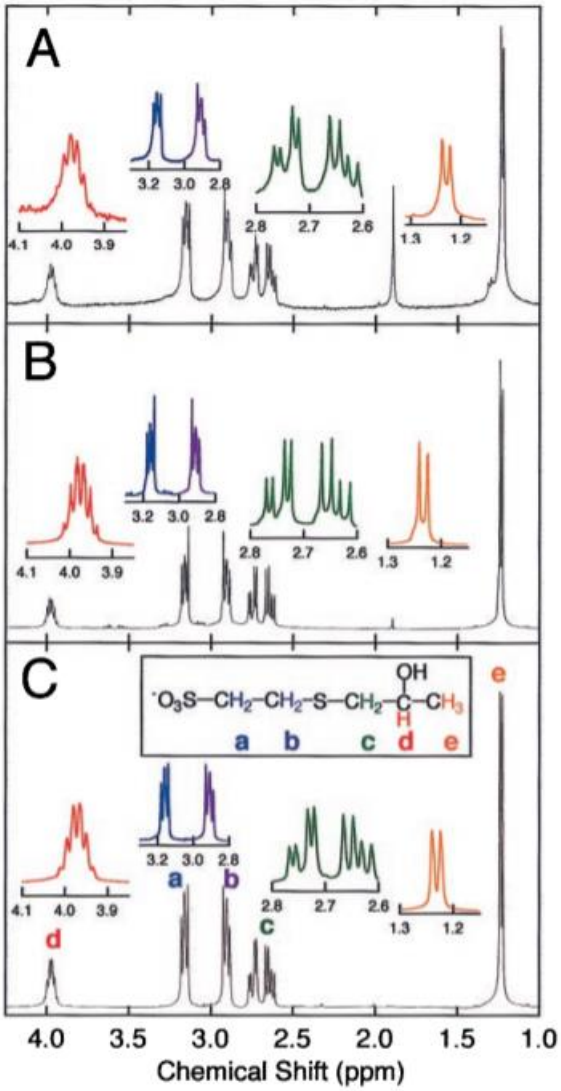

Figure 1.5. ^{1}H-NMR spectrum of the natural product epoxypropane–cofactor adduct isolated from Enzyme I (A). ^{1}H-NMR spectrum of the product of Enzyme I-catalyzed reaction of CoM with epoxypropane (B). ^{1}H-NMR spectrum of synthetic 2-hydroxypropyl–CoM (C). The signals (a-e) that correspond to the respective protons are labeled in C[25].

To determine if CoM was the C3 carrier for the next step, 2-hydroxypropyl-CoM and NAD^{+} were incubated with Enzyme II and III, and the resulting product was analyzed (Fig 1.6). It was already established that a β-kethothioether would be the product of this

reaction, so synthetic 2-ketopropyl-CoM, or the oxidized product of 2-hydroxypropyl-CoM, was also analyzed as a reference.

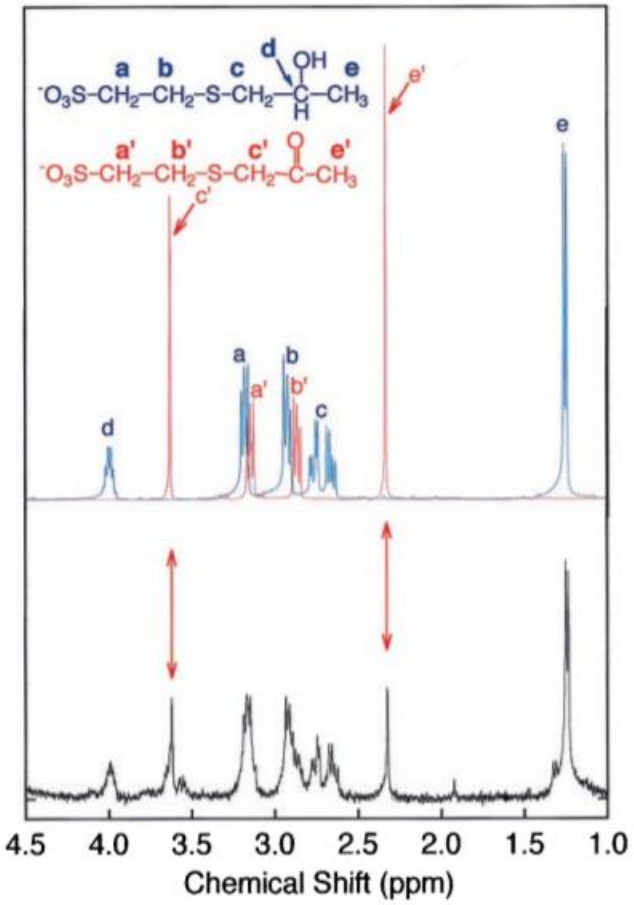

Figure 1.6. ^{1}H-NMR spectrum of the product of Enzyme II and III-catalyzed reaction of NAD^{+} and 2-hydroxypropyl–CoM (bottom panel). Spectra for synthetic 2-hydroxypropyl–CoM (blue) and 2-ketopropyl CoM (red) were overlaid to provide reference (top panel). The respective protons are labeled in the top panel. The peaks that emerge as a result of the enzymatic reaction are consistent with the formation of 2-ketopropyl CoM[25].

The peaks that appeared in the Enzyme II and III catalyzed reaction were consistent with peaks for 2-ketopropyl-CoM, indicating that CoM acts as a C3 carrier for the next step of propylene metabolism. For the final step, 2-ketopropyl-CoM, $NaH^{13}CO_3$,

and NADPH were incubated with Enzyme IV, and the resulting product was analyzed via ^{13}C-NMR (Fig 1.7).

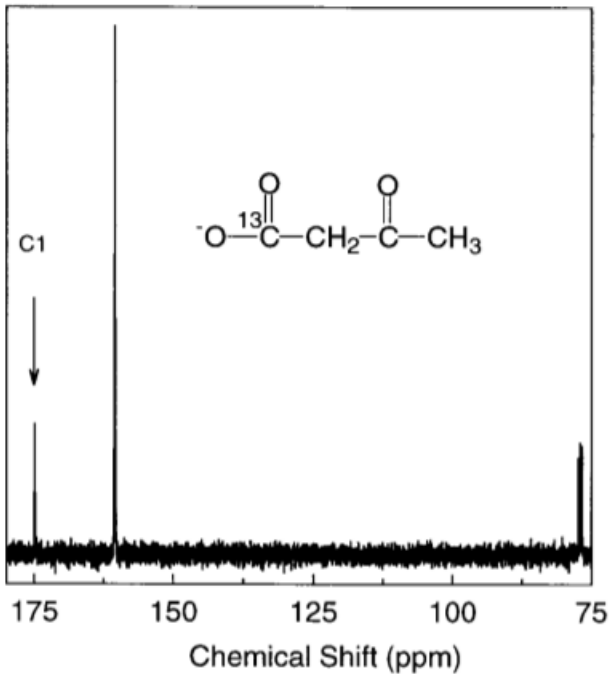

Figure 1.7. The 13C-NMR spectrum for the product of the 2-ketopropyl-CoM, $NaH^{13}CO_3$, and NADPH incubation with Enzyme IV. The peak at 176.4 ppm is consistent with acetoacetate formation while resonance at 160.3 ppm is caused by $NaH^{13}CO_3$ remaining in sample. As expected, the acetoacetate is enriched with the ^{13}C label at the C1 position[25].

The Enzyme IV-catalyzed reaction yielded a ^{13}C-enriched product consistent with the formation of acetoacetate from $^{13}CO_2$ and 2-ketopropyl-CoM, and the release of CoM. Identification of CoM in the pathway for propylene metabolism was a significant discovery, since previously, CoM was thought to be exclusive to methanogenic archaea.

A Role for CoM in Bacterial Propylene Metabolism

Propylene metabolism in *X. autotrophicus* Py2 utilizes the regenerated CoM as a C_3 carrier (Fig 1.8). CoM-dependent propylene metabolism is initiated by the uptake of propylene, which subsequently undergoes epoxidation in an NADH-dependent alkene monooxygenase (AMO) catalyzed reaction[17,22,30]. The products of this reaction are 95% (*R*)- and 5% (*S*)-epoxypropane [17,25,31]. Subsequent epoxide detoxification/carbon assimilation steps are carried out in an epoxide carboxylation pathway (ECP). Ring opening of the epoxypropane is catalyzed by epoxyalkane: coenzyme M transferase (EaCoMT) in which the electrophilic epoxide undergoes nucleophilic attack by CoM, forming 2-(*RS*)-hydroxypropyl-coenzyme M[17,32-34]. The subsequent NAD^+-dependent oxidations of the hydroxypropylthioether conjugates, or hydroxypropyl CoM (*R*- and *S*-HPC) are catalyzed by the stereoselective 2-(*RS*)-hydroxypropyl-CoM dehydrogenases(*R* and *S*-HPCDH), yielding 2-ketopropyl-coenzyme M (2-KPC)[35]. In the final 2-KPCC catalyzed reaction, 2-KPC undergoes NADPH-dependent reductive cleavage followed by carboxylation, releasing acetoacetate and CoM [18-20]. Besides *X. autotrophicus* Py2, there are other diverse bacterial species with CoM implicated in the degradation of short chain olefins; N*ocardioides* sp. JS614, several strains of *Mycobacterium*, *Pseudomonas putida* AJ, *Ochrobactrum* sp. TD, and *Rhodococcus rhodochrous* [32,33,36-40].

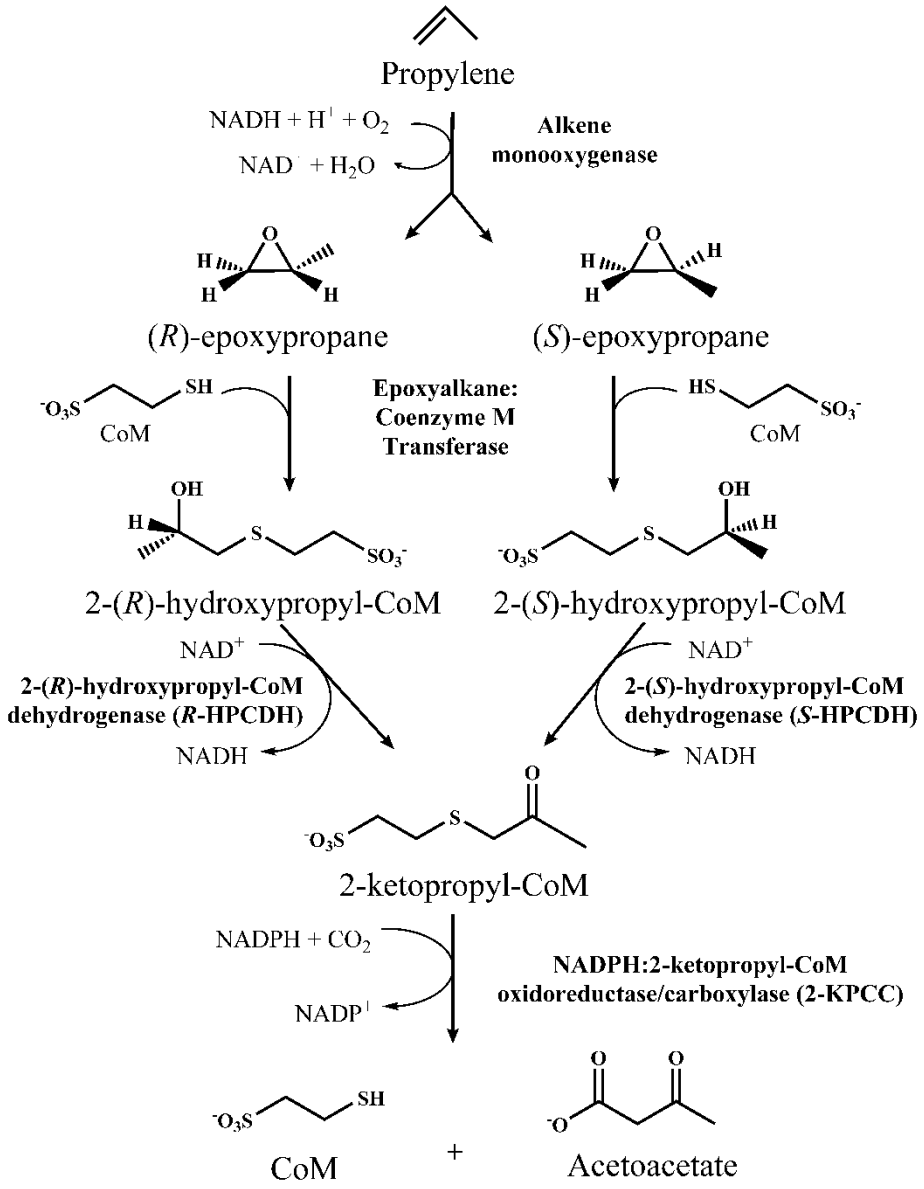

Figure 1.8. The CoM-dependent pathway for propylene metabolism in *X. autotrophicus* Py2.

Unifying Structural Features in Propylene Metabolism Enzymes

Propylene metabolism is initiated by an AMO catalyzed reaction that adds one of the oxygen atoms of O_2 to the substrate double bond, yielding epoxypropane. In contrast to methane monooxygenases and other widespread monooxygenases, AMO will not

catalyze the oxygenation of the corresponding alkane, i.e. propane[41]. The AMO of *X. autotrophicus* Py2 is a four component system that consists of; 1) an FAD and [2Fe-2S] cluster containing NADH reductase that provides the reductant for O_2 activation, 2) a [2Fe-2S] cluster containing Rieske-type ferredoxin which mediates electron transfer, 3) the catalytic center for alkene epoxidation, an epoxygenase arranged in an $\alpha_2\beta_2\gamma_2$ quaternary structure, and 4) an effector protein (Fig 1.9)[31,42,43]. Components of this system are homologous to those of aromatic monooxygenases but contain characteristics for growth on alkenes[44]. The first step of epoxypropane detoxification is catalyzed by EaCoMT, a zinc-dependent enzyme that belongs to a family of alkyl transferases, which includes enzymes such as; betaine-homocysteine methyltransferase, cobalamin-independent methionine synthases (MetE), and other methanogenic methyltransferases (MtaA, MtbA, and MtsA)[12,45].

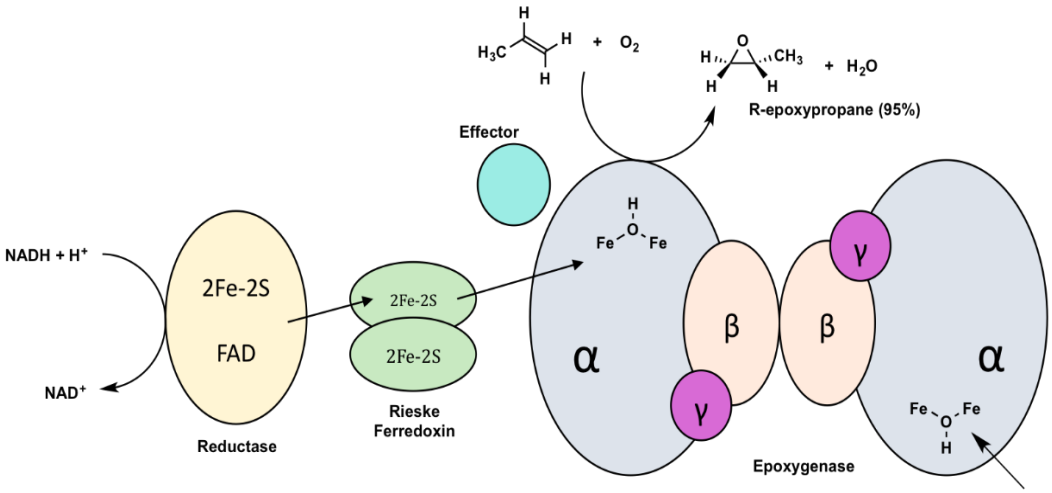

Figure 1.9. AMO from *X. autotrophicus* Py2.

In these enzymes, zinc is crucial for thiol activation during nucleophilic attack. Comparison of EaCoMTs from *Xanthobacter*, *Nocardioides*, *Mycobacterium*, and *Rhodococcus*, revealed an $HXCX_nC$ zinc binding motif shared by the MetE enzyme subclass[12]. EaCoMT is proposed to activate the substrate thiol by coordination at the zinc site, lowering the pK_a enough to facilitate deprotonation[46]. The deprotonated thiol is then poised for nucleophilic attack on the epoxypropane cosubstrate, yielding hydroxypropyl-thioether (Fig1.10A). In addition to the zinc binding motif, substrate binding sites for EaCoMTs also consist of a conserved arginine and lysine, implicating potential interactions with the sulfonate moiety of CoM. To identify possible CoM-binding side chains, a homology model for *X. autotrophicus* Py2 EaCoMT was superimposed over the homocysteine bound crystal structure for *T. maritima* MetE. The location of zinc--coordinated homocysteine provided a reference for CoM binding, ultimately revealing that positively charged arginine and lysine residues are situated to form favorable electrostatic interactions with the CoM sulfonate moiety(Fig 1.10B)[12]. The strongly favorable interactions between the positively charged active site residues and the sulfonate group may also explain the poor reactivity of EaCoMT towards other similarly small thiols, such as 2-mercaptoethanol and cysteine[47].

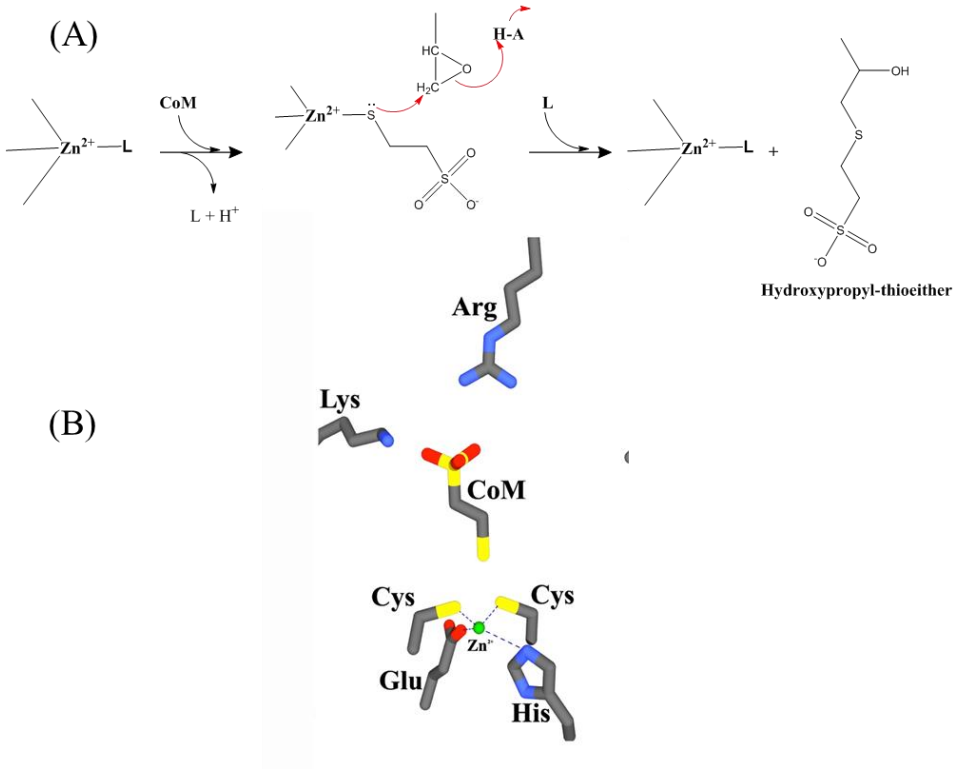

Figure 1.10. The proposed EaCoMT mechanism (A) is depicted through displacement of the exchangeable ligand (L) by CoM. The modeled EaCoMT active site (B) with coordinated CoM is shown along with additional zinc coordinating ligands [12,42].

The formation of the 2-(*RS*)-hydroxypropylethioether conjugates by EaCoMT is followed by NAD^+-dependent oxidation catalyzed by the stereoselective *R*- and *S*-HPCDH to generate 2-KPC. As members of the short-chain dehydrogenase reductase (SDR) family, *R*- and *S*-HPCDH contain the canonical serine, tyrosine, and lysine catalytic triad[48,49]. Biochemical and structural studies of *R*-HPCDH reported the presence of two arginine residues that resembles the binding site strategy of EaCoMT[50]. Like EaCoMT, the positively charged arginines are specifically oriented to favorably interact with the CoM sulfonate group, and position the substrate for catalysis. Superimposition of the *S*-HPCDH homology model on the *R*-HPCDH crystal structure revealed a

structural basis for the stereoselectivity of these enzymes, specifically, the spatial arrangement of the important positively charged residues (Fig 1.11A). Sulfonate binding sites for *R*-and *S*-HPCDH (two arginines and lysine/arginine, respectively) are separated by 105°, conferring a method for chiral discrimination. Active sites for these enzymes also include residues that appear to act as shields from bulk solvent (Fig 1.11B).

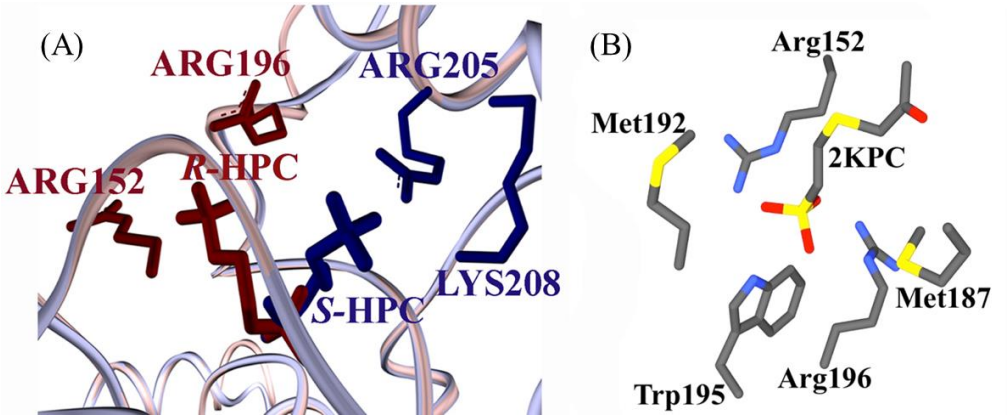

Figure 1.11. The homology model of S-HPCDH (red) was superimposed on the R-HPCDH (blue) structure (A) showing analogous sites at spatially different positions. The important residues for sulfonate binding in R-HPCDH are also depicted (B)[50].

Characterization of *R*-HPCDH established the identity and function of the catalytic serine, tyrosine, and lysine residues, which are consistent with canonical SDR enzymes[51]. Through a series of protonation and hydride transfer events, the hydroxyl group of *R*- and *S*-HPC are oxidized to ketones, yielding 2-KPC (Fig 1.12)[50].

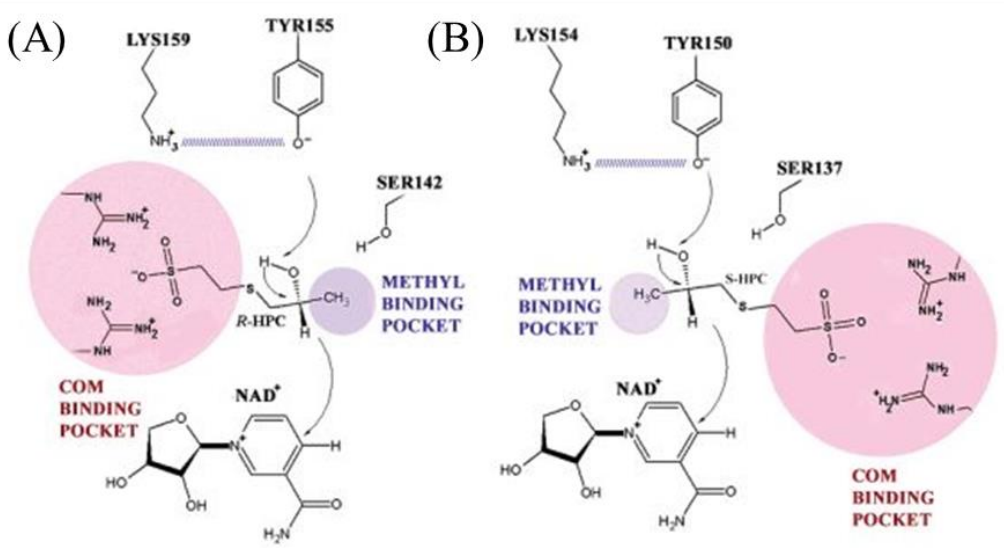

Figure 1.12. Depictions of *R*-HPCDH (A) and *S*-HPCDH (B) substrate binding, with arrows depicting the sequence in which substrate is oxidized to 2-ketopropyl-CoM[50].

During the final stage of propylene metabolism, 2-KPCC catalyzes the NADPH-dependent reductive cleavage of 2-KPC, followed by carboxylation of an unstable enolacetone intermediate. This leads to release of acetoacetate and CoM. 2-KPCC is a homodimeric enzyme with one flavin adenine nucleotide (FAD) per subunit, and belongs to the disulfide oxidoreductase (DSOR) family of enzymes[17,18,30]. Members of this family contain a redox-active pair of cysteines (GGX**C**XXXX**C**VP) that participate in the two-electron reduction of their respective substrates[52]. Extensive structural and biochemical characterization of 2-KPCC enabled the proposal a detailed mechanistic scheme initiated by NADPH reduction of FAD, which in turn reduces the oxidized cysteine pair (Fig 1.13)[18,53]. Keeping with the sulfonate binding scheme for EaCoMT and *R*- and *S*-HPCDH, 2-KPCC utilizes two active sites arginines to form electrostatic interactions with the sulfonate moiety of the 2-KPC substrate (Fig 1.14)[54]. 2-KPC binding is followed

by nucleophilic attack of the interchange cysteine thiol on the substrate thioether sulfur, breaking the S-C bond.

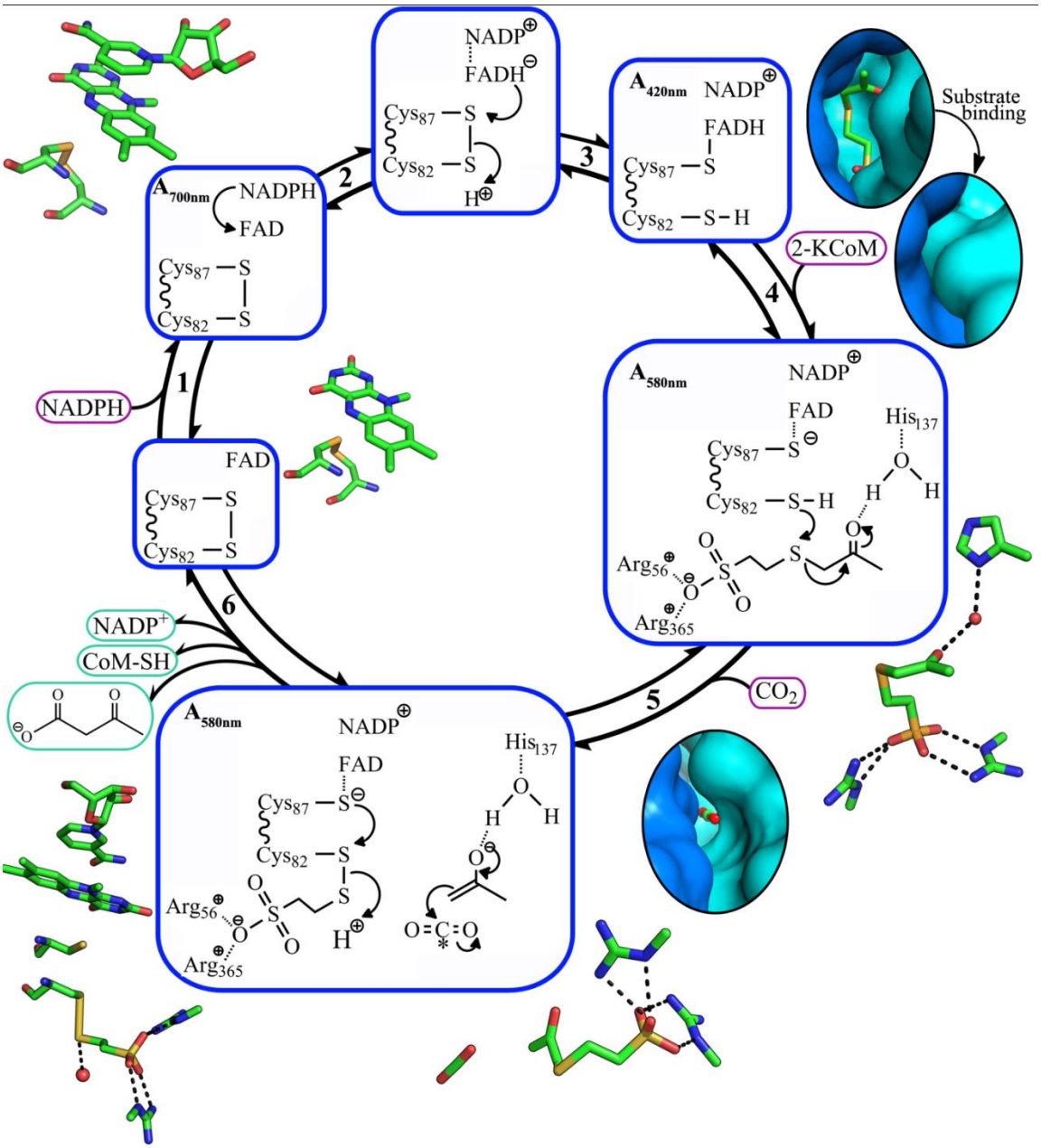

Figure 1.13. Mechanism of 2-KPCC catalyzed reaction with relevant structural features depicted[53].

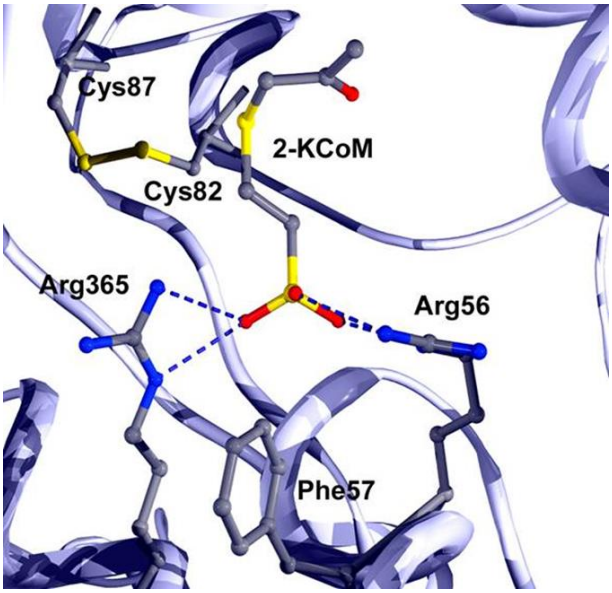

Figure 1.14. The active site of 2-KPCC is depicted with bound 2-KPC[54].

Heterolytic cleavage of 2-KPC results in enolacetone and a Cys-CoM mixed disulfide. Enolacetone can undergo two fates; carboxylation to form acetoacetate, or protonation to form acetone[18,55]. Carboxylation occurs under saturating CO_2 levels, where enolacetone undergoes nucleophilic attack on CO_2, and regeneration of CoM is achieved by protonation of the Cys-CoM mixed disulfide[18,24]. Discrimination between electrophiles (CO_2 or protons) is likely achieved by replacement of the conserved DSOR catalytic dyad (His-Glu) with residues that promote carboxylation (Phe-His)[56]. The distinguishing features of 2-KPCC among DSOR enzymes is the ability to cleave a thioether bond rather than disulfide bonds like the canonical glutathione reductase. It is the only known DSOR member that carboxylates the substrate[18,24,57]. Unifying structural features in EaCoMT, *R*- and *S*-HPCDH, and 2-KPCC demonstrate a crucial role for CoM in propylene metabolism. All four enzymes share a common strategy for binding and orienting the substrate for catalysis by association with the CoM-derived sulfonate group.

Similarities in CoM Utilization Between Methanogenesis and Propylene Metabolism

Though these pathways are present in different domains and have different purposes within the organism, they have developed interesting similarities regarding utilization of CoM. Both pathways utilize *S*-alkylation of CoM during the initial group transfer to form a thioether intermediate[12]. The methanogenic methyltransferase utilizes zinc to activate the CoM thiol for methyl group acceptance[58], and the zinc in EaCoMT facilitates an analogous CoM thiol activation for attack on the electrophilic epoxide[12,32,46]. Both pathways also utilize reductive dealkylation of their respective CoM thioethers, generating methane in methanogenesis and the enolate that undergoes carboxylation in propylene metabolism[18,54,59]. Much of the understanding of the role of CoM in pathways for methanogenesis and alkene metabolism has been supported by structural studies of enzymes bound with inhibitors, substrates or products that complement biochemical and kinetic studies[12]. A pattern has emerged amongst the enzymes of propylene metabolism, specifically EaCoMT, *R*-and *S*-HPCDH, and 2-KPCC, and the MCR of methanogenesis in which strategically placed basic amino acids interact with the acidic sulfonate moiety of CoM to properly orient the substrate for catalysis. These active site and substrate interactions suggest a structural signature for CoM binding.

It is intriguing to speculate on why CoM is utilized in both pathways when there are so many other thiols, such as cysteine or glutathione, that could also participate in this type of chemistry. Regarding propylene metabolism, it has been suggested that the elegantly small design of CoM makes the 2-hydroxypropyl-CoM conjugate a more manageable size compared to glutathione conjugates[12]. Additionally, the sulfonate handle

of CoM allows for proper orientation of the substrates in the pathway, where normally, the short-chain alkenes would lack distinctive functional groups to confer specificity in stereoselective dehydrogenase reactions. Similar rationale may explain the specific presence of CoM in methanogenesis.

Biosynthesis of CoM in Methanogenic Archaea

There are two known pathways for CoM synthesis distributed among the methanogens; a PEP-dependent pathway and an L-phosphoserine-dependent pathway (Fig 1.15, Table A.S.4) [60-67]. The CoM carbon skeleton was deduced by analyzing the extracted and derivatized products of methanoarchaea grown on stable-isotope labeled acetates (1,2-$^{13}C_2$ and 2,2,2-$^{2}H_3$ labeled acetate)[65,68]. The labeled CoM appeared to be consistent with a PEP precursor. To demonstrate that sulfite contributed the source of the CoM sulfonate moiety, cell extracts from *Methanobacterium formicum* were incubated with PEP, bisulfite, and cysteine which resulted in the formation of sulfolactate, sulfopyruvate, and sulfoacetaldehyde, which established the presence of these intermediates in the biosynthetic pathway[67]. The initial step in PEP-dependent biosynthesis of CoM is the addition of sulfite onto phosphoenolpyruvate, catalyzed by phosphosulfolactate synthase (ComA), yielding (*R*)-phosphosulfolactate[62,69].

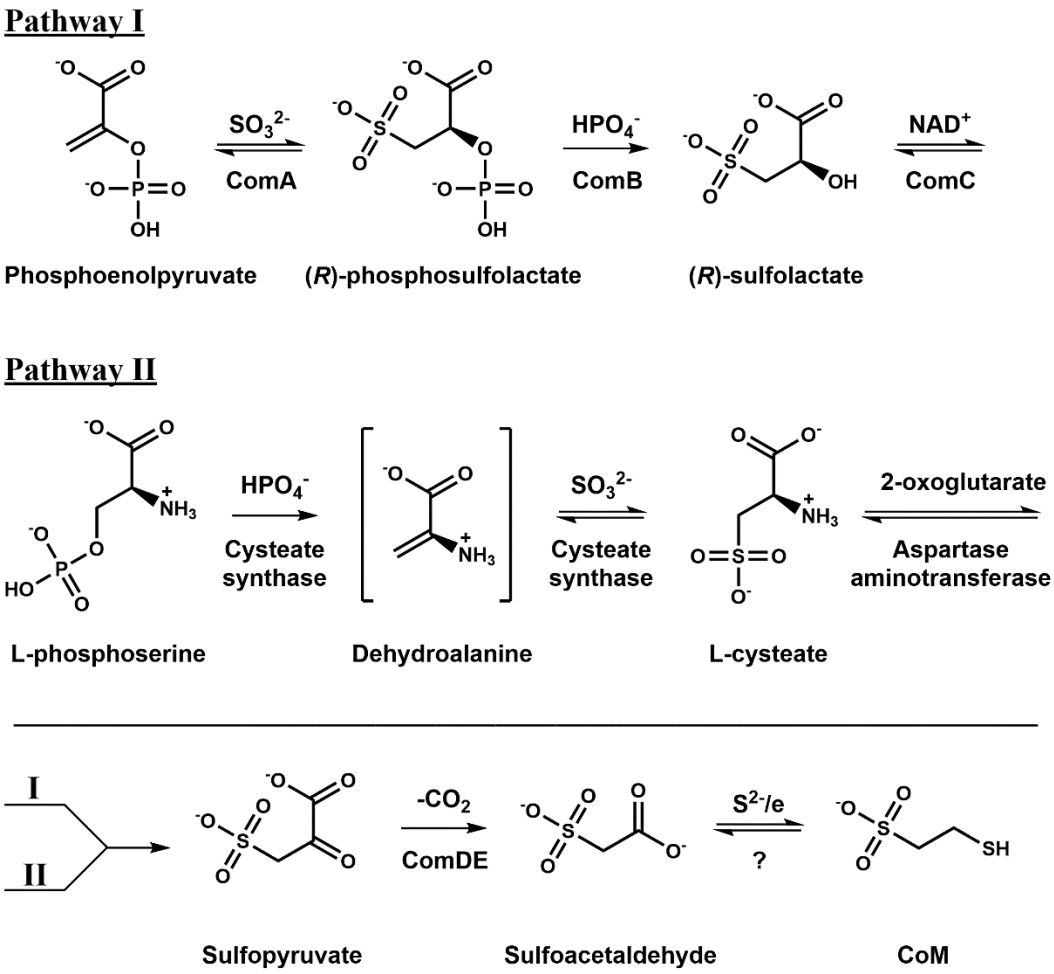

Figure 1.15. Proposed pathways for PEP- and L-phosphoserine-dependent pathways for methanoarchaeal CoM biosynthesis.

Dephosphorylation occurs in a 2-phosphosulfolactate phosphatase (ComB) catalyzed reaction, producing (*R)*-sulfolactate that subsequently undergoes a (*R)*-sulfolactate dehydrogenase (ComC) NAD^+-dependent oxidation to form sulfopyruvate[61,63,64]. A thiamine diphosphate-dependent sulfopyruvate decarboxylase (ComDE) catalyzes the decarboxylation of sulfopyruvate to sulfoacetaldehyde in what is possibly the penultimate reaction of the pathway[64]. The enzyme(s) that catalyze addition of thiol and reduction of sulfoacetaldehyde to form coenzyme M remain unknown, although experimental results

initially pointed to cysteine as the source of sulfur for the thiol moiety[64-66]. Addition of cysteine to sulfoacetaldehyde with boiled cell extracts did not yield any CoM, suggesting that the conversion to CoM is enzymatic[66]. Previous hypotheses by R.H. White et al. suggested that cysteine and sulfoacetaldehyde could form an adduct that undergoes reductive cleavage to yield CoM and other end products. However, during recent personal communications with R.H. White, it was proposed that cysteine is likely not the source of thiol due to the low abundance of free cysteine in methanogens[70]. Unpublished work by R.H. White indicates that H_2S, sulfoacetaldehyde, and dithionite readily form CoM under normal cellular conditions, making it difficult to implicate a specific enzyme(s). Whether the final biosynthetic step is spontaneous or catalyzed by enzyme(s) is not clear, however, gene homologs of *comABCDE* are distributed amongst methanogens from the orders Methanococcales, Methanobacteriales, and Methanopyrales (Class I methanogens)[60].

There are orders of methanoarchaea (Methanosarcinales and Methanomicrobiales) that do not contain *comABC* homologues (Class II methanogens), but do contain a fused *comDE* gene that is homologous to the sulfopyruvate decarboxylase in Class I methanogens[60]. Adjacent to the fused *comDE* gene is a cysteate synthase gene, which encodes a pyridoxal 5'-phosphate (PLP)-dependent enzyme that catalyzes the β-elimination of phosphate from L-phosphoserine and the addition of sulfite to yield L-cysteate. Cysteate is then transaminated by a canonical PLP-dependent aspartate aminotransferase to form sulfopyruvate, which then undergoes decarboxylation by the

ComDE homologue to form sulfoacetaldehyde[71,72]. Like the Class I methanogen biosynthetic pathway, the final enzyme(s) yielding CoM remains unknown.

Putative Pathway for Bacterial CoM Biosynthesis

Despite the significant scope of work on bacterial propylene metabolism, and methanoarchaeal CoM biosynthesis, the pathway for bacterial CoM biosynthesis remained unknown prior to the work reported in this thesis. Understanding how CoM is biosynthesized would not only be of interest for fundamental research, but will also further our understanding of the CO_2-fixing pathway for propylene metabolism, which could also contribute to better understanding of the global carbon cycle.

In 2000, J.G. Krum et al. showed that the alkene metabolic genes in *X. autotrophicus* Py2 are propylene inducible, and the synthesis of CoM is coordinately regulated with the expression of the AMO and ECP enzymes[32]. These findings suggested clustering of the respective genes under a common regulatory element, unique in its propylene sensing ability. A putative σ^{54} (RpoN)-dependent promoter was identified ~300 bp upstream from the AMO translational start[44]. Additionally, growth of *X. autotrophicus* Py2 on glucose, acetate, isopropanol, acetone, and propane did not yield any detectable amounts of CoM, further confirming the specific role for CoM in propylene metabolism. Repeated sub-culturing on alternative carbon sources (i.e. glucose, acetone, etc) resulted in the loss of the ability to grow on propylene or epoxypropane, suggesting that the necessary AMO and ECP genes for propylene metabolism are located on an extrachromosomal element maintained through selective

pressure with propylene[73]. Indeed, strains of propylene-grown *X. autotrophicus* Py2 were found to contain a single 320-kb linear megaplasmid, whereas strains repeatedly cultured on other carbon sources lacked this megaplasmid. Investigation of the region downstream from the AMO and ECP gene clusters revealed a gene that encoded a polypeptide sharing significant homology with the first enzyme present in the PEP-dependent CoM biosynthetic pathway (ComA) in *Methanocaldococcus jannaschii*.

Through proteomics approaches, C.A. Broberg et al. cataloged the proteins that were induced in response to growth on propylene, which includes the AMO, ECP, and putative CoM biosynthesis gene products (Fig 1.16)[74]. Additionally, it was speculated that a DNA-binding protein (xaut_4864) induced only under growth with propylene may be a transcriptional activator of the genes required for propylene metabolism and CoM biosynthesis.

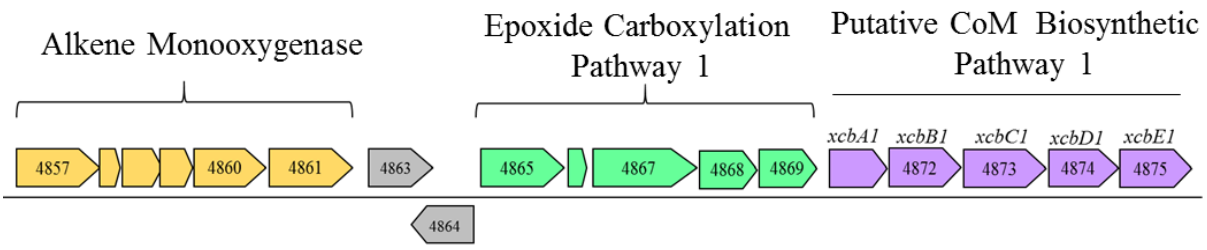

Figure 1.16. Depiction of megaplasmid region that contains the gene cluster for AMO, ECP, and the putative CoM biosynthetic pathway. Gene products are propylene inducible, and the gene that encodes the ComA homolog is denoted as *xcbB1* (adapted from Broberg, et al. 2010)[74]. Alkene-related functions for the open reading frames in gray have not been assigned. The downstream paralogous gene clusters for ECP-2 and putative CoM biosynthetic pathway 2 are not shown here.

Using data from the sequenced *X. autotrophicus* Py2 genome, the putative CoM operon consists of five partially overlapping open reading frames (ORF). The encoded products are annotated as follows: XcbA1 (hypothetical protein), XcbB1

(phosphosulfolactate synthase), XcbC1 (argininosuccinate lyase), XcbD1 (adenylosuccinate lyase family protein), and XcbE1 (1-aminocyclopropane 1-carboxylate deaminase) (refer to Table A.S.3 for list of 20 genes upstream and downstream from putative CoM operon). Farther downstream, paralogs of the ECP and putative CoM biosynthetic cluster (Table A.S.1) were also found to be propylene inducible, further supporting the relevance of the putative gene cluster. The AMO system does not appear to have additional paralogous clusters, while the extensively characterized ECP are from gene cluster 1, and are located directly downstream of AMO. The downstream ECP gene cluster (ECP-2) has yet to undergo characterization. Analysis of the proteomics profile did not reveal hits for XcbA1, but did yield matches for XcbA2 (from putative CoM biosynthetic pathway 2)[74]. The authors proposed that because *xcbA1* is classified as a pseudogene, that a lack of product could be expected.

Amongst the putative biosynthetic pathway resides the ComA homolog, XcbB1, which suggested a common starting point for bacterial and PEP-dependent methanoarchaeal CoM biosynthesis. When *M. jannachii* ComA was aligned with *xcbB1, xcbB2,* and *xcbB3* gene products, it was found that all three XcbB enzymes contained all but one of the catalytic and substrate-binding residues identified in ComA[74]. Broberg et al., proposed that these five genes are the putative CoM biosynthetic gene cluster based on four lines of evidence; 1) propylene inducible nature of the gene cluster, 2) partial overlapping of the genes within the cluster, 3) proximity of the cluster to the other alkene metabolic genes, and 4) the nearly identical makeup of the putative CoM biosynthetic

gene cluster in *X. autotrophicus* Py2 to gene clusters located in other bacteria with CoM-dependent alkene metabolism, *i.e. Nocardioides* sp. JS614.

Beyond *xcbB1*, none of the other genes in the putative CoM operon encode products homologous to enzymes from either methanoarchaeal biosynthetic pathway, suggesting that bacterial CoM is synthesized by a third, distinct pathway. While genes that encode enzymes for PEP-dependent methanoarchaeal biosynthesis are discontiguous, it appears that *X. autotrophicus* Py2 and other CoM-dependent organisms have clustered operons in remarkably similar order (Fig 1.17)[36,38]. The phylogenetically distinct *Nocardioides* JS614 and various *Mycobacteria* species are specific towards vinyl chloride and ethylene consumption, but several of these organisms also maintain their general alkene metabolism and putative CoM biosynthetic genes on a plasmid, perhaps indicating an intriguing evolutionary history[36]. Like *X. autotrophicus* Py2, strain JS614 also contains a second putative CoM biosynthetic pathway close to additional ECP homologs. While additional bioinformatics studies need to be performed to more accurately determine how the putative CoM biosynthetic genes arose in *X. autotrophicus* Py2, previous studies have speculated that the bacteria may have assimilated extracellular archaeal DNA, supported by the existence of the plasmid that houses these genes[73]. If the genes were located in the genome, there could have been a genetic recombination or insertional event, while genes located extrachromosomally may indicate that the bacteria stabilized the extrachromosomal element for a phenotype necessary for survival. This speculation may provide some insight into the origin for the ComA homolog, XcbB1, in *X. autotrophicus* Py2.

Prior to publication of the *X. autotrophicus* Py2 genome in 2007, many attempts were made to generate a CoM auxotroph through transposon mutagenesis[74]If CoM biosynthetic enzymes were inactivated by transposon, the active paralogs could compensate for the metabolic deficiencies. Multiple gene duplications events within *X. autotrophicus* Py2 highlight one of the difficulties in elucidating the pathway for bacterial CoM biosynthesis via traditional biochemical means.

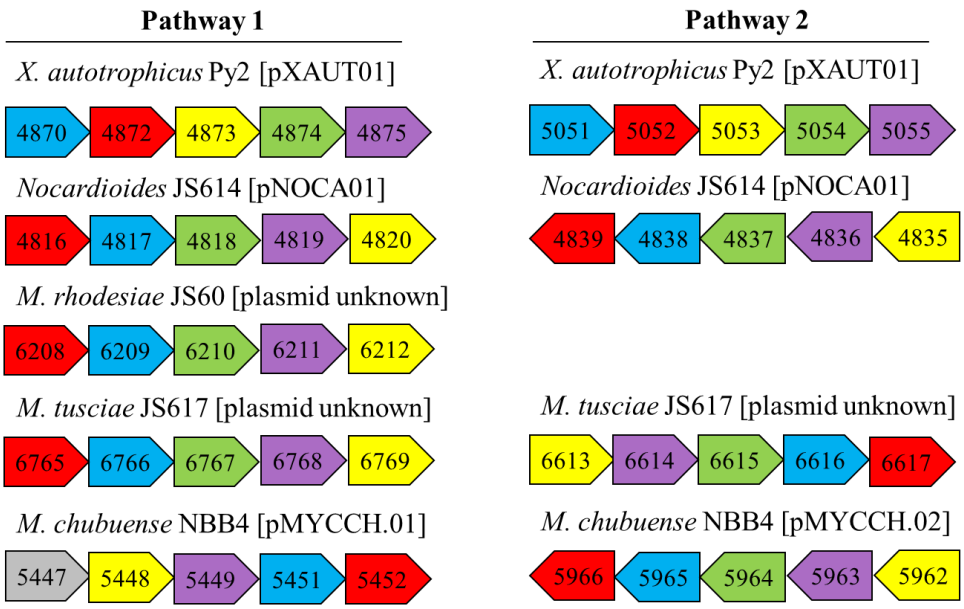

Figure 1.17. Putative CoM operons (pathway 1 & 2) are shown for *X. autotrophicus* Py2, *Nocardioides (*pathway 3 not shown), and three species of *Mycobacteria*, along with plasmid (if information is available). Using the genes from *X. autotrophicus* Py2 as a reference, the corresponding homologs in the other organisms are color matched as follows; *xcbA1* (blue), *xcbB1* (red), *xcbC1* (yellow), *xcbD1* (green), and *xcbE1* (purple). Except for *M. tusciae* JS617, all organisms shown have at least one paralogous operon.

Research Directions

A 5.7 kb putative gene cluster contains four open reading frames that are expressed in response to propylene induction[74]. This work is centered on the putative CoM biosynthetic pathway 1 (Table A.S.2), due to its proximity to the extensively

characterized AMO and ECP gene clusters. An ORF immediately upstream of the cluster, designated *xcbA1*, is annotated as a pseudo or hypothetical protein. However, this ORF possesses several stop codons throughout all three reading frames and a corresponding protein is not expressed under growth on propylene. The deduced amino acid sequence of *xcbB1* is annotated as a homolog of ComA from the CoM biosynthetic pathways of methanogenic archaea. This enzyme catalyzes the addition of sulfite to PEP to yield phosphosulfolactate as the first reaction in all known methanoarchaeal PEP-dependent pathways. We verified the production of phosphosulfolactate by ComA homolog XcbB1 indicating that bacterial CoM biosynthesis is initiated in an analogous fashion to the PEP-dependent methanogenic archaeal CoM biosynthesis pathway. Interestingly, additional genes within the cluster are not similar to those from either methanoarchaeal pathway, suggesting that the bacterial CoM is synthesized via a chemically distinct series of reactions. Conversion of phosphosulfolactate to CoM, requires net dephosphorylation, decarboxylation, and thiolation steps. XcbC1 and D1 are members of the aspartase/fumarase superfamily (AFS), and XcbE1 is a PLP containing enzyme in the Fold Type II family. The annotation of XcbC1 and XcbD1 as members of the AFS provides clear clues about the most logical trajectory by which these steps might occur. The AFS is a family of enzymes that catalyze β-elimination reactions of succinyl-containing substrates, yielding fumarate as the common unsaturated elimination product. We demonstrate herein that XcbC1 catalyzes a β-elimination reaction on the substrate phosphosulfolactate to yield sulfoacrylic acid and inorganic phosphate. To our knowledge, β-elimination reactions releasing phosphate are unprecedented among the

AFS, indicating XcbC1 is a unique phosphatase. The subsequent decarboxylation and thiolation steps are less clear, although the annotations are again enlightening of at least likely elements of the next steps. XcbD1 groups most closely with members of the adenylosuccinate lyase family within the AFS, which catalyze the reversible elimination of adenosine monophosphate (AMP) from adenylosuccinate to form fumarate.

XcbE1 shares sequence features with PLP-dependent D-cysteine desulfhydrases, which allowed us to generate a hypothetical role for XcbE1 in CoM biosynthesis. Consumption of L- and D-cysteine to produce gaseous H_2S and pyruvate indicates that this enzyme may provide the thiol moiety from cysteine during CoM biosynthesis. One of the immediate difficulties towards resolving the pathway arises from the apparent lack of canonical redox or decarboxylase enzymes amongst the enzymes proposed in this work. Recall that both methanoarchaeal pathways require a decarboxylation reaction and general redox chemistry.

In this work, investigating the putative gene products of *xcbB1* and *xcbC1* by informatics, biochemical, and spectroscopic means led us to identify roles for XcbB1 and XcbC1 in bacterial CoM biosynthesis that involves a novel metabolite and activity for an enzyme from a well-characterized, large enzyme family. Through bioinformatics and some biochemical means, it is also possible to speculate on possible schemes for the final enzymatic reactions that yield CoM. We have demonstrated that bacterial CoM biosynthesis in *X. autotrophicus* Py2 is a PEP-dependent pathway that differs from that of the methanogens, and by elucidating the XcbB1 and XcbC1 reactions, we have made

significant strides towards understanding bacterial CoM biosynthesis which evaded characterization in previous years.

References

1 McBride, B. C. & Wolfe, R. S. A new coenzyme of methyl transfer, Coenzyme M. *Biochemistry* **10**, 2317-2324 (1971).

2 Taylor, C. D. & Wolfe, R. S. Structure and Methylation of Coenzyme M ($HSCH_2CH_2SO_3$). *Journal of Biological Chemistry* **15**, 4879-4885 (1974).

3 Taylor, C. D. & Wolfe, R. S. A Simplified Assay for Coenzyme M ($HSCH_2CH_2SO_3$). *Journal of Biological Chemistry* **15**, 4886-4890 (1974).

4 Balch, W. E. & Wolfe, R. S. New Approach to the Cultivation of Methanogenic Bacteria: 2-Mercaptoethanesulfonic Acid (HS-CoM)-Dependent Growth of *Methanobacterium ruminantium* in a Pressurized Atmosphere. *Applied and Environmental Microbiology* **32**, 781-791 (1976).

5 Taylor, C. D., McBride, B. C., Wolfe, R. S. & Bryant, M. P. Coenzyme M, Essential for Growth of a Rumen Strain of *Methanobacterium ruminantium*. *Journal of Bacteriology* **120**, 974-975 (1974).

6 Balch, W. E. & Wolfe, R. S. Specificity and biological distribution of coenzyme M (2-mercaptoethanesulfonic acid). *J Bacteriol* **137**, 256-263 (1979).

7 Shima, S., Warkentin, E., Thauer, R. K. & Ermler, U. Structure and function of enzymes involved in the methanogenic pathway utilizing carbon dioxide and molecular hydrogen. *Journal of bioscience and bioengineering* **93**, 519-530 (2002).

8 Neue, H.-U. Methane Emission from Rice Fields. *BioScience* **43**, 466-474, doi:10.2307/1311906 (1993).

9 Rouviere, P. E. & Wolfe, R. S. Novel biochemistry of methanogenesis. *J Biol Chem* **263**, 7913-7916 (1988).

10 Ermler, U., Grabarse, W., Shima, S., Goubeaud, M. & Thauer, R. K. Crystal structure of methyl-coenzyme M reductase: the key enzyme of biological methane formation. *Science* **278**, 1457-1462 (1997).

11 Olson, K. D., Chmurkowska-Cichowlas, L., McMahon, C. W. & Wolfe, R. S. Structural modifications and kinetic studies of the substrates involved in the final step of methane formation in Methanobacterium thermoautotrophicum. *J Bacteriol* **174**, 1007-1012 (1992).

12 Krishnakumar, A. M. *et al.* Getting a Handle on the Role of Coenzyme M in Alkene Metabolism. *Microbiology and Molecular Biology Reviews : MMBR* **72**, 445-456, doi:10.1128/MMBR.00005-08 (2008).

13 Scheller, S., Goenrich, M., Boecher, R., Thauer, R. K. & Jaun, B. The key nickel enzyme of methanogenesis catalyses the anaerobic oxidation of methane. *Nature* **465**, 606-608, doi:10.1038/nature09015 (2010).

14 Chen, S. L., Blomberg, M. R. & Siegbahn, P. E. How is methane formed and oxidized reversibly when catalyzed by Ni-containing methyl-coenzyme M reductase? *Chemistry* **18**, 6309-6315, doi:10.1002/chem.201200274 (2012).

15 Sluis, M. K. & Ensign, S. A. Purification and characterization of acetone carboxylase from Xanthobacter strain Py2. *Proceedings of the National Academy of Sciences* **94**, 8456-8461 (1997).

16 Boyd, J. M., Ellsworth, H. & Ensign, S. A. Bacterial Acetone Carboxylase Is a Manganese-dependent Metalloenzyme. *Journal of Biological Chemistry* **279**, 46644-46651, doi:10.1074/jbc.M407177200 (2004).

17 Allen, J. R. & Ensign, S. A. Purification to homogeneity and reconstitution of the individual components of the epoxide carboxylase multiprotein enzyme complex from Xanthobacter strain Py2. *J Biol Chem* **272**, 32121-32128 (1997).

18 Clark, D. D., Allen, J. R. & Ensign, S. A. Characterization of five catalytic activities associated with the NADPH:2-ketopropyl-coenzyme M [2-(2-ketopropylthio)ethanesulfonate] oxidoreductase/carboxylase of the Xanthobacter strain Py2 epoxide carboxylase system. *Biochemistry* **39**, 1294-1304 (2000).

19 Swaving, J., de Bont, J. A., Westphal, A. & de Kok, A. A novel type of pyridine nucleotide-disulfide oxidoreductase is essential for NAD+- and NADPH-dependent degradation of epoxyalkanes by Xanthobacter strain Py2. *Journal of Bacteriology* **178**, 6644-6646 (1996).

20 Westphal, A. H., Swaving, J., Jacobs, L. & Kok, A. d. Purification and characterization of a flavoprotein involved in the degradation of epoxyalkanes by Xanthobacter Py2. *European Journal of Biochemistry* **257**, 160-168, doi:10.1046/j.1432-1327.1998.2570160.x (2013).

21 van Ginkel, C. G. & de Bont, J. A. M. Isolation and characterization of alkene-utilizing Xanthobacter spp. *Archives of Microbiology* **145**, 403-407, doi:10.1007/BF00470879 (1986).

22 Allen, J. R. & Ensign, S. A. Carboxylation of epoxides to beta-keto acids in cell extracts of Xanthobacter strain Py2. *Journal of Bacteriology* **178**, 1469-1472 (1996).

23 Ensign, S. A., Small, F. J., Allen, J. R. & Sluis, M. K. New roles for CO2 in the microbial metabolism of aliphatic epoxides and ketones. *Arch Microbiol* **169**, 179-187 (1998).

24 Small, F. J. & Ensign, S. A. Carbon dioxide fixation in the metabolism of propylene and propylene oxide by Xanthobacter strain Py2. *Journal of Bacteriology* **177**, 6170-6175 (1995).

25 Allen, J. R., Clark, D. D., Krum, J. G. & Ensign, S. A. A role for coenzyme M (2-mercaptoethanesulfonic acid) in a bacterial pathway of aliphatic epoxide carboxylation. *Proc Natl Acad Sci U S A* **96**, 8432-8437 (1999).

26 Wade, D. R., Airy, S. C. & Sinsheimer, J. E. Mutagenicity of aliphatic epoxides. *Mutat Res* **58**, 217-223 (1978).

27 Archelas, A. & Furstoss, R. Synthesis of enantiopure epoxides through biocatalytic approaches. *Annu Rev Microbiol* **51**, 491-525, doi:10.1146/annurev.micro.51.1.491 (1997).

28 Besse, P. & Veschambre, H. Chemical and biological synthesis of chiral epoxides. *Tetrahedron* **50**, 8885-8927, doi:http://dx.doi.org/10.1016/S0040-4020(01)85362-X (1994).

29 Small, F. J. & Ensign, S. A. Carbon dioxide fixation in the metabolism of propylene and propylene oxide by Xanthobacter strain Py2. *J Bacteriol* **177**, 6170-6175 (1995).

30 Allen, J. R. & Ensign, S. A. Characterization of three protein components required for functional reconstitution of the epoxide carboxylase multienzyme complex from Xanthobacter strain Py2. *Journal of Bacteriology* **179**, 3110-3115 (1997).

31 Ensign, S. A., Hyman, M. R. & Arp, D. J. Cometabolic degradation of chlorinated alkenes by alkene monooxygenase in a propylene-grown Xanthobacter strain. *Applied and Environmental Microbiology* **58**, 3038-3046 (1992).

32 Krum, J. G. & Ensign, S. A. Heterologous expression of bacterial Epoxyalkane:Coenzyme M transferase and inducible coenzyme M biosynthesis in Xanthobacter strain Py2 and Rhodococcus rhodochrous B276. *J Bacteriol* **182**, 2629-2634 (2000).

33 Coleman, N. V. & Spain, J. C. Distribution of the coenzyme M pathway of epoxide metabolism among ethene- and vinyl chloride-degrading Mycobacterium strains. *Appl Environ Microbiol* **69**, 6041-6046 (2003).

34 Liu, X. & Mattes, T. E. Epoxyalkane:Coenzyme M Transferase Gene Diversity and Distribution in Groundwater Samples from Chlorinated-Ethene-Contaminated Sites. *Applied and Environmental Microbiology* **82**, 3269-3279, doi:10.1128/AEM.00673-16 (2016).

35 Allen, J. R. & Ensign, S. A. Two short-chain dehydrogenases confer stereoselectivity for enantiomers of epoxypropane in the multiprotein epoxide carboxylating systems of Xanthobacter strain Py2 and Nocardia corallina B276. *Biochemistry* **38**, 247-256, doi:10.1021/bi982114h (1999).

36 Mattes, T. E., Coleman, N. V., Spain, J. C. & Gossett, J. M. Physiological and molecular genetic analyses of vinyl chloride and ethene biodegradation in Nocardioides sp. strain JS614. *Arch Microbiol* **183**, 95-106, doi:10.1007/s00203-004-0749-2 (2005).

37 Coleman, N. V., Mattes, T. E., Gossett, J. M. & Spain, J. C. Phylogenetic and kinetic diversity of aerobic vinyl chloride-assimilating bacteria from contaminated sites. *Appl Environ Microbiol* **68**, 6162-6171 (2002).

38 Coleman, N. V. & Spain, J. C. Epoxyalkane: coenzyme M transferase in the ethene and vinyl chloride biodegradation pathways of mycobacterium strain JS60. *J Bacteriol* **185**, 5536-5545 (2003).

39 Danko, A. S., Saski, C. A., Tomkins, J. P. & Freedman, D. L. Involvement of coenzyme M during aerobic biodegradation of vinyl chloride and ethene by Pseudomonas putida strain AJ and Ochrobactrum sp. strain TD. *Appl Environ Microbiol* **72**, 3756-3758, doi:10.1128/aem.72.5.3756-3758.2006 (2006).

40 Hartmans, S., de Bont, J. A. & Harder, W. Microbial metabolism of short-chain unsaturated hydrocarbons. *FEMS Microbiol Rev* **5**, 235-264 (1989).

41 van Ginkel, C. G., Welten, H. G. J. & de Bont, J. A. M. Oxidation of Gaseous and Volatile Hydrocarbons by Selected Alkene-Utilizing Bacteria. *Applied and Environmental Microbiology* **53**, 2903-2907 (1987).

42 Ensign, S. A. Microbial metabolism of aliphatic alkenes. *Biochemistry* **40**, 5845-5853 (2001).

43 Small, F. J. & Ensign, S. A. Alkene Monooxygenase from Xanthobacter Strain Py2: PURIFICATION AND CHARACTERIZATION OF A FOUR-COMPONENT SYSTEM CENTRAL TO THE BACTERIAL METABOLISM OF ALIPHATIC ALKENES. *Journal of Biological Chemistry* **272**, 24913-24920, doi:10.1074/jbc.272.40.24913 (1997).

44 Zhou, N.-Y., Jenkins, A., Chan Kwo Chion, C. K. N. & Leak, D. J. The Alkene Monooxygenase from Xanthobacter Strain Py2 Is Closely Related to Aromatic Monooxygenases and Catalyzes Aromatic Monohydroxylation of Benzene, Toluene, and Phenol. *Applied and Environmental Microbiology* **65**, 1589-1595 (1999).

45 Tallant, T. C., Paul, L. & Krzycki, J. A. The MtsA subunit of the methylthiol:coenzyme M methyltransferase of Methanosarcina barkeri catalyses both half-reactions of corrinoid-dependent dimethylsulfide: coenzyme M methyl transfer. *J Biol Chem* **276**, 4485-4493, doi:10.1074/jbc.M007514200 (2001).

46 Boyd, J. M. & Ensign, S. A. Evidence for a metal-thiolate intermediate in alkyl group transfer from epoxypropane to coenzyme M and cooperative metal ion binding in epoxyalkane:CoM transferase. *Biochemistry* **44**, 13151-13162, doi:10.1021/bi0505619 (2005).

47 Krum, J. G., Ellsworth, H., Sargeant, R. R., Rich, G. & Ensign, S. A. Kinetic and Microcalorimetric Analysis of Substrate and Cofactor Interactions in Epoxyalkane:CoM Transferase, a Zinc-Dependent Epoxidase. *Biochemistry* **41**, 5005-5014, doi:10.1021/bi0255221 (2002).

48 Jörnvall, H. *et al.* Short-chain dehydrogenases/reductases (SDR). *Biochemistry* **34**, 6003-6013, doi:10.1021/bi00018a001 (1995).

49 Kallberg, Y., Oppermann, U., Jornvall, H. & Persson, B. Short-chain dehydrogenases/reductases (SDRs). *Eur J Biochem* **269**, 4409-4417 (2002).

50 Krishnakumar, A. M., Nocek, B. P., Clark, D. D., Ensign, S. A. & Peters, J. W. Structural Basis for Stereoselectivity in the (R)- and (S)-Hydroxypropylthioethanesulfonate Dehydrogenases†,‡. *Biochemistry* **45**, 8831-8840, doi:10.1021/bi0603569 (2006).

51 Clark, D. D. & Ensign, S. A. Characterization of the 2-[(R)-2-Hydroxypropylthio]ethanesulfonate Dehydrogenase from Xanthobacter Strain Py2: Product Inhibition, pH Dependence of Kinetic Parameters, Site-Directed Mutagenesis, Rapid Equilibrium Inhibition, and Chemical Modification. *Biochemistry* **41**, 2727-2740, doi:10.1021/bi0118005 (2002).

52 Pai, E. F. Variations on a theme: the family of FAD-dependent NAD(P)H-(disulphide)-oxidoreductases. *Current Opinion in Structural Biology* **1**, 796-803, doi:http://dx.doi.org/10.1016/0959-440X(91)90181-R (1991).

53 Pandey, A. S., Mulder, D. W., Ensign, S. A. & Peters, J. W. Structural basis for carbon dioxide binding by 2-ketopropyl coenzyme M oxidoreductase/carboxylase. *FEBS Letters* **585**, 459-464, doi:10.1016/j.febslet.2010.12.035 (2011).

54 Nocek, B. *et al.* Structural Basis for CO2 Fixation by a Novel Member of the Disulfide Oxidoreductase Family of Enzymes, 2-Ketopropyl-Coenzyme M Oxidoreductase/Carboxylase. *Biochemistry* **41**, 12907-12913, doi:10.1021/bi026580p (2002).

55 Kofoed, M. A., Wampler, D. A., Pandey, A. S., Peters, J. W. & Ensign, S. A. Roles of the Redox-Active Disulfide and Histidine Residues Forming a Catalytic Dyad in Reactions Catalyzed by 2-Ketopropyl Coenzyme M Oxidoreductase/Carboxylase. *Journal of Bacteriology* **193**, 4904-4913, doi:10.1128/JB.05231-11 (2011).

56 Prussia, G. A. *et al.* Substitution of a conserved catalytic dyad into 2-KPCC causes loss of carboxylation activity. *FEBS Letters* **590**, 2991-2996, doi:10.1002/1873-3468.12325 (2016).

57 Argyrou, A. & Blanchard, J. S. Flavoprotein disulfide reductases: advances in chemistry and function. *Prog Nucleic Acid Res Mol Biol* **78**, 89-142, doi:10.1016/s0079-6603(04)78003-4 (2004).

58 Sauer, K. & Thauer, R. K. Methyl-coenzyme M formation in methanogenic archaea. *European Journal of Biochemistry* **267**, 2498-2504, doi:10.1046/j.1432-1327.2000.01245.x (2000).

59 Pandey, A. S., Nocek, B., Clark, D. D., Ensign, S. A. & Peters, J. W. Mechanistic Implications of the Structure of the Mixed-Disulfide Intermediate of the Disulfide Oxidoreductase, 2-Ketopropyl-Coenzyme M Oxidoreductase/Carboxylase. *Biochemistry* **45**, 113-120, doi:10.1021/bi051518o (2006).

60 Graham, D. E., Taylor, S. M., Wolf, R. Z. & Namboori, S. C. Convergent evolution of coenzyme M biosynthesis in the Methanosarcinales: cysteate synthase evolved from an ancestral threonine synthase. *Biochem J* **424**, 467-478, doi:10.1042/bj20090999 (2009).

61 Graham, D. E., Graupner, M., Xu, H. & White, R. H. Identification of coenzyme M biosynthetic 2-phosphosulfolactate phosphatase. A member of a new class of Mg(2+)-dependent acid phosphatases. *Eur J Biochem* **268**, 5176-5188 (2001).

62 Graham, D. E., Xu, H. & White, R. H. Identification of coenzyme M biosynthetic phosphosulfolactate synthase: a new family of sulfonate-biosynthesizing enzymes. *J Biol Chem* **277**, 13421-13429, doi:10.1074/jbc.M201011200 (2002).

63 Graupner, M., Xu, H. & White, R. H. Identification of an archaeal 2-hydroxy acid dehydrogenase catalyzing reactions involved in coenzyme biosynthesis in methanoarchaea. *J Bacteriol* **182**, 3688-3692 (2000).

64 Graupner, M., Xu, H. & White, R. H. Identification of the gene encoding sulfopyruvate decarboxylase, an enzyme involved in biosynthesis of coenzyme M. *J Bacteriol* **182**, 4862-4867 (2000).

65 White, R. H. Biosynthesis of coenzyme M (2-mercaptoethanesulfonic acid). *Biochemistry* **24**, 6487-6493, doi:10.1021/bi00344a027 (1985).

66 White, R. H. Characterization of the enzymic conversion of sulfoacetaldehyde and L-cysteine into coenzyme M (2-mercaptoethanesulfonic acid). *Biochemistry* **27**, 7458-7462, doi:10.1021/bi00419a043 (1988).

67 White, R. H. Intermediates in the biosynthesis of coenzyme M (2-mercaptoethanesulfonic acid). *Biochemistry* **25**, 5304-5308, doi:10.1021/bi00366a047 (1986).

68 Graham, D. E. & White, R. H. Elucidation of methanogenic coenzyme biosyntheses: from spectroscopy to genomics. *Nat Prod Rep* **19**, 133-147 (2002).

69 Wise, E. L., Graham, D. E., White, R. H. & Rayment, I. The structural determination of phosphosulfolactate synthase from Methanococcus jannaschii at 1.7-A resolution: an enolase that is not an enolase. *J Biol Chem* **278**, 45858-45863, doi:10.1074/jbc.M307486200 (2003).

70 Liu, Y., Sieprawska-Lupa, M., Whitman, W. B. & White, R. H. Cysteine Is Not the Sulfur Source for Iron-Sulfur Cluster and Methionine Biosynthesis in the Methanogenic Archaeon Methanococcus maripaludis. *The Journal of Biological Chemistry* **285**, 31923-31929, doi:10.1074/jbc.M110.152447 (2010).

71 Weinstein, C. L. & Griffith, O. W. Cysteinesulfonate and beta-sulfopyruvate metabolism. Partitioning between decarboxylation, transamination, and reduction pathways. *J Biol Chem* **263**, 3735-3743 (1988).

72 Helgadottir, S., Rosas-Sandoval, G., Soll, D. & Graham, D. E. Biosynthesis of phosphoserine in the Methanococcales. *J Bacteriol* **189**, 575-582, doi:10.1128/jb.01269-06 (2007).

73 Krum, J. G. & Ensign, S. A. Evidence that a linear megaplasmid encodes enzymes of aliphatic alkene and epoxide metabolism and coenzyme M (2-mercaptoethanesulfonate) biosynthesis in Xanthobacter strain Py2. *J Bacteriol* **183**, 2172-2177, doi:10.1128/jb.183.7.2172-2177.2001 (2001).

74 Broberg, C. A. & Clark, D. D. Shotgun proteomics of Xanthobacter autotrophicus Py2 reveals proteins specific to growth on propylene. *Arch Microbiol* **192**, 945-957, doi:10.1007/s00203-010-0623-3 (2010).

CHAPTER TWO

COENZYME M BIOSYNTHESIS IN BACTERIA INVOLVES PHOSPHATE ELIMINATION BY A UNIQUE MEMBER OF THE ASPARTASE/FUMARASE SUPERFAMILY

Contribution of Authors and Co-Authors

Manuscript in Ch. 2, Appendix B

Author: Sarah E. Partovi

Contributions: Experimental design and interpretation, involvement in all experiments

Co-Author: Florence Mus

Contributions: Q-TOF MS

Co-Author: Andrew E. Gutknecht

Contributions: XcbC1 molybdenum blue studies

Co-Author: Hunter A. Martinez

Contributions: XcbE1 studies

Co-Author: Brian P. Tripet

Contributions: ^{1}H-NMR

Co-Author: B. Mark Lange

Contributions: Q-TOF MS

Co-Author: Jennifer L. DuBois

Contributions: Experimental design and interpretation

Co-author: John W. Peters

Contributions: Experimental design and interpretation

Manuscript Information Page

Sarah E. Partovi, Florence Mus, Andrew E. Gutknecht, Hunter A. Martinez, Brian P. Tripet, Bernd Markus Lange, Jennifer L. DuBois, and John W. Peters

Journal of Biological Chemistry

Status of Manuscript:
____ Prepared for submission to a peer-reviewed journal
_**X**_ Officially submitted to a peer-review journal
____ Accepted by a peer-reviewed journal
____ Published in a peer-reviewed journal

American Society for Biochemistry and Molecular Biology

Abstract

Coenzyme M (CoM) was thought to be present solely in methanogenic archaea for nearly 30 years. In the late 1990s, CoM was reported to play a role in bacterial propene metabolism, though no biosynthetic pathway for CoM has yet been discovered in any bacterium. We identified four putative CoM biosynthetic enzymes encoded by *xcbB1*, *C1*, *D1*, and *E1*, through bioinformatics and proteomic approaches in the metabolically versatile bacterium, *Xanthobacter autotrophicus* Py2. Only XcbB1 is homologous to a known CoM biosynthetic enzyme (ComA), indicating that the proposed pathway is unique to bacteria. We verified that the ComA homolog produces phosphosulfolactate from phosphoenolpyruvate (PEP), demonstrating that bacterial CoM biosynthesis is initiated in an analogous fashion to the PEP-dependent methanogenic archaeal pathway. Informatics analysis showed XcbC1 and D1 are members of the aspartase/fumarase superfamily (AFS), and XcbE1 is a pyridoxal 5'-phosphate-containing enzyme with homology to D-cysteine desulfhydrases. Known AFS members catalyze β-elimination reactions of succinyl-containing substrates, yielding fumarate as the common unsaturated elimination product. We demonstrated that XcbC1 catalyzes a β-elimination reaction on the substrate phosphosulfolactate to yield inorganic phosphate and a novel metabolite, sulfoacrylic acid. β-elimination reactions releasing phosphate are unprecedented among the AFS, indicating XcbC1 is a unique phosphatase. Direct demonstration of activities for XcbB1 and C1 strengthens their hypothetical assignment to a CoM biosynthetic pathway, and suggests functions for XcbD1 and E1. These results

allow us to propose a complete pathway for CoM, unique to the bacterial kingdom of life, for the first time.

Introduction

Coenzyme M (2-mercaptoethanesulfonate, CoM) was once thought to be exclusive to methanogenesis in archaea, where it functions as a C1 carrier and plays a key role in the biosynthesis of methane gas (1-5). In the late 1990s, CoM was discovered to serve as a C3 carrier in a bacterial pathway for alkene metabolism in the proteobacterium *Xanthobacter autotrophicus* Py2 (6). Since then, other bacterial species from the Actinobacterial phylum have also been shown to use CoM in the metabolism of alkenes such as ethylene (6-11). In *X. autotrophicus* Py2, propylene is converted to acetoacetate that is subsequently funneled into the TCA cycle in the form of two molecules of acetyl CoA, where it serves as a carbon source for growth. The pathway begins with the epoxidation of propylene by an NADH-dependent alkene monooxygenase, forming propylene oxide. This is followed by nucleophilic attack by CoM to break the epoxide ring and form an enantiomeric mixture of *R*- and *S*-hydroxypropyl-CoM, catalyzed by epoxyalkane: CoM transferase (12-17). CoM then functions as a carrier, orienting *R*- and *S*-hydroxypropyl groups as oxidation substrates for a pair of stereoselective short chain dehydrogenases, yielding 2-ketopropyl-CoM (16-18). In the final step of the pathway, CoM again serves to orient the 2-ketopropyl group for reductive cleavage and carboxylation, forming acetoacetate and free CoM (16,17,19-22). CoM in essence serves

an analogous role in propylene metabolism as it has in methanogenesis, in promoting the proper orientation of these small organic substrates (16).

Methanogens have two known pathways for CoM synthesis, in which the carbon backbone for CoM is derived either from phosphoenolpyruvate (PEP) or L-phosphoserine (Scheme 2.1).

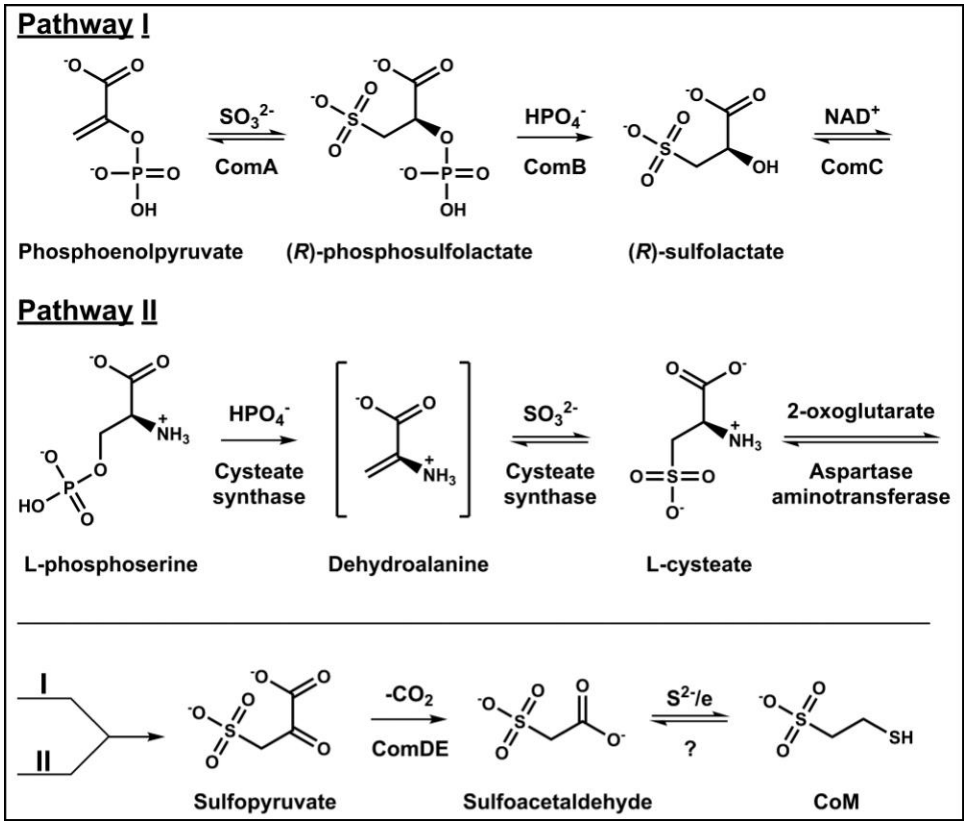

Scheme 2.1. The PEP-dependent and L-phosphoserine dependent pathways to CoM in methanoarchaea. Pathway I and Pathway II respectively are depicted. Both pathways culminate in production of sulfopyruvate which undergoes decarboxylation and reduction plus thiol addition to yield CoM.

The PEP-dependent pathway is initiated by a phosphosulfolactate synthase (ComA), which catalyzes the nucleophilic addition of sulfite to PEP (23,24). The phosphosulfolactate product subsequently undergoes oxidative dephosphorylation to

yield sulfopyruvate (25-28). Decarboxylation of sulfopyruvate, yielding sulfoacetaldehyde, is presumably followed by reduction and thiol addition to generate CoM (29,30). The L-phosphoserine-dependent pathway begins with the concerted elimination of phosphate and addition of sulfite to generate L-cysteate. L-cysteate is subsequently transaminated to form the common intermediate with the PEP dependent pathway, sulfopyruvate (31), after which stage the pathways are presumed to follow the same chemical steps to CoM.

Though it is essential for alkene metabolism, a bacterial pathway for CoM synthesis has never been described. The genes responsible for alkene metabolism in the bacterium *X. autotrophicus* Py2 are located on a 320 kb linear megaplasmid (pXAUT01) (Figure 2.1) (32,33).

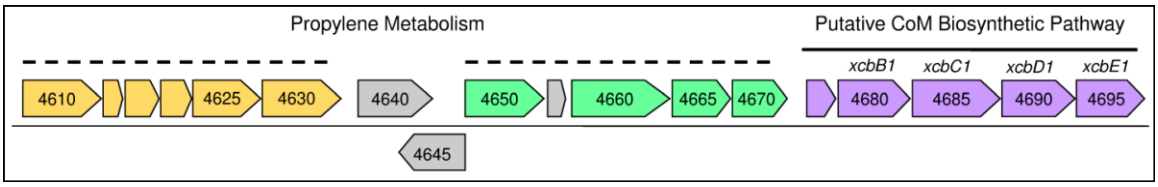

Figure 2.1 The 320 kb linear megaplasmid of *X. autotrophicus* Py2 contains the genes for the putative CoM biosynthetic pathway (purple) immediately downstream from the genes that encode the enzymes responsible for propylene metabolism. Alkene monooxygenase subunits are yellow and the remaining four enzymes involved in transforming propylene oxide to acetoacetate are shown in green. Alkene-related functions for the open reading frames in gray have not been assigned. The locus tags shown are truncated for clarity, and contain the prefix “xaut_RS2” in the pXAUT01 plasmid.

Proteomic experiments showed that proteins encoded in a gene cluster adjacent to the alkene metabolizing genes were co-expressed with enzymes involved in propylene metabolism under conditions of propylene-dependent growth (14,32). These experiments also revealed additional copies of the same genes. Only the cluster directly adjacent to the

alkene metabolizing genes is considered in this work, and these are designated as *xcbB1*, *C1*, *D1*, and *E1* (XAUT_RS24680, RS24685, RS24690, and RS24695, respectively).

One of the genes in the cluster (*xcbB1*) is a homolog of *comA* suggesting that the bacterial pathway for CoM biosynthesis, is PEP-dependent. Additional genes within the cluster, however, are not similar to those from either methanoarchaeal pathways, suggesting that the bacterial CoM is synthesized via a chemically distinct series of reactions. The adjacent *xcbC1* gene encodes a member of the aspartase/fumarase superfamily (AFS). Enzyme families within this superfamily include the argininosuccinate lyases (ASL)/δ2-crystallins, with which the XcbC1 gene product has the closest similarity, as well as class II fumarases, aspartases, and adenylosuccinate lyases (ADL). All of these AFS members catalyze β-elimination reactions that result in the formation of an unsaturated organic product (34).

In this work, we demonstrate that the ComA homolog XcbB1 catalyzes the conversion of PEP to phosphosulfolactate. We also show that XcbC1 then catalyzes a β-elimination using phosphosulfolactate as the substrate, releasing phosphate and sulfoacrylic acid as the analogous unsaturated product. This is a new activity for a member of the AFS and a highly unusual mechanism for biological dephosphorylation. Based on the confirmation of these two activities, bioinformatic analyses of the sequences for XcbD1 and E1, and partial biochemical characterization of XcbE1, we can now propose a complete biosynthetic pathway for CoM biosynthesis in bacteria.

Methods

Growth of *Xanthobacter autotrophicus* Py2

Cells were grown as previously described in phosphate buffer, assorted nutrients, and trace minerals at 30 °C with shaking (180 rpm) in Erlenmeyer flasks sealed with rubber septum stoppers(68,69). The cells in liquid medium were sparged with compressed air for ~15 min and propene gas was injected into the headspace (10% volume) every 12 hours. The cultures were allowed to reach an optical density at 600 nm (OD_{600}) of ~1-1.5 before harvesting by centrifugation at 6000 x *g* for 10 minutes. Aliquots of 5-10 mL were reserved for genomic DNA extraction using the DNeasy Blood and Tissue protocol for gram-negative bacteria.

Amplification of Genes for Putative CoM Biosynthesis

Sequences for the putative biosynthetic operon were obtained from the NCBI database file for the pXAUT01 megaplasmid. Primers (Integrated DNA Technologies, San Diego, CA) were designed for *xcbB1* (XAUT_RS24680), *xcbC1* (XAUT_RS24685), and *xcbE1* (XAUT_RS24695) using the respective locus tags given in parentheses (Table S1). Restriction sites were added in order to clone each gene with an added N-terminal His-tag into a Duet Expression System (Novagen). The forward and reverse restriction sites for each ORF were: XcbB1, Sac1/Nde1; XcbC1, BamHI/BglII; XcbE1, PstI/EcoRV. Each amplicon was initially cloned into a pGEM-T vector and transformed into JM109 competent cells for propagation, before being cloned into a Duet vector. XcbB1 and XcbE1 weres inserted into multiple cloning site 1 (MCS1) of individual pETDuet-1

(Amp^R) vectors, while XcbC1 and was cloned under MCS1 of pACYCDuet-1 (Cm^R). Sequences were verified via Davis Sequencing (Davis, CA).

Expression and Purification of Putative CoM Biosynthesis Gene Products

BL21(DE3) competent cells were transformed with each construct, XcbB1-pETDuet-1, XcbC1-pACYCDuet-1, and XcbE1-pETDuet-1; and cells were grown on lysogeny broth (LB) agar plates supplemented with ampicillin (Amp) (0.1 mg/mL) or chloramphenicol (Cm) (0.034 mg/mL), as specified for each construct. A single colony was used to inoculate an overnight culture in liquid LB+Amp or Cm medium. Expression was initiated with 10% volume of the overnight culture (XcbE1 expression included 40 µM pyridoxine) and incubated at 37°C with shaking at 250 rpm until the culture reached an OD_{600} of 0.6-0.8. Protein expression was induced with 1 mM IPTG and the cells moved to a 30°C incubator with shaking at 180 rpm. Protein expression proceeded for 3 h before the cells were harvested by centrifugation (7500 x *g*, 10 min) followed by flash freezing of the pellets in liquid nitrogen.

For purification, frozen cell pellets were resuspended in lysis buffer (20 mM Tris, 500 mM NaCl, 5 mM imidazole, pH 8) and homogenized with the addition of lysozyme, DNase, and PMSF. Cell pellets from cultures larger than 1 L were lysed using a microfluidizer (M-110L Microfluidics Corporation, Newton, MA). Lysates were cleared by centrifugation: 45,000 x *g* for 30 min when using a gravity flow column, or 105,000 x *g* for 1 h prior to fast protein liquid chromatography (FPLC, Bio-Rad). The Ni-NTA columns were equilibrated to the lysis buffer prior to loading the cleared lysate. For FPLC elution, a 75 mL gradient from 0-100% elution buffer was used. The elution buffer

contained 20 mM Tris, 500 mM NaCl, 300 mM imidazole, and 20% glycerol. SDS-PAGE and Western blot anti-His tag antibodies (alkaline phosphatase conjugated monoclonal immunoglobulin, from hybridoma clone His-1 from SIGMA catalog # A5588. Lot # 096M4841V) were used to determine the purity of the protein as well as integrity of the His-tag. Buffer exchange of the pure protein into imidazole-free pH 8 buffer (20 mM Tris, 100 mM NaCl) was carried out via centrifuge filtration as a final step prior to storage at -80 °C in 10% glycerol.

Determining Sulfite Uptake by the XcbB1-Catalyzed Reaction

An assay using a fluorescent sulfite indicator was adapated from prior methods (23). Reaction mixtures contained 100 mM Tris (pH 8), 100 mM NaCl, 5 mM $MgCl_2$, 1 mM $NaHSO_3$, and 1 mM PEP in 50 µL. The assay mixture was incubated at 30°C for 5 min before addition of 0.1 mg XcbB1 enzyme in 50 mM Tris, 50 mM NaCl, and 20% glycerol (pH 8). The reaction was incubated at 30°C for a further 5 min prior to addition of 5 µL of terminating solution (0.5 M arginine, 0.1 M EDTA adjusted to pH 12.8 with NaOH). Post-termination, 3 µL of 50 mM monobromobimane (mBBr) dissolved in acetonitrile was added to the assay. The reaction was then incubated in the dark for 15 min at room temperature and diluted to 1 mL using 50 mM glycine, 10 mM EDTA (pH 10). Fluorescence of the sulfite-mBBr adducts was measured on a Cary Eclipse fluorescence spectrophotometer: excitation wavelength 410 nm, emission 480 nm, 350V photomultiplier tube. Standard curves were generated using a gradient from 0-1 mM $NaHSO_3$ in the reaction buffers. Data fit to linear equations (Kaleidagraph) were used to calculate concentrations of sulfite in enzymatic reactions.

Measuring Inorganic Phosphate Production by the XcbC1-Catalyzed Reaction

Phosphosulfolactate produced by XcbB1 was used as the substrate for XcbC1 in a coupled reaction, and the resulting inorganic phosphate quantified. Samples containing 50 mM Tris (pH 8), 50 mM NaCl, 5 mM $MgCl_2$, 0.1 mg XcbB1 enzyme, 1 mM sulfite, 1 mM PEP, and dH_2O in a final volume of 500 µL were incubated at 30°C for 30 min, followed by incubation at 95°C for 10 min to stop XcbB1 activity. The samples were centrifuged for 10 min at 14,000 x *g* and the supernatant was used for the subsequent reaction. To the supernatant, 0.1 mg XcbC1 was added to begin consumption of phosphosulfolactate. The reaction was allowed to continue for an additional 30 min before termination as with XcbB1. The supernatant was then used for phosphate determination.

Formation of inorganic orthophosphate can be detected using ammonium molybdate to form colored molybdenum blue complexes (25,70). A procedure was adapted from prior methods (71,72). Briefly: to a 500 µL sample, 100 µL of 2.5 M H_2SO_4 was added, followed by 100 µL of 2.5% ammonium molybdate. 10 µL of reducing solution (0.2 g 1-amino-2-naphthol-4-sulfonic acid, 1.2 g sodium bisulfite, and 1.2 g sodium sulfite in 100 mL) was added, followed by distilled H_2O to bring the volume to 1 mL. The samples were thoroughly mixed, then incubated at 50°C for 15 min. Absorbance was monitored at 700 nm using a Thermo Spectronic Biomate 3. Concentrations of phosphate were calculated from a standard curve generated using KH_2PO_4 (0-1 mM).

Determination of XcbE1 Activity with an Assay for H_2S Formation

The production of H_2S can be detected using a method that converts H_2S to methylene blue with the addition of *N'*,*N'*-dimethyl-*p*-phenylenediamine dihydrochloride (DPPD) 20 mM in 7.2 M HCl, and 30 mM $FeCl_3$ in 1.2 M HCl (73). Enzymatic assays were conducted in sealed crimp vials containing 250 µL reaction buffer (50 mM Tris, 50 mM NaCl, pH 8), 0.1mg XcbE1, and dH_2O to 450 µL. 50 µL of 10 mM L-cysteine was injected through the septum to initiate the reaction. Reactions were incubated for 1h at 30°C, followed by quench and derivatization with 100 µL each of DPPD and acidified $FeCl_3$. Color development proceeded for 30 min at room temperature. Absorption was measured at 670 nm and referenced to a Na_2S standard (0-150 µM) generated under identical conditions.

Mass Spectrometric Analysis of Reaction Products

Sample buffers were prepared at 1 mM Tris, 1 mM $MgCl_2$, pH 8 to avoid ion suppression. XcbB1 (0.1 mg) was incubated with 5 mM PEP and 5 mM sulfite for 45 mins at 30°C prior to molecular weight cut-off filtration to remove enzyme. To determine if phosphosulfolactate was consumed by XcbC1, 0.1 mg XcbC1 was added to the quenched XcbB1 reactions and allowed to react for 20 or 45 mins. Samples were quenched by molecular weight cut-off filtration, and were analzyed by Q-TOF MS without additional derivatization or extractions.

Q-TOF MS

Analytes were detected with a 6530 series Q-TOF MS, equipped with an electrospray ionization source (operated in negative polarity mode), and data were analyzed with the MassHunter Workstation software version B.03.01 (Agilent Technologies) Samples were introduced via direct injection.

Time Resolved ^{1}H-NMR

Time-resolved ^{1}H-NMR experiments were performed using a 600 MHz (^{1}H Larmor Frequency) Bruker AVANCE III solution NMR spectrometer equipped with a helium-cooled ^{1}H-optimized, inverse detection, (^{1}H, ^{15}N, ^{13}C) TCI cryoprobe (Bruker Corporation, Billerica, MA). Samples were prepared by first diluting 0.1 mg XcbB1 in 550 µL buffer (50 mM Tris, 50 mM NaCl, 5 mM $MgCl_2$, 10% v/v D_2O pH 8), followed by an initial scan to determine baseline peaks. The substrates PEP and bisulfite were then added to the reaction at varying concentrations (minimum 2 mM PEP for ease of detection) and monitored over the course of 30 mins, with NMR experiments every 2 mins. 1D ^{1}H NMR spectra were acquired using the Bruker supplied noesygppr1d pulse sequence with 32 scans, a spectral width of 12 ppm and data collected into 32K data points. Spectral processing and analysis was performed using the Topspin™ software. Approximately 0.1 mg XcbC1 was added to the reaction upon completion of the XcbB1 time course. The reaction was again monitored over 30 mins with scans every 2 mins as above.

Phylogeny and Homology Modeling

27 diverse members of the AFS including 6 argininosuccinate lyase family members were used to construct the maximum-likelihood tree on MEGA 6.06 with 100 bootstrap replications. The resulting tree was prepared for publication using FigTree v1.4.2. Homology models for XcbC1 were constructed with SWISSMODEL, using the crystal structure of T161D variant duck δ2-crystallin with bound argininosuccinate (1TJW, 76% query coverage, 28% ID).

Results and Discussion

Sequence Analyses Identify Gene Families and Suggest Possible Roles for Putative CoM Biosynthetic Genes

The four putative CoM biosynthetic genes under study have deduced amino acid sequence similarities to characterized enzymes, providing clues into the likely chemical steps associated with bacterial CoM biosynthesis. The *xcbB1* gene is homologous to *comA*, which encodes the phosphosulfolactate synthase that initiates PEP-dependent CoM biosynthetic pathway in methanogens. The pathway in *X. autotrophicus* Py2 is consequently presumed to be PEP-dependent. The adjacent *xcbC1* and *xcbD1* genes encode members of the AFS. Enzyme families within this superfamily catalyze reversible β-elimination reactions that result in the formation of an unsaturated organic product (35-53). The last gene in the cluster, *xcbE1,* encodes a PLP-dependent enzyme homologous to D-cysteine desulfhydrases. Using these preliminary sequence analyses, hypothetical roles for the enzymes in CoM biosynthesis have been proposed (Scheme 2.2).

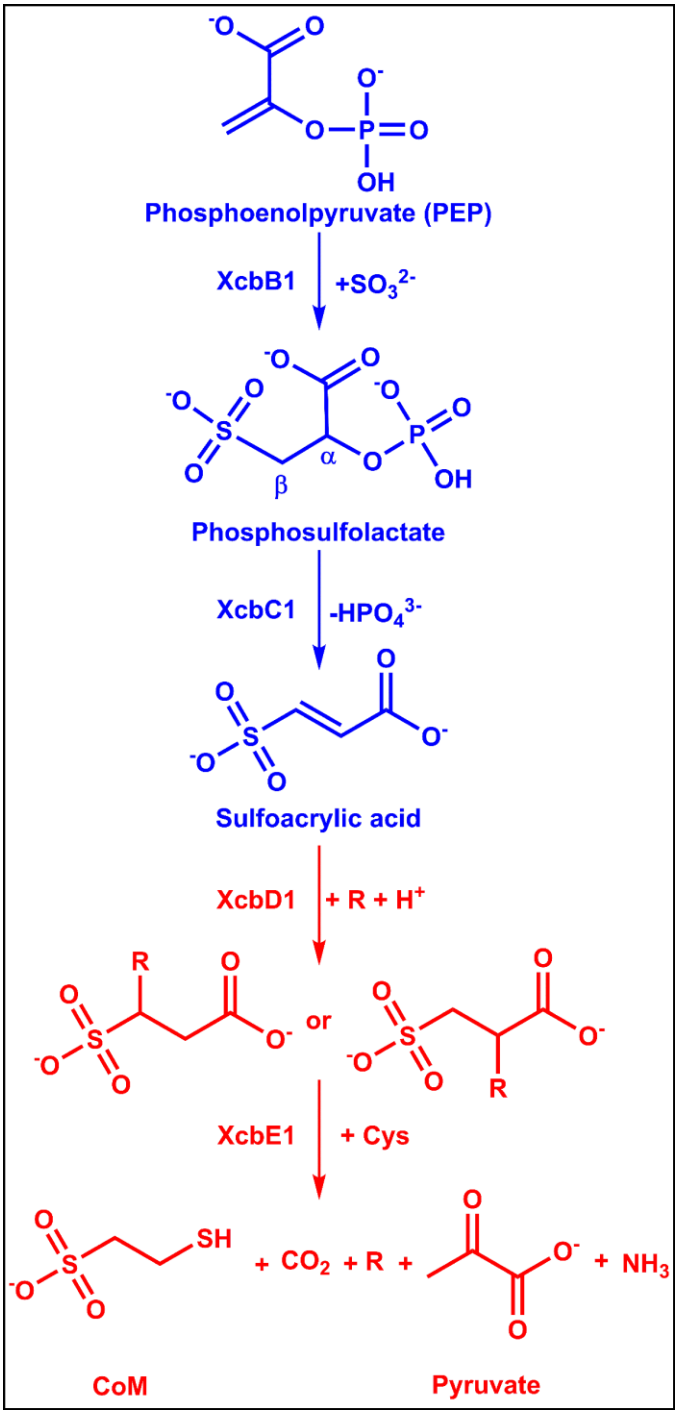

Scheme 2.2. Proposed bacterial pathway for CoM biosynthesis. Steps shown in blue are supported by data reported in this study. Steps shown in red are proposed based on bioinformatics analyses. Cysteine desulfhydrase activity has additionally been demonstrated for XcbE1 in the presence of either L- or D-Cys.

Homology between XcbB1 and ComA suggested that the pathway may begin with the addition of sulfite to PEP to form phosphosulfolactate. Conversion of this pathway intermediate to CoM requires net dephosphorylation, decarboxylation, and thiolation steps. The annotation of XcbC1 and XcbD1 as members of the AFS provides clear clues about the most logical trajectory by which these steps might occur. Within the AFS, XcbC1 has the strongest homology to the arginosuccinate lyases (Figure 2.2). Enzymes in this family catalyze the reversible β-elimination of argininosuccinate through general base proton abstraction from the C_β of the succinate moiety, yielding arginine and fumarate (35). Phosphosulfolactate is a loose structural analog of arginosuccinate, containing a potential proton abstraction site at the C_β position relative to the phosphoryl group. A proton abstraction analogous to that catalyzed by argininosuccinate lyases would lead to elimination of phosphate and formation of a carbon-carbon double bond, yielding sulfoacrylic acid. This product, in turn, is a structural analog of fumarate, the coproduct of the β-elimination of arginine.

The subsequent decarboxylation and thiolation steps are less clear, although the annotations are again enlightening of at least likely elements of the next steps. XcbD1 groups most closely with members of the adenylosuccinate lyase family within the AFS (Figure 2.2), which catalyze the reversible elimination of adenosine monophosphate (AMP) from adenylosuccinate to form fumarate (52). We propose that the most likely role for XcbD1 is therefore in catalyzing an analogous reaction in the addition direction, in which a substrate is added across the double bond.

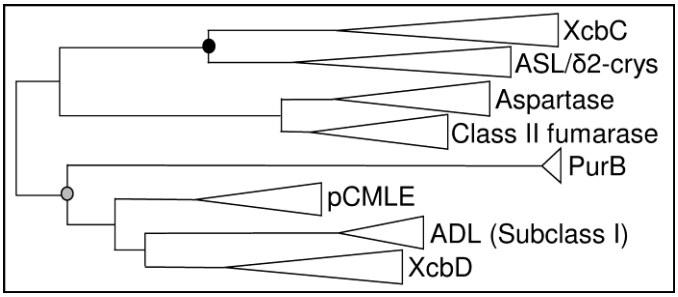

Figure 2.2. Bioinformatics analysis of XcbC1 (WP_011992986) and XcbD1 (WP_011992987) sequences identifies the AFS families to which each belongs. The maximum-likelihood tree (100 bootstrap reps) was constructed for XcbC1 and appears to show two sub-branches for argininosuccinate-lyase type enzymes. Bootstrap values are shown only for nodes of relevance to this work, as indicated by circles; ≥90 (black), 80-89 (grey). The canonical argininosuccinate lyase/δ2-crystallin enzymes appear to occupy a separate clade from the XcbC-type enzymes that may be involved in a pathway for CoM biosynthesis, and XcbD appears to form an additional subgroup in the adenylosuccinate lyase clade.

Attempts to use AMP as a substrate have not resulted in formation of adenylated product (data not shown). Addition of H^+ and an as-yet undetermined co-substrate across the sulfoacrylic acid double bond (Scheme 2.2) would yield the putative substrate for XcbE1, the final enzyme in the pathway. XcbE1is homologous to pyridoxal 5'-phosphate (PLP)-dependent D-cysteine desulfhydrases that catalyze the α,β-elimination of D-Cys to yield H_2S, pyruvate, and ammonia (54). We tested XcbE1 for desulfhydrase activity via H_2S formation assays and found that both D- and L-Cys isomers were effective substrates, where XcbE1 specific activity was 27.31± 2.32 nmol $H_2S/min^{-1}mg\text{-}XcbE1^{-1}$ for L-Cys and 5.04 ± 1.95 nmol $H_2S/min^{-1}mg\text{-}XcbE1^{-1}$for D-Cys (Fig B.S.1). It is attractive to propose therefore that XcbE1 supplies cysteine-derived sulfur that is ultimately incorporated into CoM. It is attractive to propose therefore that XcbE1 supplies cysteine-derived sulfur that is ultimately incorporated into CoM. However, without knowing the

product of the XcbD1 reaction, the cosubstrate for XcbE1 the mechanism of thiolation cannot yet be determined. In addition, the substrate of XbcE1 will also require decarboxylation to arrive at the CoM product. PLP-dependent enzymes catalyze a number of reactions, including decarboxylation, transamination, racemization, and elimination/replacement reactions of a variety of predominantly amino acid substrates (55,56). Many PLP-dependent enzyme reactions moreover share common intermediates, and several enzymes have been shown to be bifunctional, catalyzing combinations of reactions that utilize the basic PLP reaction chemistry (55). Examples include the decarboxylation and transamination catalyzed by dialkylglycine decarboxylase and the γ-elimination/β-replacement catalyzed by threonine synthase (57,58). It is therefore conceivable that XcbE1 could be a bifunctional PLP enzyme, catalzying a more complicated final step coupling for example thiolation and decarboxylation in the production of CoM (Scheme 2.2).

XcbB1 Catalyzes the Conversion of Phosphoenolpyruvate to Phosphosulfolactate

To begin to test these proposed steps of the pathway, we first examined the ComA homolog, XcbB1. ComA catalyzes the addition of sulfite to PEP to yield phosphosulfolactate, an unusual metabolite that, according to currently annotated KEGG pathway assignments, is unique to the methanogen PEP-dependent CoM biosynthetic pathway. An active site Mg^{2+} in ComA coordinates the enol form of PEP, facilitating nucleophilic addition of sulfite and protonation of the adduct by a conserved active site lysine to form phosphosulfolactate (24). The predicted phosphosulfolactate-producing activity of the ComA homolog XcbB1 was initially examined via sulfite consumption

assays using monobromobimane (mBBr) as a fluorescent label for free sulfite (Figure 2.3A). Sulfite consumption increased specifically when XcbB1 was incubated with the substrates PEP and sulfite, with a specific activity of 487.51 ± 45.54 nmol sulfite min^{-1} mg^{-1}. This specific activity is approximately 20% of the activity reported for ComA from *Methanocaldococcus jannaschii*, supporting the conclusion that XcbB1 and ComA share the same physiological function (23). Q-TOF MS was subsequently used to identify phosphosulfolactate as the product (Figure 2.3B). The predicted m/z for phosphosulfolactate in negative ion mode ((M-H)-species) was 248.94, which matched the m/z of the emergent signal in XcbB1-catalyzed reactions. Additionally, the isotope distribution matched the predicted isotope distributions within 5% of their predicted values.

At pH 8, the pair of singlets associated with the PEP vinyl moiety (5.15 and 5.35 ppm) showed clear signs of consumption in the presence of bisulfite (HSO_3-) and XcbB1. PEP consumption was temporally coupled to phosphosulfolactate production, detected via the increase of a characteristic doublet signal (3.36/3.35 ppm) upfield. The phosphosulfolactate triplet signal was not visible, likely due to the suppression of the water peak, plus the additional Tris and glycerol peaks in the 3.5-4.8 ppm region. The reaction went to completion within 30 mins, consistent with the general time course for sulfite consumption expected from the specific activity measured in Figure 2.3A. We therefore assign XcbB1 as a PEP-dependent phosphosulfolactate synthase (EC:4.4.1.19).

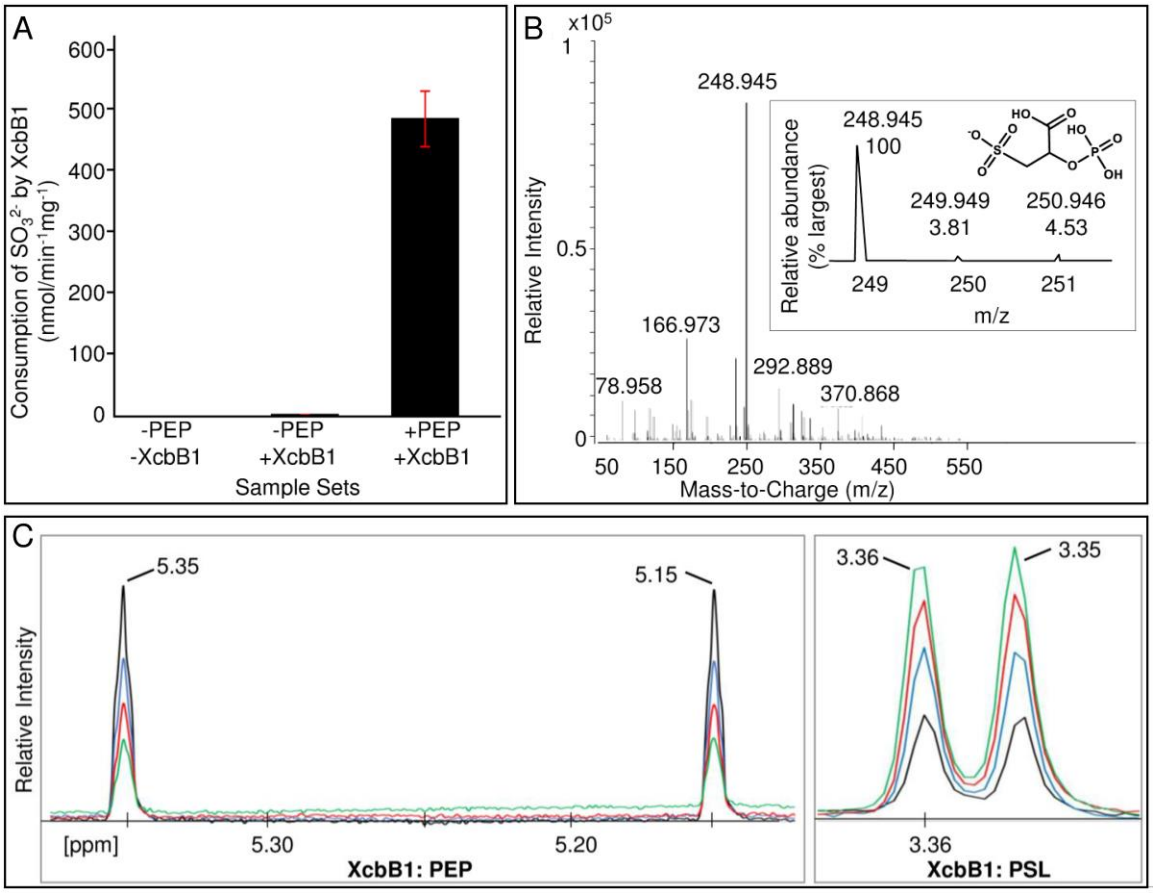

Figure 2.3. The XcbB1 reaction was established using biochemical and spectroscopic means. Using fluorescence spectroscopy, the consumption of 1 mM sulfite by purified XcbB1 was measured with or without presence of 1 mM PEP (A). An increase in sulfite consumption is observed specifically in samples containing PEP.MS analysis of the products of the XcbB1 catalyzed reaction (B) demonstrate production of phosphosulfolactate from 5 mM PEP and 5 mM sulfite. The inset panel shows the isotope distribution of phosphosulfolactate along with the corresponding ratios. The predicted m/z 248.945 and the respective predicted isotope distribution agrees with the findings. Time resolved ^{1}H-NMR spectroscopy of the XcbB1 reaction (C) shows the consumption of 2 mM PEP with the addition of 1 mM sulfite in the left panel with the concomitant yield of phosphosulfolactate (PSL) on the right. Spectra were monitored continuously over time. For clarity, 4 time points are shown; 0-2 mins (black), 8-10 mins (blue), 16-18 mins (red), and 28-30 mins (green). For all experiments, samples included 0.1 mg XcbB1 in pH 8 buffer, and incubated at 30°C.

XcbC1 Catalyzes the β-elimination of Phosphate from
Phosphosulfolactate to form Sulfoacrylic Acid

The proposed substrate for XcbC1 is the phosphosulfolactate generated by the upstream enzyme, XcbB1. In keeping with its sequence-based assignment to the arginosuccinate lyase family, the proposed β-elimination to yield phosphate was monitored using a coupled assay involving XcbB1, XcbC1, and molybdenum blue as a phosphate indicator (Figure 2.4A). When equimolar amounts of XcbB1 and XcbC1 were present in solution with a large excess of PEP and sulfite, a robust level of phosphate production was observed (specific activity = 29.74 ± 8.3 nmol PO_4^{3-} min^{-1} mg-XcbC1^{-1}). We therefore concluded that XcbC1 catalyzes the dephosphorylation of phosphosulfolactate, which was in turn generated by the upstream catalyst, XcbB1.

Canonical alkaline/acid phosphatases are typically metal-dependent enzymes that catalyze the hydrolysis of phosphomonoesters using metal-activated water, resulting in inorganic phosphate and alcohol products (59-65). A classic phosphohydrolase-type reaction would be expected to yield sulfolactate from phosphosulfolactate (Fig B.S.3A). However, Q-TOF MS analysis of the reaction products indicated that sulfoacrylic acid was the organic product (Figure 2.4B), based on its measured m/z (150.967, (M-H)- species, negative ion mode) and isotope pattern. These matched predicted values for sulfoacrylic acid (m/z =150.97) rather than sulfolactate (m/z = 168.98). This suggested that XcbC1 does not catalyze a simple hydrolytic reaction on the phosphosulfolactate substrate; rather, the reaction requires concomitant release of phosphate and a proton to form an unsaturated product, consistent with β−elimination (see below).

Time resolved ^{1}H-NMR of the XcbC1 reaction directly demonstrated that disappearance of the doublet signal attributed to phosphosulfolactate was coupled with t1Hhe appearance of a new pair of doublets further downfield (6.96/6.93 and 6.53/6.50 ppm, integrated to 1). These doublets match the predicted ^{1}H-NMR spectrum for sulfoacrylic acid (Figure 2.4C, B.S.3B). The measured spectrum furthermore bears no overlap with the ^{1}H-NMR spectrum observed for a sulfolactate standard (B.S.2B), confirming the production of a new double bond. The large j-values for the pair of doublets (16.08) indicate significant separation of the olefinic hydrogens relative to each other, meaning that the XcbC1 product exists specifically in the *trans* conformation. The conversion of phosphosulfolactate to sulfoacrylic acid proceeded to completion within approximately 12-14 mins, again consistent with the reaction time scale indicated by the phosphate release data in Figure 2.4A. We therefore conclude that XcbC1 is an unusual AFS-type phosphatase that catalyzes a β-elimination reaction using phosphosulfolactate as the substrate.

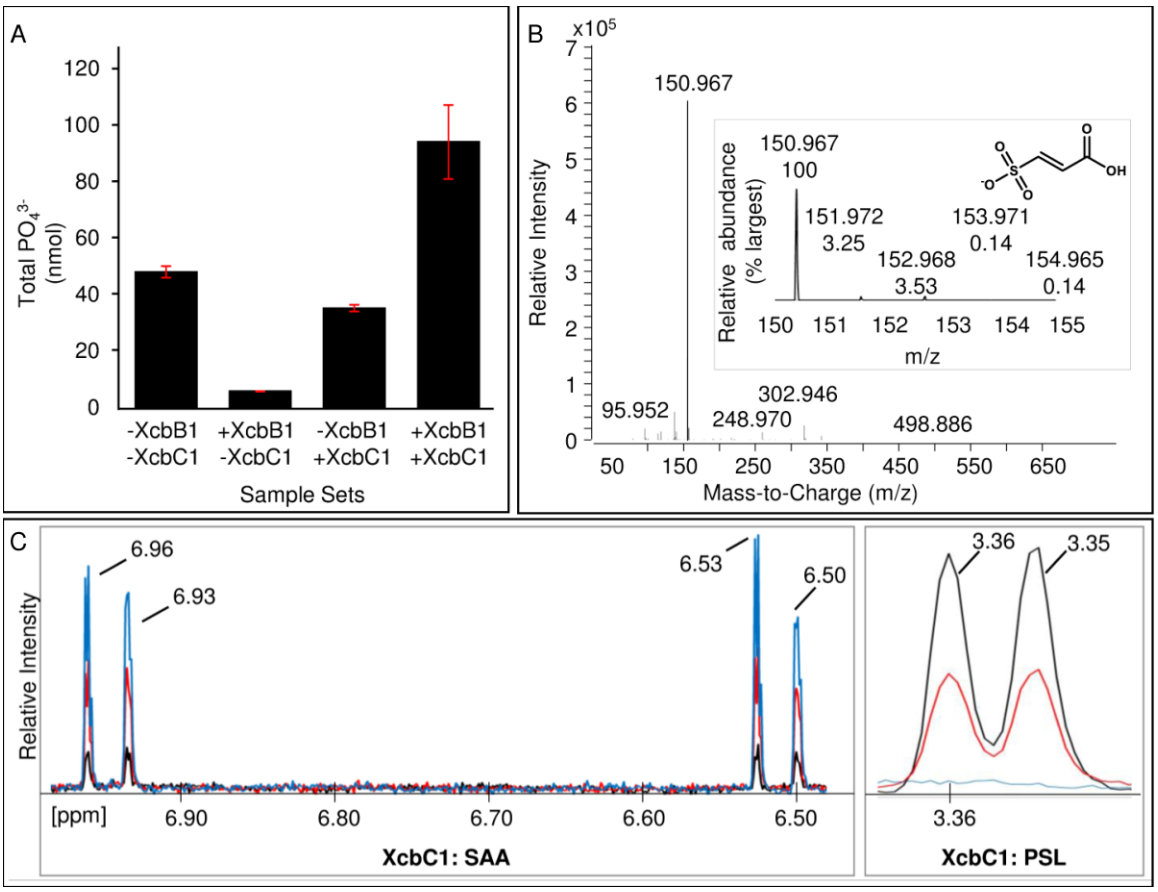

Figure 2.4. The XcbC1 reaction was established through biochemical and spectroscopic means. The production of phosphate was monitored from a coupled assay containing 1 mM PEP, 1 mM sulfite, and one, both, or neither enzyme (XcbB1 and XcbC1) (A). Inorganic phosphate, measured via absorbance using the molybdenum blue assay, was produced only in the presence of both XcbB1 and C1, suggesting that the latter removes phosphate from the XcbB1 product, phosphosulfolactate. The products of the coupled assay initiated by 5 mM PEP and 5 mM sulfite were analyzed by MS (B). The inset panel shows the isotope distribution of sulfoacrylic acid along with the corresponding ratios. The predicted m/z 150.970 and the respective predicted isotope distribution is in agreement with the results. Time resolved ^{1}H-NMR showed conversion of PSL to sulfoacrylic acid (SAA) (C) over time by the XcbB1/C1 coupled reaction, initiated by 2 mM PEP and 1 mM sulfite. For clarity, only 3 time points are shown; 0-2 mins (black), 8-10 mins (red), and 28-30 mins (blue). XcbC1 appears to fully convert PSL before the 30 min endpoint. For all experiments, samples included 0.1 mg XcbB1 in pH 8 buffer, and incubated at 30°C.

Modeling XcbC1 Active Site Reactivity

The sequence of XcbC1 was analyzed in light of canonical AFS structures and mechanisms, in order to understand the features that permit its unique reactivity. AFS members share a signature GSSxxPxKxN sequence, tertiary/quaternary fold and active site structure, and a general acid-base catalytic strategy, even while their sequence identities may be comparitively low (20-30%) (Fig B.S.4)(40). Canonical AFS enzymes have been proposed to use a general base for proton abstraction from the Cβ atom of the substrate followed by collapse of the carbanion intermediate and cleavage of the substrate. Product release may be facilitated by donation of a proton from an active site acid to the leaving group (34). Mutagenesis and structural studies point toward the strictly conserved first serine of the GSSxxPxKxN motif as the base (35,50,66). Interactions with backbone amides or the β-carboxylate group of the substrate may stabilize the catalytic Ser in its oxyanion form (41,48). The catalytic acid has been proposed to be an incompletely conserved histidine residue in ASL/δ2-crystallin, adenylosuccinate lyases, and fumarate lyases, with various replacements in aspartases and members of the pCMLE family (35,40,50). Finally, a strictly conserved lysine has been shown to interact with and position the α-carboxylate group of the substrate (41,66). The substrate-binding cavity otherwise appears to be variable, with various residues stabilizing substrates through an extensive hydrogen bonding network (50,66).

A homology-modeled structure for XcbC1 was generated using the crystal structure for a closely related δ2-crystallin in its argininosuccinate-bound form (Figure 2.5A) (40).

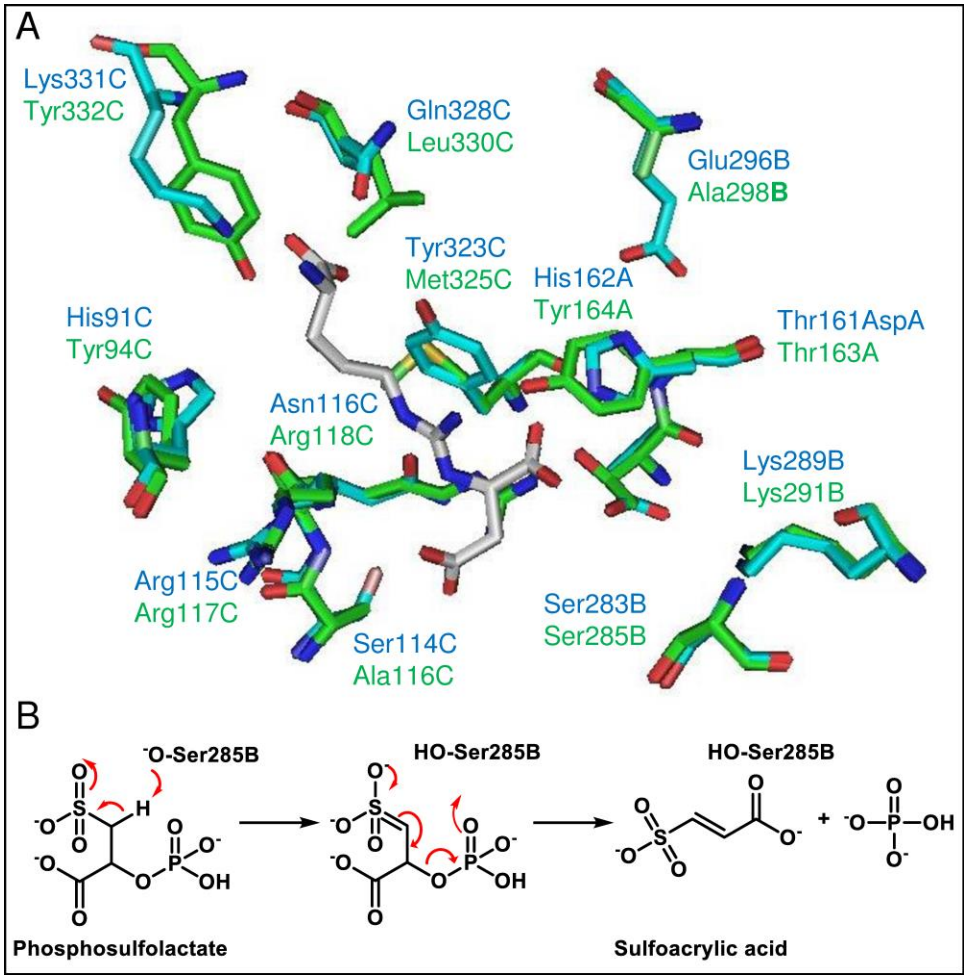

Figure 2.5. The active site of a canonical δ2-crystallin from duck with bound argininosuccinate (1TJW, 76% coverage with 28% ID) with superimposed homology model for XcbC1 (cyan and green, respectively) (A). Side chains from each respective chain are denoted with A, B, or C. The proposed XcbC1 mechanism via an argininosuccinate-lyase type reaction (B) through a general base proton abstraction followed by elimination of the phosphate leaving group is shown.

Residues from the crystal structure that were proposed to interact with the substrate are superimposed with the corresponding residues from the XcbC1 homology model. XcbC1 appears to retain the catalytic base (Ser285B, XcbC1 numbering) and strictly conserved lysine (Lys291B), but very little else. Apart from the residues important for catalysis, the other residues highlighted for δ2-crystallin form a stabilizing

hydrogen bonding network around argininosuccinate (40,67). Notably, the catalytic His is absent in the XcbC1 model, with Tyr164A-Ala298B replacing His162A-Glu296B. Previous mutagenesis studies of aspartase from *Bacillus* sp. YM55-1 showed that the histidine is not absolutely required for activity, and when considered with the incomplete conservation of the residue, may indicate that the protonation of the substrate leaving group varies amongst the superfamily (34,43). Using the homology model and known AFS chemistry, it is possible to propose a catalytic mechanism for XcbC1 (Figure 2.5B). Like the canonical AFS enzymes, the conserved Ser285B could feasibly initiate the general base catalyzed reaction through Cβ proton abstraction of the phosphosulfolactate substrate, with stabilization from Lys291B and putative H-bond donors present in the binding site. If the phosphoryl group of phosphosulfolactate is already singly protonated, it is possible that acid catalysis is not needed to facilitate phosphate release (phosphate p*K*as= 2.12 and 7.21).

Conclusions

Investigating the putative gene products of *xcbB1* and *xcbC1* by informatics, biochemical, and spectroscopic means revealed a PEP-dependent pathway for bacterial CoM biosynthesis that is distinct from the PEP-dependent pathway in methanogens. Out of the four enzymes possibly involved in CoM biosynthesis, only XcbB1 is homologous to the pathway enzyme ComA, which is known to encode the first step in the PEP-dependent CoM biosynthesis in methanogens. XcbB1 catalyzes the addition of sulfite to PEP to yield phosphosulfolactate, which is delivered as the substrate for the subsequent XcbC1 reaction. The β-elimination of phosphate catalyzed by XcbC1 yields sulfoacrylic

acid and inorganic phosphate. To our knowledge, this reaction has not been observed before in AFS enzymes, marking a novel activity for an enzyme from a large, well-characterized family, as well as a novel pathway intermediate. Though the activity of XcbD1 remains unidentified, we have implicated an important role for PLP-dependent XcbE1 in providing the source of the CoM thiol derived from Cys. This work will serve as the framework for future studies aimed at uncovering the final stages of the biosynthetic pathway. By elucidating the XcbB1 and XcbC1 reactions, we have made significant strides towards understanding bacterial CoM biosynthesis which evaded characterization in previous years.

Acknowledgements

This material is based on the work supported by the U.S. Department of Energy, Office of Science, Office of Basic Energy Services, under Award Number DE-FG02-04ER15563. Support for the NMR instruments console upgrades and Montana State University's NMR Center has been provided by the NIH Shared Instrumentation Grant (SIG) program [NIH: 1S10RR13878 and 1S10RR026659], the NSF MRI program [NSF: DBI-1532078] the Murdock Charitable Trust, and Montana State University's Vice President for Research Economic Development's office. We thank Dr. George Gauss for technical support and helpful suggestions. We also thank Garrett Moraski and Dr. Robert White for their insightful synthetic advice.

Conflict of Interest

The authors declare that they have no conflict of interest with the content of this article.

Author Contributions

SP, FM, AG, HM, BML and BT ran the experiments and analyzed the results. AG assisted on the molybdenum blue studies, while HM assisted on XcbE1 studies. SP, FM, and BML conducted Q-TOF MS studies and analyzed the results. SP and BT ran the ^{1}H-NMR studies and analyzed the results. SP, JD, and JP planned the experiments and conceived the idea of the project with input from FM, BML, and BT. SP, JD, and JP wrote the paper with input and approval from all authors.

References

1 Balch, W. E. & Wolfe, R. S. New Approach to the Cultivation of Methanogenic Bacteria: 2-Mercaptoethanesulfonic Acid (HS-CoM)-Dependent Growth of *Methanobacterium ruminantium* in a Pressurized Atmosphere. *Applied and Environmental Microbiology* **32**, 781-791 (1976).

2 Balch, W. E. & Wolfe, R. S. Specificity and biological distribution of coenzyme M (2-mercaptoethanesulfonic acid). *J Bacteriol* **137**, 256-263 (1979).

3 McBride, B. C. & Wolfe, R. S. A new coenzyme of methyl transfer, Coenzyme M. *Biochemistry* **10**, 2317-2324 (1971).

4 Taylor, C. D., McBride, B. C., Wolfe, R. S. & Bryant, M. P. Coenzyme M, Essential for Growth of a Rumen Strain of *Methanobacterium ruminantium*. *Journal of Bacteriology* **120**, 974-975 (1974).

5 Wolfe, R. S. in *The Molecular Basis of Bacterial Metabolism* Vol. 41 *41. Colloquium der Gesellschaft für Biologische Chemie 5.–7. April 1990 in Mosbach/Baden* (eds Günter Hauska & RudolfK Thauer) Ch. 1, 1-12 (Springer Berlin Heidelberg, 1990).

6 Allen, J. R., Clark, D. D., Krum, J. G. & Ensign, S. A. A role for coenzyme M (2-mercaptoethanesulfonic acid) in a bacterial pathway of aliphatic epoxide carboxylation. *Proc Natl Acad Sci U S A* **96**, 8432-8437 (1999).

7 Coleman, N. V., Mattes, T. E., Gossett, J. M. & Spain, J. C. Phylogenetic and kinetic diversity of aerobic vinyl chloride-assimilating bacteria from contaminated sites. *Appl Environ Microbiol* **68**, 6162-6171 (2002).

8 Liu, X. & Mattes, T. E. Epoxyalkane:Coenzyme M Transferase Gene Diversity and Distribution in Groundwater Samples from Chlorinated-Ethene-Contaminated Sites. *Applied and Environmental Microbiology* **82**, 3269-3279, doi:10.1128/AEM.00673-16 (2016).

9 Mattes, T. E., Coleman, N. V., Spain, J. C. & Gossett, J. M. Physiological and molecular genetic analyses of vinyl chloride and ethene biodegradation in Nocardioides sp. strain JS614. *Arch Microbiol* **183**, 95-106, doi:10.1007/s00203-004-0749-2 (2005).

10 Small, F. J., Tilley, J. K. & Ensign, S. A. Characterization of a new pathway for epichlorohydrin degradation by whole cells of xanthobacter strain py2. *Appl Environ Microbiol* **61**, 1507-1513 (1995).

11 van Ginkel, C. G., Welten, H. G. J. & de Bont, J. A. M. Oxidation of Gaseous and Volatile Hydrocarbons by Selected Alkene-Utilizing Bacteria. *Applied and Environmental Microbiology* **53**, 2903-2907 (1987).

12 Ensign, S. A., Hyman, M. R. & Arp, D. J. Cometabolic degradation of chlorinated alkenes by alkene monooxygenase in a propylene-grown Xanthobacter strain. *Applied and Environmental Microbiology* **58**, 3038-3046 (1992).

13 Small, F. J. & Ensign, S. A. Alkene Monooxygenase from Xanthobacter Strain Py2: PURIFICATION AND CHARACTERIZATION OF A FOUR-COMPONENT SYSTEM CENTRAL TO THE BACTERIAL METABOLISM OF ALIPHATIC ALKENES. *Journal of Biological Chemistry* **272**, 24913-24920, doi:10.1074/jbc.272.40.24913 (1997).

14 Krum, J. G. & Ensign, S. A. Heterologous expression of bacterial Epoxyalkane:Coenzyme M transferase and inducible coenzyme M biosynthesis in Xanthobacter strain Py2 and Rhodococcus rhodochrous B276. *J Bacteriol* **182**, 2629-2634 (2000).

15 Krum, J. G., Ellsworth, H., Sargeant, R. R., Rich, G. & Ensign, S. A. Kinetic and Microcalorimetric Analysis of Substrate and Cofactor Interactions in Epoxyalkane:CoM Transferase, a Zinc-Dependent Epoxidase. *Biochemistry* **41**, 5005-5014, doi:10.1021/bi0255221 (2002).

16 Krishnakumar, A. M. *et al.* Getting a Handle on the Role of Coenzyme M in Alkene Metabolism. *Microbiology and Molecular Biology Reviews : MMBR* **72**, 445-456, doi:10.1128/MMBR.00005-08 (2008).

17 Ensign, S. A. Microbial metabolism of aliphatic alkenes. *Biochemistry* **40**, 5845-5853 (2001).

18 Allen, J. R. & Ensign, S. A. Two short-chain dehydrogenases confer stereoselectivity for enantiomers of epoxypropane in the multiprotein epoxide carboxylating systems of Xanthobacter strain Py2 and Nocardia corallina B276. *Biochemistry* **38**, 247-256, doi:10.1021/bi982114h (1999).

19 Clark, D. D., Allen, J. R. & Ensign, S. A. Characterization of five catalytic activities associated with the NADPH:2-ketopropyl-coenzyme M [2-(2-ketopropylthio)ethanesulfonate] oxidoreductase/carboxylase of the Xanthobacter strain Py2 epoxide carboxylase system. *Biochemistry* **39**, 1294-1304 (2000).

20 Westphal, A. H., Swaving, J., Jacobs, L. & Kok, A. d. Purification and characterization of a flavoprotein involved in the degradation of epoxyalkanes by

Xanthobacter Py2. *European Journal of Biochemistry* **257**, 160-168, doi:10.1046/j.1432-1327.1998.2570160.x (2013).

21 Kofoed, M. A., Wampler, D. A., Pandey, A. S., Peters, J. W. & Ensign, S. A. Roles of the Redox-Active Disulfide and Histidine Residues Forming a Catalytic Dyad in Reactions Catalyzed by 2-Ketopropyl Coenzyme M Oxidoreductase/Carboxylase. *Journal of Bacteriology* **193**, 4904-4913, doi:10.1128/JB.05231-11 (2011).

22 Pandey, A. S., Mulder, D. W., Ensign, S. A. & Peters, J. W. Structural basis for carbon dioxide binding by 2-ketopropyl coenzyme M oxidoreductase/carboxylase. *FEBS Letters* **585**, 459-464, doi:10.1016/j.febslet.2010.12.035 (2011).

23 Graham, D. E., Xu, H. & White, R. H. Identification of coenzyme M biosynthetic phosphosulfolactate synthase: a new family of sulfonate-biosynthesizing enzymes. *J Biol Chem* **277**, 13421-13429, doi:10.1074/jbc.M201011200 (2002).

24 Wise, E. L., Graham, D. E., White, R. H. & Rayment, I. The structural determination of phosphosulfolactate synthase from Methanococcus jannaschii at 1.7-A resolution: an enolase that is not an enolase. *J Biol Chem* **278**, 45858-45863, doi:10.1074/jbc.M307486200 (2003).

25 Graham, D. E., Graupner, M., Xu, H. & White, R. H. Identification of coenzyme M biosynthetic 2-phosphosulfolactate phosphatase. A member of a new class of Mg(2+)-dependent acid phosphatases. *Eur J Biochem* **268**, 5176-5188 (2001).

26 White, R. H. Biosynthesis of coenzyme M (2-mercaptoethanesulfonic acid). *Biochemistry* **24**, 6487-6493, doi:10.1021/bi00344a027 (1985).

27 White, R. H. Intermediates in the biosynthesis of coenzyme M (2-mercaptoethanesulfonic acid). *Biochemistry* **25**, 5304-5308, doi:10.1021/bi00366a047 (1986).

28 Graupner, M., Xu, H. & White, R. H. Identification of an archaeal 2-hydroxy acid dehydrogenase catalyzing reactions involved in coenzyme biosynthesis in methanoarchaea. *J Bacteriol* **182**, 3688-3692 (2000).

29 Graupner, M., Xu, H. & White, R. H. Identification of the gene encoding sulfopyruvate decarboxylase, an enzyme involved in biosynthesis of coenzyme M. *J Bacteriol* **182**, 4862-4867 (2000).

30 White, R. H. Characterization of the enzymic conversion of sulfoacetaldehyde and L-cysteine into coenzyme M (2-mercaptoethanesulfonic acid). *Biochemistry* **27**, 7458-7462, doi:10.1021/bi00419a043 (1988).

31 Graham, D. E., Taylor, S. M., Wolf, R. Z. & Namboori, S. C. Convergent evolution of coenzyme M biosynthesis in the Methanosarcinales: cysteate synthase evolved from an ancestral threonine synthase. *Biochem J* **424**, 467-478, doi:10.1042/bj20090999 (2009).

32 Broberg, C. A. & Clark, D. D. Shotgun proteomics of Xanthobacter autotrophicus Py2 reveals proteins specific to growth on propylene. *Arch Microbiol* **192**, 945-957, doi:10.1007/s00203-010-0623-3 (2010).

33 Krum, J. G. & Ensign, S. A. Evidence that a linear megaplasmid encodes enzymes of aliphatic alkene and epoxide metabolism and coenzyme M (2-mercaptoethanesulfonate) biosynthesis in Xanthobacter strain Py2. *J Bacteriol* **183**, 2172-2177, doi:10.1128/jb.183.7.2172-2177.2001 (2001).

34 Puthan Veetil, V., Fibriansah, G., Raj, H., Thunnissen, A. M. & Poelarends, G. J. Aspartase/fumarase superfamily: a common catalytic strategy involving general base-catalyzed formation of a highly stabilized aci-carboxylate intermediate. *Biochemistry* **51**, 4237-4243, doi:10.1021/bi300430j (2012).

35 Wiegant, W. M. & De Bont, J. A. M. A New Route for Ethylene Glycol Metabolism in *Mycobacterium* E44. *Journal of General Microbiology* **120**, 325-331 (1980).

36 Vishniac, W. & Santer, M. The Thiobacilli. *Bacteriol Rev* **21**, 195-213 (1957).

37 Bessey, O. A., Lowry, O. H. & Brock, M. J. A method for the rapid determination of alkaline phosphates with five cubic millimeters of serum. *J Biol Chem* **164**, 321-329 (1946).

38 Fiske, C. H. & Subbarow, Y. THE COLORIMETRIC DETERMINATION OF PHOSPHORUS. *Journal of Biological Chemistry* **66**, 375-400 (1925).

39 Palmer, R. E. An experiment to quantitate organically bound phosphate: With special emphasis on biochemical molecules. *Journal of Chemical Education* **62**, 898, doi:10.1021/ed062p898 (1985).

40 Todorovic, B. & Glick, B. R. The interconversion of ACC deaminase and D-cysteine desulfhydrase by directed mutagenesis. *Planta* **229**, 193-205, doi:10.1007/s00425-008-0820-3 (2008).

41 Bhaumik, P., Koski, M. K., Bergmann, U. & Wierenga, R. K. Structure determination and refinement at 2.44 A resolution of argininosuccinate lyase from Escherichia coli. *Acta Crystallogr D Biol Crystallogr* **60**, 1964-1970, doi:10.1107/s0907444904021912 (2004).

42 Farrell, K. & Overton, S. Characterization of argininosuccinate lyase (EC 4.3.2.1) from Chlamydomonas reinhardtii. *Biochem J* **242**, 261-266 (1987).

43 Garrard, L. J., Bui, Q. T., Nygaard, R. & Raushel, F. M. Acid-base catalysis in the argininosuccinate lyase reaction. *J Biol Chem* **260**, 5548-5553 (1985).

44 Patejunas, G., Barbosa, P., Lacombe, M. & O'Brien, W. E. Exploring the role of histidines in the catalytic activity of duck delta-crystallins using site-directed mutagenesis. *Exp Eye Res* **61**, 151-154 (1995).

45 Paul, A., Mishra, A., Surolia, A. & Vijayan, M. Cloning, expression, purification, crystallization and preliminary X-ray studies of argininosuccinate lyase (Rv1659) from Mycobacterium tuberculosis. *Acta Crystallographica Section F: Structural Biology and Crystallization Communications* **69**, 1422-1424, doi:10.1107/S1744309113031138 (2013).

46 Sampaleanu, L. M. *et al.* Structural studies of duck delta2 crystallin mutants provide insight into the role of Thr161 and the 280s loop in catalysis. *Biochem J* **384**, 437-447, doi:10.1042/bj20040656 (2004).

47 Tsai, M. *et al.* Substrate and product complexes of Escherichia coli adenylosuccinate lyase provide new insights into the enzymatic mechanism. *J Mol Biol* **370**, 541-554, doi:10.1016/j.jmb.2007.04.052 (2007).

48 Viola, R. E. L-aspartase: new tricks from an old enzyme. *Adv Enzymol Relat Areas Mol Biol* **74**, 295-341 (2000).

49 Puthan Veetil, V., Raj, H., Quax, W. J., Janssen, D. B. & Poelarends, G. J. Site-directed mutagenesis, kinetic and inhibition studies of aspartate ammonia lyase from Bacillus sp. YM55-1. *The FEBS journal* **276**, 2994-3007, doi:10.1111/j.1742-4658.2009.07015.x (2009).

50 Woods, S. A., Schwartzbach, S. D. & Guest, J. R. Two biochemically distinct classes of fumarase in Escherichia coli. *Biochim Biophys Acta* **954**, 14-26 (1988).

51 Yoon, M. Y. *et al.* Acid-base chemical mechanism of aspartase from Hafnia alvei. *Arch Biochem Biophys* **320**, 115-122 (1995).

52 Banerjee, S. *et al.* Structural and kinetic studies on adenylosuccinate lyase from Mycobacterium smegmatis and Mycobacterium tuberculosis provide new insights on the catalytic residues of the enzyme. *The FEBS journal* **281**, 1642-1658, doi:10.1111/febs.12730 (2014).

53 Brosius, J. L. & Colman, R. F. Three Subunits Contribute Amino Acids to the Active Site of Tetrameric Adenylosuccinate Lyase: Lys268 and Glu275 Are Required†. *Biochemistry* **41**, 2217-2226, doi:10.1021/bi011998t (2002).

54 Bulusu, V., Srinivasan, B., Bopanna, M. P. & Balaram, H. Elucidation of the substrate specificity, kinetic and catalytic mechanism of adenylosuccinate lyase from Plasmodium falciparum. *Biochim Biophys Acta* **1794**, 642-654, doi:10.1016/j.bbapap.2008.11.021 (2009).

55 Fyfe, P. K., Dawson, A., Hutchison, M. T., Cameron, S. & Hunter, W. N. Structure of Staphylococcus aureus adenylosuccinate lyase (PurB) and assessment of its potential as a target for structure-based inhibitor discovery. *Acta Crystallogr D Biol Crystallogr* **66**, 881-888, doi:10.1107/s0907444910020081 (2010).

56 Kozlov, G., Nguyen, L., Pearsall, J. & Gehring, K. The structure of phosphate-bound Escherichia coli adenylosuccinate lyase identifies His171 as a catalytic acid. *Acta Crystallographica Section F: Structural Biology and Crystallization Communications* **65**, 857-861, doi:10.1107/S1744309109029674 (2009).

57 Lee, T. T., Worby, C., Bao, Z. Q., Dixon, J. E. & Colman, R. F. His68 and His141 are critical contributors to the intersubunit catalytic site of adenylosuccinate lyase of Bacillus subtilis. *Biochemistry* **38**, 22-32, doi:10.1021/bi982299s (1999).

58 Toth, E. A. & Yeates, T. O. The structure of adenylosuccinate lyase, an enzyme with dual activity in the de novo purine biosynthetic pathway. *Structure* **8**, 163-174, doi:https://doi.org/10.1016/S0969-2126(00)00092-7 (2000).

59 Yang, J. *et al.* Crystal structure of 3-carboxy-cis,cis-muconate lactonizing enzyme from Pseudomonas putida, a fumarase class II type cycloisomerase: enzyme evolution in parallel pathways. *Biochemistry* **43**, 10424-10434, doi:10.1021/bi036205c (2004).

60 Soutourina, J., Blanquet, S. & Plateau, P. Role of D-cysteine desulfhydrase in the adaptation of Escherichia coli to D-cysteine. *J Biol Chem* **276**, 40864-40872, doi:10.1074/jbc.M102375200 (2001).

61 Eliot, A. C. & Kirsch, J. F. Pyridoxal phosphate enzymes: mechanistic, structural, and evolutionary considerations. *Annu Rev Biochem* **73**, 383-415, doi:10.1146/annurev.biochem.73.011303.074021 (2004).

62 Toney, M. D. Reaction specificity in pyridoxal phosphate enzymes. *Arch Biochem Biophys* **433**, 279-287, doi:10.1016/j.abb.2004.09.037 (2005).

63 Watanabe, Y. & Shimura, K. BIOSYNTHESIS OF THREONINE FROM HOMOSERINE .5. NATURE OF AN INTERMEDIARY PRODUCT. *Journal of Biochemistry* **43**, 283-294 (1956).

64 Keller, J. W. *et al.* Pseudomonas cepacia 2,2-dialkylglycine decarboxylase. Sequence and expression in Escherichia coli of structural and repressor genes. *J Biol Chem* **265**, 5531-5539 (1990).

65 Bull, H., Murray, P. G., Thomas, D., Fraser, A. M. & Nelson, P. N. Acid phosphatases. *Molecular Pathology* **55**, 65-72 (2002).

66 Kim, E. E. & Wyckoff, H. W. Reaction mechanism of alkaline phosphatase based on crystal structures. Two-metal ion catalysis. *J Mol Biol* **218**, 449-464 (1991).

67 Millán, J. L. Alkaline Phosphatases: Structure, substrate specificity and functional relatedness to other members of a large superfamily of enzymes. *Purinergic Signalling* **2**, 335-341, doi:10.1007/s11302-005-5435-6 (2006).

68 Sharma, U., Pal, D. & Prasad, R. Alkaline Phosphatase: An Overview. *Indian Journal of Clinical Biochemistry* **29**, 269-278, doi:10.1007/s12291-013-0408-y (2014).

69 Simopoulos, T. T. & Jencks, W. P. Alkaline phosphatase is an almost perfect enzyme. *Biochemistry* **33**, 10375-10380 (1994).

70 Stec, B., Holtz, K. M. & Kantrowitz, E. R. A revised mechanism for the alkaline phosphatase reaction involving three metal ions1. *Journal of Molecular Biology* **299**, 1303-1311, doi:https://doi.org/10.1006/jmbi.2000.3799 (2000).

71 Tabaldi, L. A. *et al.* Effects of metal elements on acid phosphatase activity in cucumber (Cucumis sativus L.) seedlings. *Environmental and Experimental Botany* **59**, 43-48, doi:https://doi.org/10.1016/j.envexpbot.2005.10.009 (2007).

72 Fibriansah, G., Veetil, V. P., Poelarends, G. J. & Thunnissen, A.-M. W. H. Structural Basis for the Catalytic Mechanism of Aspartate Ammonia Lyase. *Biochemistry* **50**, 6053-6062, doi:10.1021/bi200497y (2011).

73 Sampaleanu, L. M., Vallée, F., Slingsby, C. & Howell, P. L. Structural Studies of Duck δ1 and δ2 Crystallin Suggest Conformational Changes Occur during Catalysis. *Biochemistry* **40**, 2732-2742, doi:10.1021/bi002272k (2001).

CHAPTER THREE

A PYRIDOXAL 5'-PHOSPHATE-DEPENDENT ENZYME MAY PROVIDE A SOURCE FOR THE COENZYME M THIOL MOIETY

Introduction

The previous chapter described a plausible pathway initiated by the XcbB1 catalyzed addition of sulfite to PEP yield phosphosulfolactate, followed by XcbC1 catalyzed β-elimination of phosphate to yield sulfoacrylic acid. The remaining stages still require further investigation, but some speculation can be made regarding the other two enzymes considered in this work: XcbD1 and XcbE1 (refer to Ch.4 for XcbD1). XcbE1 was briefly discussed previously, but will be further expanded in this chapter. This enzyme is annotated as 1-aminocyclopropane-1-carboxylate deaminase (ACCD), but bioinformatics indicate that XcbE1 shares more sequence features with D-cysteine desulfhydrases. These are part of a large family of pyridoxal 5'-phosphate (PLP)-dependent enzymes.

PLP-Dependent Enzymes

The PLP-dependent enzymes are responsible for catalyzing several important reactions on predominantly amino acid substrates, including transamination, decarboxylation, removal or replacement of chemical groups at α, β, or γ positions, and interconversion of L and D forms of amino acids[1,2]. The first conserved reaction among all known PLP-dependent enzymes involves a Schiff base exchange reaction (Fig 3.1). In

the resting state, PLP-dependent enzymes contain an internal aldimine in the form of a catalytic lysine-bound PLP that acts as a Schiff base. The incoming amine-containing substrate displaces the ε-amine from the internal aldimine, forming an external aldimine. From this point, there is a distinct divergence in the assorted catalyzed reactions[1].

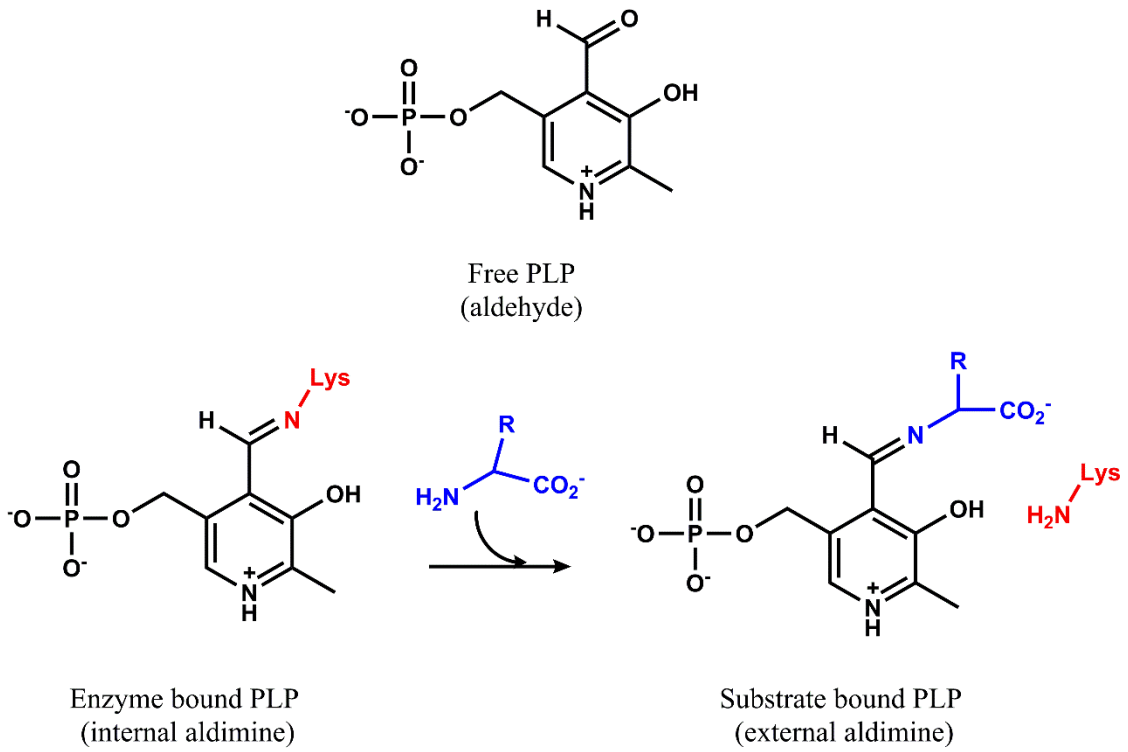

Figure 3.1 The general scheme for PLP-dependent reactions is depicted. Free PLP exists as an aldehyde, which is converted to a Schiff base (internal aldimine) upon binding to the enzyme active site lysine. Displacement of the active site lysine by the incoming nucleophile, or amino acid substrate, results in formation of the external aldimine Schiff base.

PLP-dependent reactions make up 4% of all catalogued reactions in the Enzyme Commission (EC) database, and catalyze a number of reactions on a variety of predominantly amino acid substrates[2]. Though the scope of these enzymes seems vast,

PLP-dependent reactions can be arranged by the position on the respective substrate where the net reaction occurs. Decarboxylation, transamination, racemization, and electrophilic elimination/replacement reactions are typically performed on the C_α position while reactions at the C_β and C_γ positions include eliminations or replacements[2]. Since many PLP-dependent reaction pathways share common intermediates, several enzymes have been shown to catalyze combination reactions that utilize the basic chemistry, such as; the decarboxylation and transamination of aminoisobutyrate and pyruvate to form acetone, CO_2, and L-alanine, catalyzed by diakylglycine decarboxylase, or the γ-elimination/β-replacement of *O*-phospho-L-homoserine and H_2O to L-threonine and inorganic phosphate catalyzed by threonine synthase[2-4].

Ultimately, a simple mechanistic strategy serves as the unifying feature for all PLP-dependent enzymes (Fig 3.2).

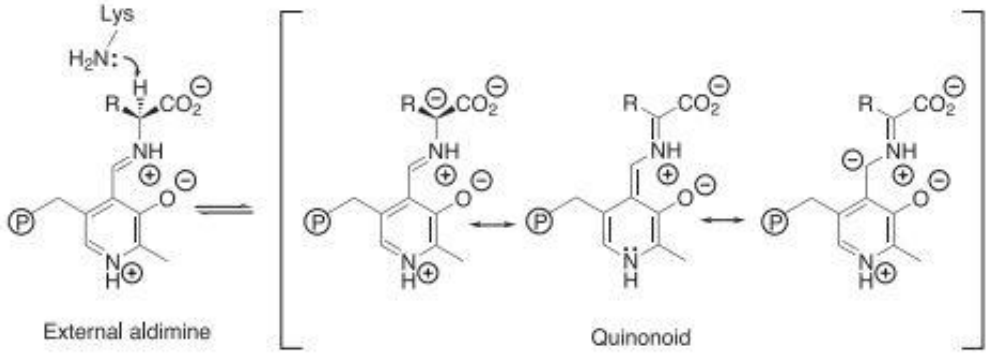

Figure 3.2. Delocalization of the negative charge on the C_α position formed during formation of the external aldimine is facilitated by the conjugated system of the PLP cofactor in the quinonoid intermediate[2].

During formation of the external aldimine (described previously), the negative charge at the C_α position that is formed as a result of the condensation of PLP with the substrate is stabilized by the PLP cofactor. Stabilization of the carbanion (typically referred to as the quiononoid intermediate) is facilitated by delocalization of the negative charge throughout the conjugated ring system of PLP, thereby acting as an "electron sink"[2]. Free PLP retains this innate catalytic capability, albeit very slowly, meaning that the apoenzyme is responsible for enforcing substrate specificity and enhancing the rate of reaction between the substrate and enzyme-bound PLP.

All the solved structures for PLP-dependent enzymes fall into five fold types[5,6]. The majority of known structures are classified as Fold Type I (aspartate aminotransferase family), which function as homodimers with two active sites per dimer[2]. Fold Type II (tryptophan synthase family) enzymes structures are similar to Fold Type I enzymes, but remain evolutionarily distinct. One key difference is that Fold Type II enzyme active sites are composed of residues from a single monomer, instead of residue contributions from both monomers, yet still functions as a homodimer. Fold Type III and V (alanine racemase and glycogen phosphorylase family, respectively) exhibit mechanistic departures from the rest of the family, in that they utilize the phosphate group of the PLP cofactor for catalysis, rather than the aldehyde for Schiff base formation. Fold Type IV (D-amino acid aminotransferase family) resemble Fold Type I and II enzymes, in that they also function as homodimers. However, the cofactor binding site for Fold Type IV is oriented in a near mirror image of the Fold Type I and II binding sites, exposing the *re* face, rather than *si* face, to solvent[7]. Structural studies revealed that

PLP-enzyme structures do not correlate with reaction type; instead, each fold type has enzymes representative of multiple reaction types[2,8].

XcbE1 is homologous to D-cysteine desulfhydrases, a sub-family within the Fold Type II/tryptophan synthase family. In NCBI's Conserved Domain Database (CDD), other enzymes in this family include; cysteine synthase, ACCD, cystathionine β-synthase, threonine synthase, L-cysteate sulfolyase, serine dehydratase, and L-serine-ammonia lyase[9].

Cysteine Desulfhydrases

L-cysteine Desulfhydrase. L-cysteine desulfhydrases are found in the KEGG pathway (L-cysteine hydrogen sulfide-lyase [deaminating] E.C. 4.4.1.1) under several names, including cystathionine γ-lyase, as part of a class of carbon-sulfur lyases. A multifunctional PLP-dependent enzyme, it can catalyze several different reactions, including the α,β-elimination of L-cysteine to H_2S, pyruvate, and ammonia[10-12]. The reaction scheme was proposed to start with enzyme-bound L-cysteine undergoing proton abstraction and H_2S elimination, followed by release of bound aminoacrylate that hydrolyzes to form pyruvate and ammonia (refer to next section for similar D-cysteine scheme). Earlier studies indicated that this reaction may be reversible when alkylmercaptans, pyruvate and ammonia are incubated with the enzyme, yielding (*S*)-alkyl-L-cysteine (**R**SCH_2CHNH_2COOH) when the α,β-elimination steps are reversed[12]. L-cysteine desulfhydrase-type enzymes are part of the Fold Type I/aspartate aminotransferase family of PLP-dependent enzymes, and are not to be confused with the [4Fe-4S]-containing L-cysteine desulfidase that also decomposes L-cysteine to H_2S,

pyruvate, and ammonia and lacks PLP[13]. The unrelated PLP-dependent cysteine desulfurases like NifS and IscS also catalyze L-cysteine, but use a different strategy to yield elemental sulfur (S^0) and alanine[14,15]. These enzymes use PLP and an active site cysteine to form persulfide (R-S-SH) groups with substrate L-cysteine, and the resulting S^0 is incorporated into some downstream product, making these enzymes key players in sulfur transfer. A proposed mechanism for NifS suggests that the L-cysteine amino group forms the expected external aldimine or Schiff base with the PLP cofactor, followed by nucleophilic attack of the substrate cysteine thiol by the active site cysteine thiolate anion[14]. This results in repulsion of a stabilized anion of alanine and formation of enzyme-bound cysteinyl persulfide (R-S-SH), which in the even that a sulfur acceptor is not present, the persulfide decomposes to S^0 or if reductant is present, H_2S.

<u>D-cysteine Desulfhydrase</u>. The closely related D-cysteine desulfhydrase (EC 4.4.1.15) and ACCD (EC 3.5.99.7) enzymes are part of the Fold Type II/tryptophan synthase family of PLP-dependent enzymes. D-cysteine desulfhydrases catalyze the α,β-elimination of D-cysteine to H_2S, pyruvate and ammonia, and ACCD catalyzes the ring breaking of the cyclopropanoid1-aminocyclopropane-1-carboxylic acid (ACC) to α-ketobutyrate and ammonia (Fig 3.3)[16].

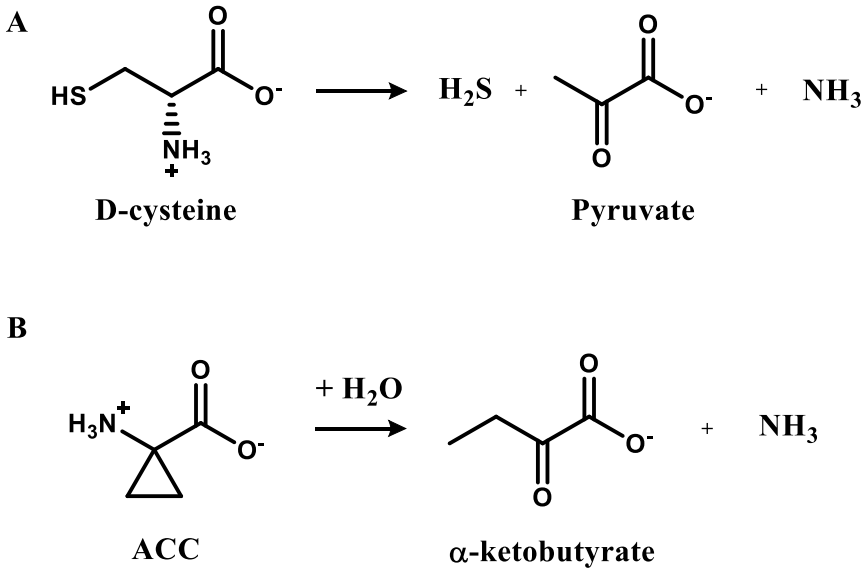

Figure 3.3. The simplified scheme for canonical D-cysteine desulfhydrases (A) is shown with a scheme for ACCD enzymes (B).

The significant sequence identity between ACCD and D-cysteine desulfhydrase enzymes has resulted in many sequences being labeled as putative ACCD genes, with only a small percentage of these proteins being experimentally shown to actually catalyze the degradation of 1-aminocyclopropane-1-carboxylate (ACC)[17]. The D-cysteine desulfhydrase enzyme in *E. coli* catalyzes the α,β-elimination reaction of D-cysteine as well as D-cysteine derivatives (D-cystine, DL-selenocystine, β-chloro-D-alanine, *O*-acetyl-D-serine) to produce H_2S that can be used by the cell as a source of sulfur[16]. Like L-cysteine desulfhydrases, D-cysteine desulfhydrases are stereoselective for the respective stereoisomer of cysteine[14,16-18]. While attempting to differentiate between a true ACCD enzyme and D-cysteine desulfhydrase, Todorovic et al. investigated two amino acid residues in the active sites of both proteins that may confer substrate bias[17]. Their findings suggested that true ACCDs contained a conserved Glu and Leu residue,

while D-cysteine desulfhydrase-type proteins contained a Ser or Thr replacement at the indicated sites[17,19]. In the *Solanum lycopersicum* D-cysteine desulfhydrase, these Ser/Thr sites were mutated back to the Glu and Leu residues, which resulted in newfound ACCD activity and the loss of desulfhydrase activity[17]. Canonical D-cysteine desulfhydrase mechanisms follow the typical mode of catalysis for PLP-dependent enzymes to release H_2S, followed by non-enzymatic tautomerization and hydrolysis to generate the other reaction products (Fig 3.4)[20].

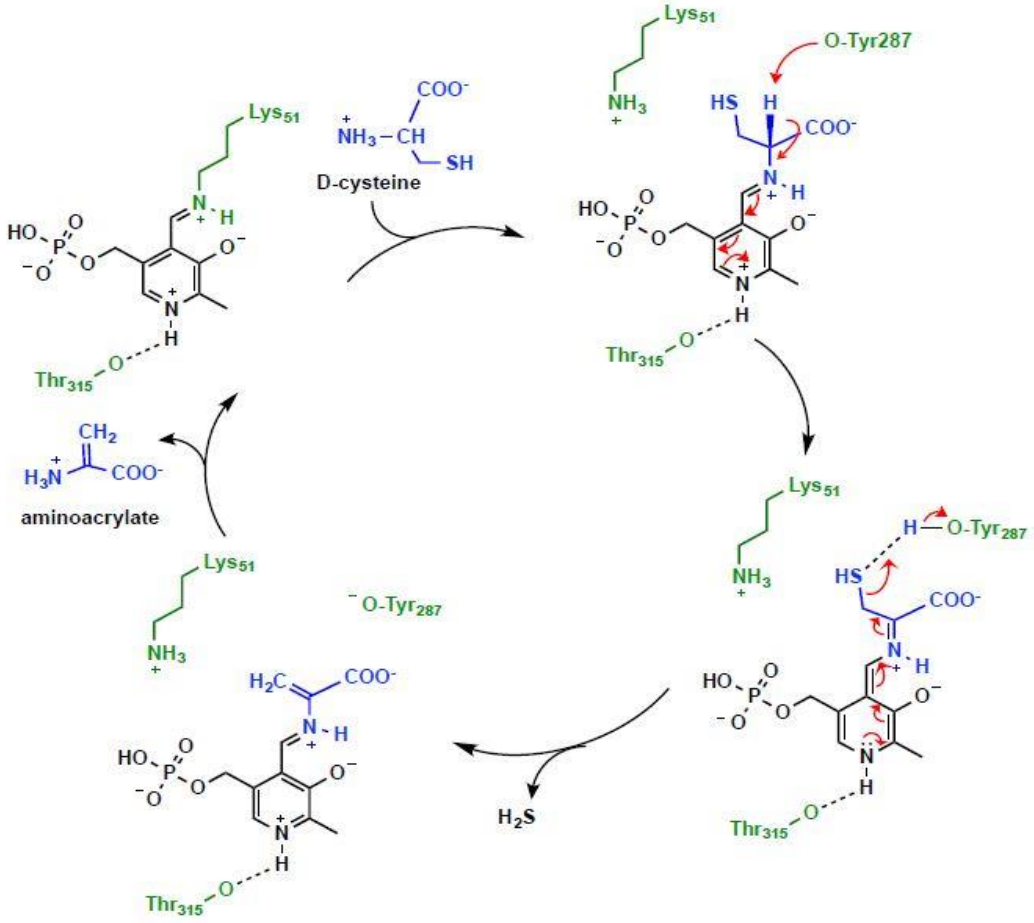

Figure 3.4 The catalytic mechanism for D-cysteine desulfhydrase in *Salmonella typhimurium*. (1) PLP bound to Lys51 as Schiff base forming internal aldimine. (2) Imine

exchange between the amino group of D-cysteine and internal aldimine, forming external aldimine, and deprotonation of α-carbon by the Tyr287 phenolate, facilitating the formation of a quinonoid complex. (3) Protonated Tyr287 releases –SH from external aldimine as H_2S, reverting Tyr287 to the phenolate form, and forming the PLP-aminoacrylate complex. (4) Second imine exchange between PLP-aminoacrylate complex and Lys51, releasing aminoacrylate and regenerating the original Lys51-PLP Schiff base. The aminoacrylate is nonenzymatically deaminated by hydrolysis, forming pyruvate and ammonia[20].

Previous work done with *E. coli* D-cysteine desulfhydrase suggests that this enzyme may be responsible for mitigating D-cysteine toxicity in the cell by utilizing it as a source of thiol[16,21,22]. While there are several *E. coli* proteins involved in detoxification, transport, and utilization of D-cysteine as a thiol source, it is still unclear what specific circumstances would expose the bacterium to this seemingly uncommon amino acid[16,23]. Detoxification of D-cysteine to generate toxic H_2S gas may seem counterintuitive, but the role of endogenously generated H_2S in mediating various physiological effects has gained traction in more recent years[24,25]. H_2S is also important in the sulfur cycle, and as a source of energy for green/purple sulfur bacteria. A weak acid (pK_{a1} is 6.9 and pK_{a2} is >12[26]), H_2S exists as HS^-:H_2S at 3:1 at physiological pH (pH 7.4)[27]. While more studies are needed to elucidate the signaling roles of endogenous H_2S, as well as elucidating the reason for the disconnect between enzyme K_Ms (mM range) and intracellular concentrations of cysteine or homocysteine (~tens to hundreds of micromolar range)[10], it is possible to suggest a role for a propylene inducible D-cysteine desulfhydrase in *X. autotrophicus* Py2.

Hypothesized Role of XcbE1 in CoM Biosynthesis

D-cysteine desulfhydrases catalyze the α,β-elimination of D-cysteine to yield gaseous H_2S, pyruvate, and NH_3, potentially providing a source of thiol for the cell while remediating the toxic effects of D-cysteine. Initially, it was proposed that cysteine provided the source of thiol for the final stage of CoM biosynthesis in methanogenic archaea (refer to Ch. 1). Though there is some speculation whether cysteine or endogenous H_2S provides the thiol source, and the identity of the enzyme(s) remains unknown, it is established that reductive thiol addition occurs in the last stage of both PEP- and L-phosphoserine-dependent methanoarchaeal CoM biosynthesis pathways.

It is attractive to propose therefore that XcbE1 supplies cysteine-derived sulfur that is ultimately incorporated into CoM. Since many PLP-dependent enzyme reactions moreover share common intermediates, and several enzymes have been shown to be bifunctional, it is conceivable that XcbE1 could be a bifunctional PLP enzyme, catalzying a more complicated final step that results in the production of CoM. We have proposed a scheme that requires XcbE1 to utilize two substrates (cysteine and unknown intermediate) and in a bifunctional role (thiol addition and decarboxylation). To probe the role of XcbE1 in CoM biosynthesis, we examined the reaction through several means, including co-substrate screening and UV/vis, LC-MS, and NMR methods.

Methods

Amplification of *xcbE1*

X. autotrophicus Py2 was grown as described in Ch. 2. Sequences for the putative biosynthetic operon were obtained from the NCBI database file for the pXAUT01 megaplasmid. Primers (Integrated DNA Technologies, San Diego, CA) were designed for *xcbE1* (XAUT_RS24695):

[Fwd: 5'- ACACTGCAGATGGAGCAGCCTGACATGCGG-3'] and

[Rev: 5'- AGCGATATCTCACGCGGTTCCATCGACGAAC -3'].

Restriction sites were added to clone *xcbE1* (F: PstI/ R: EcoRV) with an added N-terminal His-tag into a Duet Expression System (Novagen). Amplicons were initially cloned into a pGEM-T vector and transformed into JM109 competent cells for propagation, before being cloned into a Duet vector. XcbE1 was inserted into multiple cloning site 1 (MCS1) of a pETDuet-1 (Amp^R) vector, and sequences were verified via Davis Sequencing (Davis, CA).

Expression and Purification of XcbE1

The XcbE1-pETDuet-1 construct was transformed into BL21(DE3) competent cells and grown on ampicillin-supplemented (0.1 mg/mL) lysogeny broth (LB+Amp) agar plates. A single colony was used to inoculate an overnight culture in liquid LB+Amp medium.

A larger scale purification protocol was implemented for expression from XcbE1-pETDuet-1, but scaled down growths were easily achieved using the typical growth

conditions for *E. coli* in standard incubators (i.e. 250 rpm). 16 L fermenter cultures were grown from an overnight culture inoculum at 10% volume in LB+AMP supplemented with 40 µM of the PLP-precursor pyridoxine (400 rpm, 37°C). Expression was initiated with 10% volume of the overnight culture and incubated at 37°C with agitation at 400 rpm until the culture reached an OD600 of 0.6-0.8. Protein expression was induced with 1 mM IPTG, with continued agitation for 3 hrs at 30 °C .

For purification, frozen cell pellets were resuspended in lysis buffer (20 mM Tris, 500 110 mM NaCl, 5 mM imidazole, pH 8) and homogenized with the addition of lysozyme, DNase, and PMSF. Cultures larger than 1 L were lysed using a microfluidizer (M-110L Microfluidics 112 Corporation, Newton, MA). The lysed pellets were centrifuged (105,000 x g, 1h) and the clarified lysate loaded onto a Ni-NTA column. The Ni-NTA columns were equilibrated to the lysis buffer prior to loading the cleared lysate. For FPLC elution, a 75 mL gradient from 0-100% elution buffer was used. The elution buffer contained 20 mM Tris, 500 mM NaCl, 300 mM imidazole, and 20% glycerol. SDS-PAGE and Western blot (anti-His tag antibodies) were used to determine the purity of the protein (~34 kDa) as well as integrity of the His-tag. Purified protein exhibited a bright yellow color, indicative of the PLP cofactor. Pure protein was concentrated by centrifugation-filtration (Merck Millipore) and buffer exchanged into the imidazole-free buffer (20 mM Tris, 100 mM NaCl) via a P2 desalting column (Bio-Rad). The protein was stored at -80°C with 10% glycerol.

XcbE1 Phylogenetics

22 PLP-dependent enzymes including ACCD, canonical D-cysteine desulfhydrases, canonical L-cysteine desulfhydases, and D-cysteine desulfhydrase-type enzymes from other organisms with CoM-dependent alkene metabolism were selected for comparison to both XcbE1 and XcbE2 sequences. Phylogenetic trees were generated using MEGA (Version 6.06).

Determination of Activity with an Assay for H_2S Formation

The production of H_2S can be detected using a method that converts H_2S to methylene blue with the addition of N',N'- 174 dimethyl-*p*-phenylenediamine dihydrochloride (DPPD) (20 mM in 7.2 M HCl) and 30 mM $FeCl_3$ in 1.2 M HCl[17]. Enzymatic assays were conducted in sealed crimp vials containing 400 µL reaction buffer (100 mM Tris, 100 mM NaCl, pH 8). 100 µL of 10 mM L-or D-cysteine was injected through the septum to initiate the reaction. Reactions were incubated for 1h at 30°C, followed by quench and derivatization with 100 µL each of DPPD and acidified $FeCl_3$. Color development proceeded for 30 min at room temperature. Absorption was measured at 670 nm and referenced to a standard curve generated under identical conditions from Na2S (0-100 µM).

Screening XcbE1 Reaction for Aldehyde/Ketone Products

The production of pyruvate was initially detected using an aldehyde/ketone indicator, 2,4-dinitrophenylhydrazine. 500 uL enzymatic reactions containing cysteine were incubated at 30°C over various time points, then quenched with 200 ul 2,4-dinitrophenylhydrazine in 3 M HCl. The reaction proceeded for 10 minutes at 37°C, and

then color development was initiated by adding 600 uL of 2 M NaOH. After approximately 5 minutes, the samples were diluted 1:10 and the absorbance was measured at 440 nm. Commercially available pyruvic acid was used as a control, and the threshold was tested with a range from 0-5 mM pyruvic acid.

Measurement of Pyruvate Production

Pyruvate production can be quantified using a coupled assay with lactate dehydrogenase (LDH)[16,17].The LDH-catalyzed conversion of pyruvate to lactate is NADH-dependent, and the oxidation of NADH can be monitored via its absorbance at 340 nm. Enzymatic assays contained reaction buffer (100 mM Tris, 100 mM NaCl), purified XcbE1, 2 mM D- or L- cysteine, 120 µM NADH and 10 µL 5 mg/mL rabbit muscle LDH (Sigma). Absorbance was measured at 340 nm (ε340 = 6220 M-1 cm-1) every 0.1 s for 6 min at 30°C following Cys addition on a Cary60 UV-Vis (Agilent) in kinetics mode. The final concentration of pyruvate was quantified at the end of each reaction. Assay reagents were sealed into crimp vials and incubated for 1 h at 30°C, followed by boiling for 10 min to inactivate the enzymes. The absorbance at 340 nm (relative to no-enzyme controls) was used as a measure of total pyruvate produced.

Detection of Cysteine Consumption

Consumption of cysteine was measured using a ninhydrin assay[28,29]. Under acidic conditions, ninhydrin is specific for labeling the amino group of cysteine over the other amino acids. Enzymatic reactions were carried out as described above and terminated with 100 µL of acetic acid. 250 mg ninhydrin was dissolved in 10 mL glacial acetic acid:concentrated HCl 60:40 v/v%. 200 µL of this ninhydrin reagent mixture was added

to each terminated enzymatic reaction. The samples were boiled for 10 min, then rapidly cooled before the addition of 600 µL 95% EtOH. Sample absorption was immediately measured at 560 nm on a Cary50 UV-Vis (Agilent). Cysteine concentrations were calculated from a standard curve using 0-1 mM cysteine.

Confirming PLP-Dependence

Hydroxylamine is a known inhibitor of PLP-dependent enzymes[30]. Purified XcbE1 was dialyzed against buffer containing 5 mM hydroxylamine for 16 h. The dialyzed aliquot of XcbE1 was assayed for H_2S formation (as described previously) against a non-dialyzed batch for activity comparison.

Determination if Thiol-Specific Alkylating Agent Inhibits XcbE1 Activity

Cysteine desulfurases utilize an active site cysteine to carry out catalysis of L-cysteine[14]. Since it appears that XcbE1 may contain a cysteine in the location of the NifS active site cysteine (Cys325, *Azotobacter vinelandii* numbering), an inhibition assay was adapted from prior methods[14]. In uncrimped 3 ml vials, 2.7 nmol of XcbE1 was incubated with 0, 0.675, 1.35, 2.7, and 5.4 nmol of *N*-ethylmaleimide (NEM) for 3 hrs at ambient temperature in 50 mM Tris, 50 mM NaCl buffer, pH 8. Each vial was then crimped, and to each sample, 1 mM L-cysteine was injected and then incubated at 30 °C for 30 mins prior to injecting the necessary reagents for H_2S methylene blue formation, described above.

XcbE1 Crystal Screens

Purified XcbE1 was prepared for crystallization using Disposable PD-10 Desalting Columns containing Sephadex G-25 resin (GE Healthcare Life Sciences) equilibrated with crystallization buffer (10 mM Tris, 10 mM NaCl, pH 8). Crystal screens used for initial set-up were: 1) Hampton Index, 2) Salt RX, 3) PEG-Rx 1 and 2, 4)HR PEG-ion/HR Natrix, 5)Crystal Screen Lite and Cryo 6) Emerald Cryo 1 and 2 (Hampton Research, Aliso Viejo, CA) and were set up using were set up using a Digilab Honeybee crystallization robot (Digilab Inc., Marlborough, MA). Second round crystallizations were carried out in a 24 well plate using 1 mL total of mother liquor and 2 µL purified enzyme; All wells were pH 6, with 0.05 M sodium cacodylate and 0.01 M $CaCl_2$ held constant while PEG was varied at 6, 8, 10, 12, and 14, and 16% w/v across the wells, with KCl present at 100, 150, 200, and 250 mM down the wells. Prepared screens were incubated at 18°C.

Proposed Co-Substrate Activity Screens

Assays with Proposed Cosubstrates. Screens to identify potential cosubstrates for XcbE1 that may react with either H_2S gas or cysteine itself were carried out using various CoM intermediate analogs; vinyl sulfonic acid (Sigma), isethionic acid (Sigma), 3-sulfolactate(Chempacific), or sulfoacetaldehyde (synthesis described in next section). Proposed cosubstrates were added to the previously described H_2S assays in varying concentrations up to 2 mM with L-or D-cysteine were and compared to samples where cysteine was the only substrate present. Levels of H_2S production could indicate if XcbE1 may be utilizing H_2S or cysteine for a bifunctional reaction.

Synthesis and Biological Preparation of Sulfoacetaldehyde. Synthesis of the sulfoacetaldehyde bisulfite adduct (SABA) was adapted from prior methods[31] and carried out by charging a round bottom flask with 2.93 mL of 2-bromo-1,1-dimethyoxyethane and 5 mL 1 M HCl. The mixture was heated to 100°C and refluxed until homogenized into solution. The solution was cooled slightly and approximately 35 mL of an aqueous solution consisting of 3.78 g sodium sulfite and 1.95 g sodium metabisulfite was added dropwise. Once complete, the solution was heated to 100°C and refluxed for 40 hrs. Recrystallization was carried out twice, using 1:1 ethanol:dH_2O, after drying, ~4.7 g of product was recovered. Mass spectrometry, ^{1}H-NMR and ^{13}C-NMR were used to confirm structure (SABA = 250.1 g/mol).

The bisulfite protecting group was removed from SABA for use in assays by dissolving SABA to 0.5 M in dH_2O to 250 µL total volume. 500 µL of 0.5 M $BaCl_2$ was added, and the resulting precipitate was centrifuged at 14,000 x g, with supernatant retained. To the supernatant, 500 µL of 0.5 M Na_2SO_4 was added, and the resulting precipitate was centrifuged at 14,000 x g. Retained supernatant (free sulfoacetaldehyde = 123.1 g/mol) was then used in experiments. Free aldehyde can be detected by adding 25 µL of 0.1 M Purpald reagent dissolved in 0.5 M NaOH to enzymatic assays Samples tubes were left open overnight, and after overnight oxidation, Purpald-aldehyde adducts were detected at 550 nm on a Cary50 UV-Vis (Agilent).

Detection of CoM using HPLC-FLD

Derivatization of small thiols was adapted from a prior procedure[32]. Enzymatic reactions were set up using buffer (50 mM Tris, 50 mM NaCl, pH 8), varying concentrations of XcbE1, and 0-2 mM L-cysteine, and 0-2 mM sulfoacetaldehyde, with dH_2O to bring the final volume to 500 µL. Samples were allowed to incubate from 15-45 mins at 30°C. Once the desired time was completed, 250 µL of enzyme reaction was added to 250 µL of MOPS/TCEP derivatization buffer (20 mM MOPS, 50 mM NaCl, 5 mM TCEP, and 10% glycerol, pH 7.2). A preparation of 3 mg of N-(1-pyrenyl)maleimide (NPM) was dissolved in 10 mL acetonitrile (1 mM final concentration), and 500 µL of the NPM/ACN was added to the 1:1 enzyme reaction/derivatization buffer mix. Samples were allowed to derivatize for 10 minutes at room temperature, followed by 10 µL of 2 M HCl to quench the reaction. To the quenched derivatization reactions, 1 mL acetone was added to precipitate any protein, and samples were frozen at least 1 hr to overnight. Before HPLC-FLD analysis, samples were centrifuged for 15 mins at 14,000 x g and supernatant was retained. Control samples of commercially available CoM (0-1 mM) and sulfoacetaldehyde were treated in the exact manner described for enzymatic reactions.

HPLC-FLD analysis was performed on an Agilent 1100 series instrument outfitted with a fluorescence detector. A Luna 5u C18(2) column was used, with 100Å pore size, 150 x 4.6 mm dimensions (Phenomenex, Inc., Torrance, CA) and fitted with a guard column consisting of C18 4 x 3.0 mm SecurityGuard Cartridges (Phenomenex, Inc., Torrance, CA). Mobile phases consisted of; A – 90% dH2O, 10% ACN, 0.1% *o*-

phosphoric acid, and 0.1% acetic acid, and B - 90% ACN, 10% dH2O, 0.1% *o*-phosphoric acid, and 0.1% acetic acid. Separation of thiols was achieved using the following method; 0-2 mins: 30% B, 2.1-5 mins: 45% B, 5.1-21 mins: 45-100% B, 21-24 mins: 100% B, 24.1-27 mins: 30% B.

Results and Discussion

XcbE1 Bioinformatics Provides Preliminary Insight Into Activity

Structural studies of the D-cysteine desulfhydrase in *Salmonella typhimurium* indicated the following active site residues: Asn 50, Lys51 (PLP binding), Ser78, Asn79, His80, Tyr261, Tyr287, Thr288, Thr315, and Gln77[20]. These residues are all conserved in *X. autotrophicus* Py2 XcbE1, except for Thr315 and Gln77. However, the active sites for the ACCD from *Hansenula saturnus*[19] contains several of these conserved residues (Asn50, Lys51, Ser78, Asn79, *S. typhimurium* numbering) in addition to the conserved Glu/Leu residues that confer substrate bias. Alignment of the XcbE1 amino acid sequence with the ACCD from *H. saturnus* and D-cysteine desulfhydrase from *S. typhimurium* indicates that XcbE1 contains a similar D-cysteine desulfhydrase Thr/Ser replacement at the canonical ACCD Glu/Leu (Fig 1).

```
                310         320         330         340
XcbE1  VYTGKAMAGY GALVGAGRYG EAATVLFLHS GGLPSLFVDG
ACCD   VYEGKSMQGL IALIKEDYFK PGANVLYVHL GGAPALSAYS
DCD    VYTGKAMAGL IDGISQKRFN DDGPILFIHT GGAPALFAYH
```

Figure 3.5. A section of the *X. autotrophicus* Py2 XcbE1 amino acid alignment with the *H. saturnus* ACCD and *S. typhimurium* D-cysteine desulfhydrase (DCD) is shown, with yellow highlight showing the Thr/Ser residues for XcbE1 and D-cysteine desulfhydrase replacing the blue highlighted canonical Glu/Leu residues of ACCD.

Investigation of the paralogous downstream XcbE2 sequence revealed an identical Thr/Ser replacement. This observation suggests that XcbE1 was erroneously annotated as an ACCD protein, when instead it may be a D-cysteine desulfhydrase. Phylogenetics indicate that XcbE1 and its homologs from *Nocardioides* and *Mycobacterium* share a common ancestor with D-cysteine desulfhydrase and ACCD, where the D-cystine desulfhydrase and XcbE1 are closer to the mutual ancestor than ACCD (Fig 3.6).

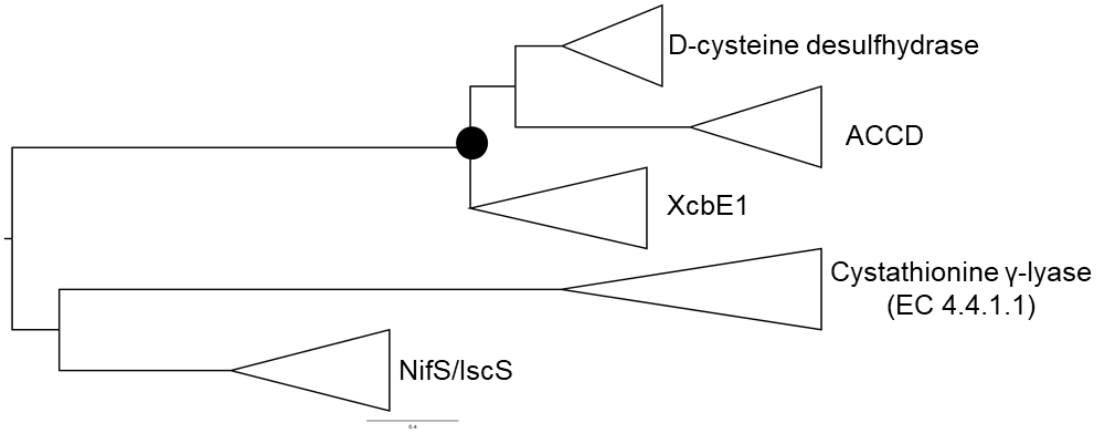

Figure 3.6. Cysteine desulfhydrase/desulfurase type enzymes from 25 organisms were grouped in a phylogenetic tree (100 bootstrap replications). The bootstrap value (black circle = >90) for the clade most relevant to this work is shown. The clade containing cystathionine γ-lyase and NifS/IscS did not originally show any value, likely due to large degree of separation between the groups shown in the tree.

We proposed that XcbE1 may be bifunctional, but the nature of its function(s) is unclear from a bioinformatics perspective. With relatively low amino acid sequence identity amongst the substantial PLP-dependent family of enzymes, it can difficult to determine what key residues distinguish enzymes that carry out other basic PLP reaction types.

XcbE1 was also compared to other cysteine desulfhydrases and cysteine desulfurases, including NifS and IscS. NifS is involved in nitrogenase maturation and catalyzes the removal of elemental sulfur from L-cysteine to yield alanine[14]. The active site Cys325 in NifS appears to be conserved in XcbE1, IscS and L-cysteine desulfhydrase, but is not present in the canonical D-cysteine desulfhydrase (Fig 3.7).

```
                320         330         340
XcbE1 IIHDGFIGAG YGIASPAGMS ALERAARCEG
NifS  IAFEYIEGEA ILLLLNKVGI AASSGSACTS
IscS  LSFNYVEGES LIMSLR--DL AVSSGSACTS
DCD   LLWDDYFAPG YGVPNDEGME AVKLLARLEG
LCD   LSFNYVEGES LLMSLK--DI AVSSGSACTS
```

Figure 3.7. XcbE1 was aligned with four other enzymes, and an active site cysteine from NifS (Cys325) appears to be conserved in all enzymes (yellow highlight) except for D-cysteine desulfhydrase (blue highlight). The enzymes are from the following organisms: NifS and IscS; *Azotobacter vinelandii*, D-cysteine desulfhydrase (DCD); *E. coli*, and L-cysteine desulfhydrase (LCD); *Pseudomonas putida*.

Purification of XcbE1

Addition of pyridoxine (PLP precursor) increased expression of soluble XcbE1 relative to insoluble material. Elution of XcbE1 from any column used was immediately visible by eye, due to the yellow color attributed to the PLP cofactor (Fig 3.8).

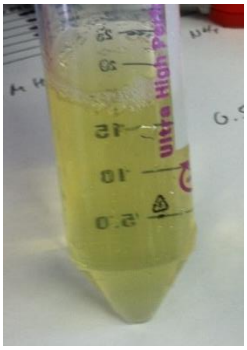

Figure 3.8. Eluted XcbE1 exhibits yellow color indicative of the PLP-cofactor.

UV/vis scans of purified XcbE1 can provide additional confirmation of PLP occupancy at with the characteristic ε-amino-group of lysine bound-PLP peak at 417 nm (ε = 5020 M^{-1} cm^{-1}) (Figure 3.9). Purifications typically yield enzyme with 85-95% PLP occupancy.

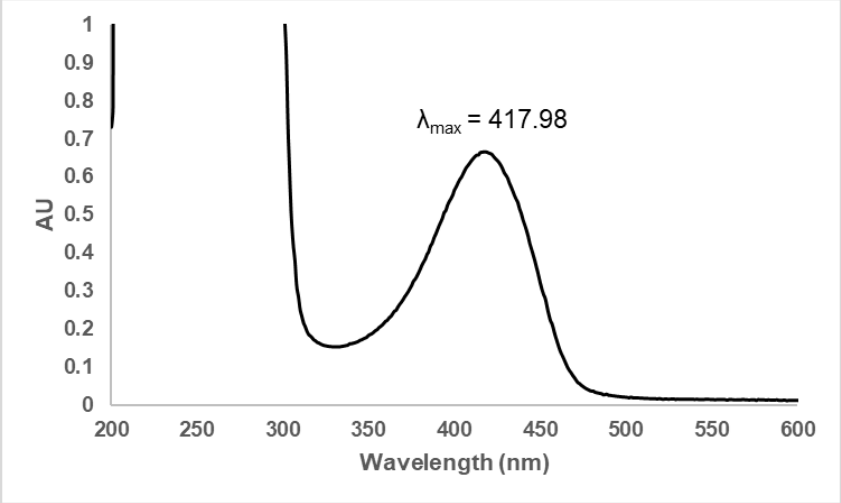

Figure 3.9. UV/Vis scans of purified XcbE1 exhibits a characteristic enzyme bound-PLP peak at 417-420 nm. Free PLP has been reported to exhibit absorbance anywhere from 325-388 nm[33], which is undetectable in the shown figure, likely due to insufficient concentration for detection.

Testing XcbE1 for Canonical D-cysteine Desulfhydrase Activity

XcbE1 activity in the context of CoM biosynthesis was not inherently obvious, necessitating a series of assays to establish what, if any, reaction XcbE1 may catalyze. The most logical course resulted in assaying for canonical D-cysteine desulfhydrase activity (D-cysteine → H_2S + pyruvate + ammonia). A common method for detecting H_2S formation involves formation of methylene blue which can be readily compared on UV/Vis. Some studies suggest that the methylene blue method has some serious critical issues, including dimer/trimer formation of methylene blue that does not follow Beer's law, leading to erroneous results[34]. While this assay may not be suitable for concrete quantitative results, it provides a relatively easy, and inexpensive method for quick comparison of simplified enzymatic reactions in aqueous conditions. To establish a general background for XcbE1 reactivity, the enzyme was incubated with D- and L-cysteine, and L-alanine and assayed for H_2S formation (Fig 3.10). In lieu of more precise methods for measuring H2S, we found that specific activity was 27.31 ± 2.32 nmol $H_2S/min^{-1}mg\text{-}XcbE1^{-1}$ for L-cysteine and 5.04 ± 1.95 nmol $H_2S/min^{-1}mg\text{-}XcbE1^{-1}$for D-cysteine.

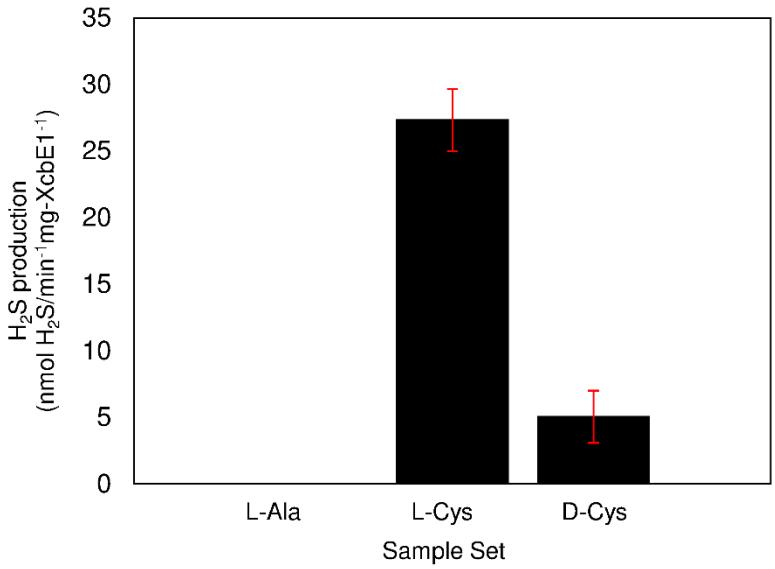

Figure 3.10. A methylene blue activity assay measuring levels of H_2S gas was used to determine relative activity of XcbE1 when supplemented with D- or L-Cys, with L-Ala used as a control. Specific activity was 27.31 ± 2.31 nmol $H_2S/min^{-1}mg\text{-}XcbE1^{-1}$ for L-Cys and 5.04 ± 1.95 nmol $H_2S/min^{-1}mg\text{-}XcbE1^{-1}$for D-cys.

Surprisingly, XcbE1 could catalyze both stereoisomers of cysteine, marking a departure from canonical D-cysteine desulfhydrases that are specific for D-cysteine[16,20,21]. However, formation of H_2S establishes only part of the reaction, and does not fully confirm canonical D-cysteine desulfhydrase activity since some L-cysteine desulfurases yield alanine as an additional product, rather than pyruvate[14]. Using this assay, XcbE1 pH optimum was pH 8 (Fig 3.11). For any experiments that involve the addition of additional cosubstrates (described later in the chapter), it is crucial to ensure that any experimental additives do not significantly alter the pH of the enzymatic assay since pH shifts in either direction reduce XcbE1 activity by approximately 50-75%, which could potentially generate false positives.

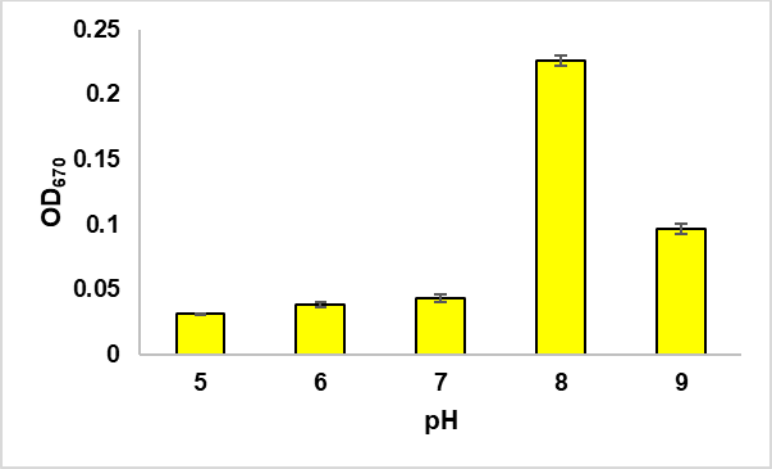

Figure 3.11. Using the H_2S methylene blue assay, XcbE1 reactions at pH 8 yield highest levels of H_2S production.

Rapid, preliminary detection of the presence of a ketone in solution, such as pyruvate, can be carried out using 2,4-dinitrophenylhydrazine (ε = 4000 M^{-1} cm^{-1} for indicator-product adduct), a general aldehyde/ketone indicator (Fig 3.12). Much like the H_2S methylene blue formation assay, this method of detection would not be appropriate for a complex biological matrix, but provided a simple means for confirmation for the presence of an aldehyde or ketone. Based on canonical D-cysteine desulfhydrase references, the putative aldehyde/ketone is pyruvate. Incubation of XcbE1 with L-cysteine resulted in a clear signal at 440 nm that correlates with the signal given by the pyruvate control. As expected, alanine does not yield any peaks, establishing that XcbE1 is generating an aldehyde or ketone.

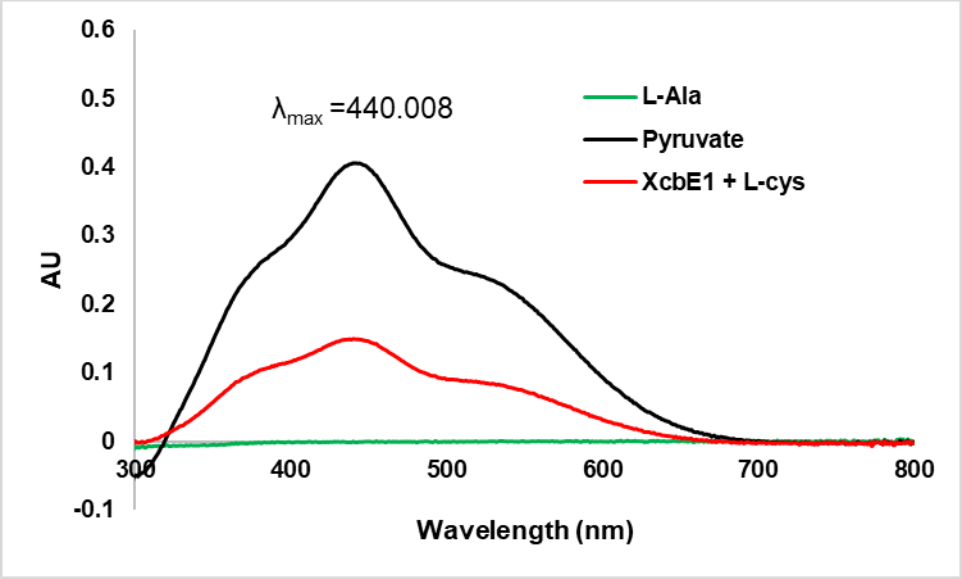

Figure 3.12. Confirmation of the presence of a ketone or aldehyde (putatively pyruvate) was achieved using 2,4-dinitrophenylhydrazine. The respective concentrations for samples shown are as follows: 1 mM L-alanine, 1 mM pyruvate, and XcbE1 + 1 mM L-cysteine.

Further confirmation of pyruvate generation by XcbE1 was achieved through the coupled assay with LDH, and allowed for preliminary kinetic data. The conversion of pyruvate to lactate in an NADH-dependent reduction catalyzed by LDH can be monitored by monitoring the decrease in absorption of NADH at 340 nm ($\varepsilon = 6220\ M^{-1}\ cm^{-1}$)[35,36]. Inititial rates of reaction for each D- and L-cysteine were calculated at various concentrations of substrate and fitted to a curve via Kaleidagraph (Fig 3.13). Both D- and L-cysteine isomers were effective substrates where V_{max} and K_m for each D- an L-cysteine were 49.01 nmol/min^{-1}mg^{-1} and 9.45 µM, and 78.78 nmol/min^{-1}mg^{-1} and 3.52 µM, respectively. Additionally, utilization of a specific coupled assay confirms the identity of the XcbE1 reaction co-product as pyruvate. Ammonia is presumed to be the other product based on canonical D-cysteine desulfhydrase reactions, as described earlier.

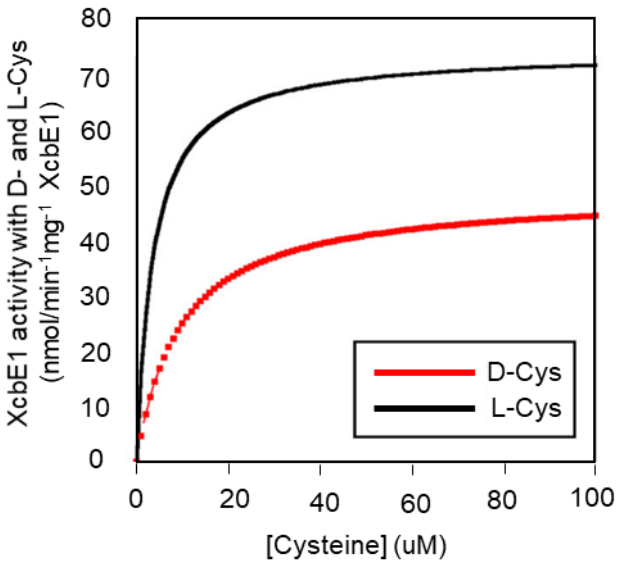

Figure 3.13. Plotted curves for pyruvate production at varying concentrations of D-and L-cysteine indicate that XcbE1 generates pyruvate as a product, and can utilize both isomers.

Cysteine detection methods described herein use ninhydrin as a detection reagent, and can provide an alternative assay method if H_2S detection is inadequate (data not shown). However, the ninhydrin assay also comes with some issues, including rapid sample degradation.

To confirm that XcbE1 is PLP-dependent, an aliquot of purified enzyme was dialyzed against buffer containing the classic PLP-inhibitor, hydroxylamine. The XcbE1 batch that did not undergo dialysis, along with the dialyzed batch, was incubated with cysteine and assayed for H_2S formation (data not shown). The dialyzed batch did not exhibit activity towards cysteine, indicating that XcbE1 is PLP-dependent and suggesting that H_2S is released through the expected enzyme-bound PLP mechanism (Fig 3.14).

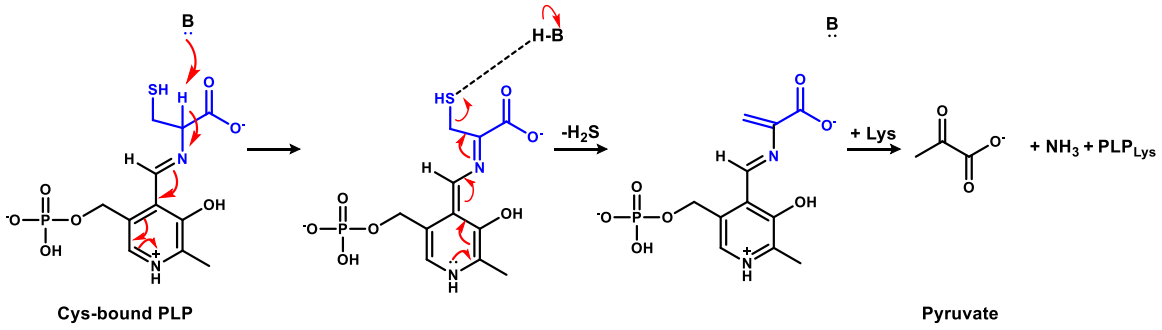

Figure 3.14. The proposed truncated mechanism for XcbE1 is depicted, with the cysteine-bound PLP (i.e. external aldimine) undergoing proton abstraction from the cysteine C_{α}, initiating the reaction. Release of H_2S is followed by displacement of the aminoacrylate moiety by the active site lysine, re-forming the internal aldimine for further catalysis. The displaced aminoacrylate moiety hydrolyzes to form pyruvate and ammonia.

Screening XcbE1 Reactions for Proposed Cosubstrates

L- and D-cysteine desulfhydrase activity has been established for XcbE1, but probing the role of XcbE1 in the context of CoM biosynthesis proved to be more challenging. The unexpected ability to catalyze L-cysteine where canonical D-cysteine desulfhydrases will not react suggests that XcbE1 may facilitate other reactions. Our goal was to determine if XcbE1 provides cysteine-derived sulfur to CoM for the thiol moiety, either solely through release of H_2S, or through use of a bifunctional mechanism that requires a cosubstrate to act with cysteine. The identity of the XcbD1 product would likely delineate the nature of the XcbE1 reaction, but we faced significant challenges with XcbD1, to be elaborated in Ch. 4. We proposed several CoM analogs that could reasonably act as the final intermediate or cosubstrate prior to XcbE1 catalysis; isethionate, vinyl sulfonate, sulfolactate, and sulfoacetaldehyde (Fig 3.15).

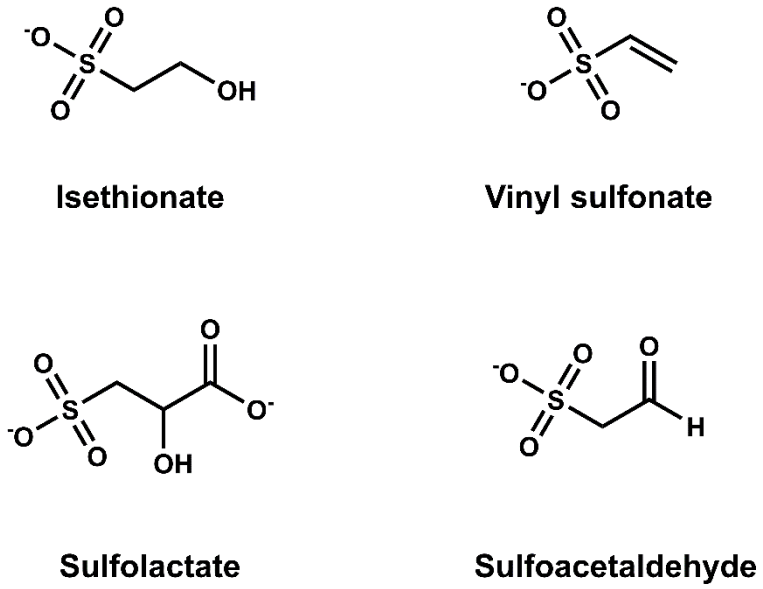

Figure 3.15. Derivatives of CoM were conceived as final intermediates and/or cosubstrates for the XcbE1 reaction.

Though we currently know more about the trajectory of the pathway, at the time of these experiments, we proposed derivatives that contained a sulfonic acid moiety, were devoid of phosphate groups, and contained a 2-3 carbon backbone (2 carbon if free of carboxylic acid or 3 carbon with carboxylic acid group). Sulfolactate is an intermediate in the PEP-dependent methanoarchaeal biosynthetic pathway, while sulfoacetaldehyde is the final intermediate in both methanoarchaeal pathways. Isethionate is a small alcohol that could undergo minimal transformations to form CoM and vinyl sulfonate is a dehydrated derivative of isethionate that could conceivably undergo even fewer transformations to yield CoM. We proposed that any viable cosubstrate would either undergo a bifunctional XcbE1 reaction with cysteine, or capture H_2S through enzymatic/spontaneous means. Ideally, the H_2S methylene blue assay could provide the most preliminary information for identifying a potential cosubstrate, i.e. if cysteine or H_2S are sequestered for the proposed

CoM reaction, then levels of H_2S will be reduced compared to the XcbE1 and cysteine only reaction. At the time these substrates were proposed, the XcbC1 reaction was not fully established and there was no real proposal yet for XcbD1, so some of these substrates seem illogical for a transformation from sulfoacrylic acid to CoM, hence why they have been archived. However, the methods and analysis used with these compounds may be useful in the future when testing out other compounds, or if the product of XcbD1 is identified.

Isethionate and vinyl sulfonate. Isethionate and vinyl sulfonate are not associated with either methanoarchaeal pathway for CoM biosynthesis, but loosely fit the criteria for a molecule that could reasonably act as an intermediate in the pathway for CoM biosynthesis. Isethionate and vinyl sulfonate were independently incubated at equimolar concentrations with cysteine, and compared to samples that did not contain either cosubstrate on the basis of H_2S formation (Fig 3.16A). When the samples were incubated for 1 hr, it appeared that there were reduced levels of H_2S in the XcbE1 with L-cysteine and vinyl sulfonate. The simplicity of vinyl sulfonate was appealing, and we envisioned an *anti*-markovnikov type reaction where H_2S would be added across the vinyl group, forming CoM. This observation was followed up with a time course comparing levels of H_2S in samples from 0-15 mins (Fig 3.16B). With inconclusive results from the time point assay, vinyl sulfonate was then added to the XcbE1 + L-cys reaction in vast excess (5 mM:0.5 mM), resulting in no significant change to the H_2S levels (data not shown). Additional attempts to probe the reaction were similarly inconsistent and inconclusive, with H_2S levels not being reduced significantly enough to attribute to an additional

reaction. We attributed the minor H_2S reduction to inconsistencies in the methylene blue assay, and possibly some spontaneous addition of cysteine thiol/H_2S to vinyl sulfonate. Therefore, we ruled out isethionate and vinyl sulfonate from consideration for the potential cosubstrate.

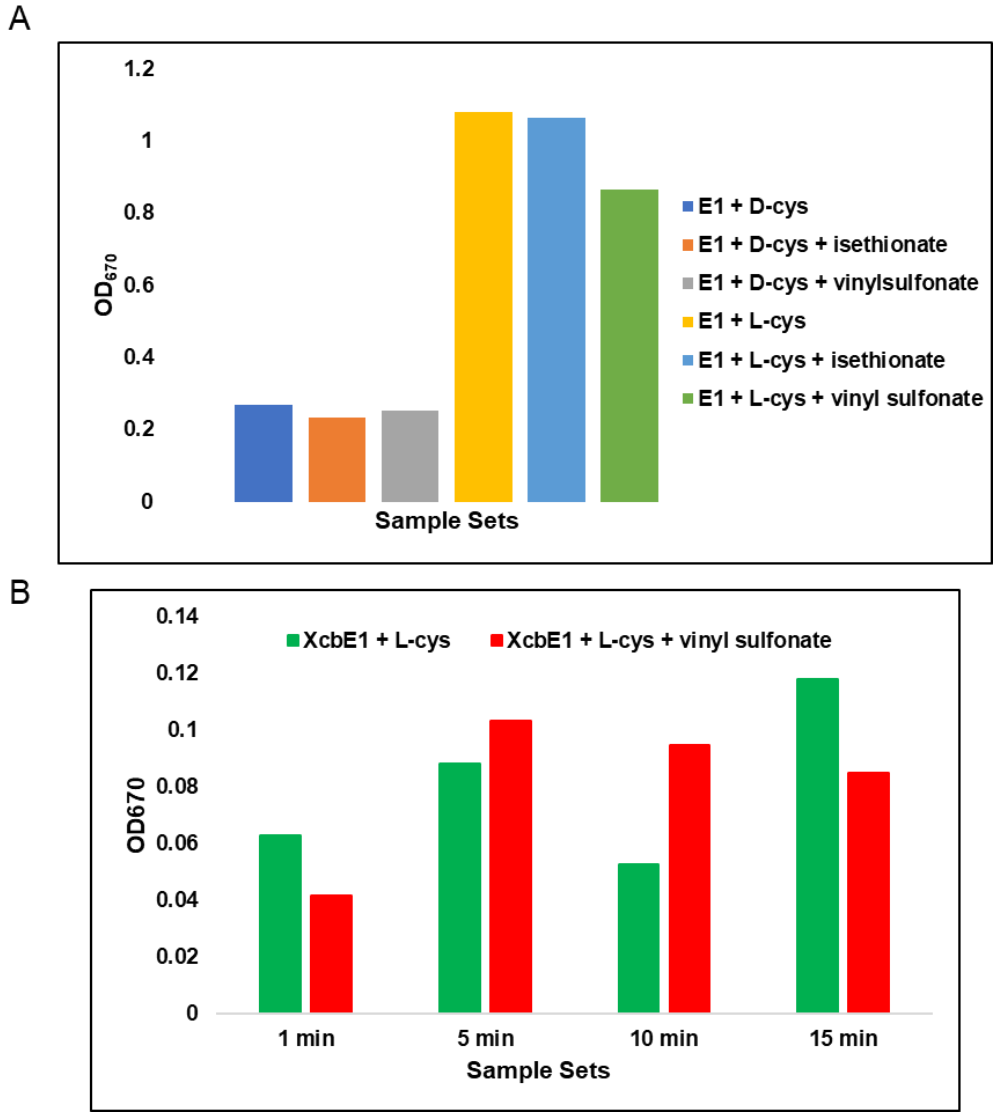

Figure 3.16. XcbE1 (0.1 mg) was incubated with 2 mM D-or L- cysteine plus either 2 mM isethionate or vinyl sulfonate and compared to samples containing only XcbE1 with D-or L-cysteine at pH 8 for 1 hr prior to derivatization with the H_2S methylene blue assay (A). Preliminary results indicated some reduction in H_2S levels when vinyl sulfonate was

present. H_2S formation was measured at time points from 0-15 minutes with XcbE1 incubated with 2 mM L-cysteine and 2 mM vinyl sulfonate, and compared to XcbE1 plus L-cysteine only (B). Results appear inconsistent and inconclusive.

Sulfolactate. Sulfolactate is the third intermediate in the PEP-dependent methanoarchaeal CoM biosynthetic pathway, and was considered as a potential cosubstrate in the XcbE1 reaction. Ch. 2 described the first two reactions established for bacterial CoM biosynthesis, culminating in the production of sulfoacrylic acid. This intermediate is proposed to be the XcbD1 substrate, a member of the AFS that catalyzes reversible β-elimination reactions. Due sulfoacrylic acids analogous tructure to fumarate and lack of saturated carbons, we proposed a fumarase-type reaction in which water is added across the double bond to yield sulfolactate as the cosubtrate to XcbE1. Sulfolactate was then incubated with XcbE1 and L-cysteine as described for vinyl sulfonate and isethionate (Fig. 3.17).

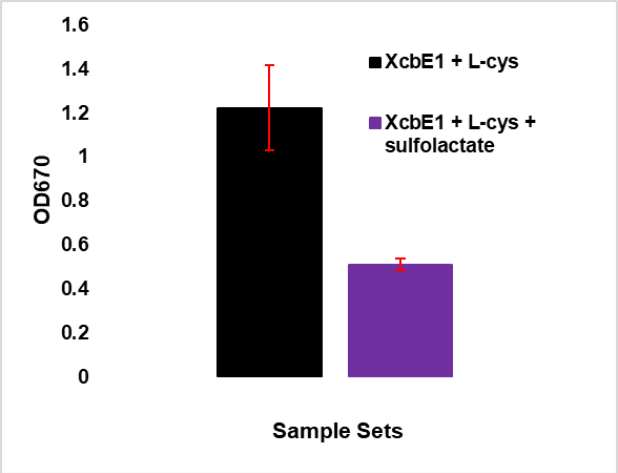

Figure 3.17. XcbE1 (0.1 mg) was incubated with 2 mM L- cysteine plus 2 mM sulfolactate and compared to samples containing only XcbE1 with L-cysteine for 1 hr at pH 8.

Preliminary results for sulfolactate indicated more significantly reduced H_2S levels compared to vinyl sulfonate, which led to further experimentation to determine whether sulfolactate was: 1) a viable cosubstrate for the XcbE1 reaction, 2) an XcbE1 inhibitor, or 3) involved in a side reaction with cysteine/H_2S that resulted in an unexpected product.

HPLC-FLD and NPM derivatization were utilized to determine if CoM was produced during incubation of XcbE1 with L-cysteine and sulfolactate (Fig 3.18). Using synthetic CoM standards, the HPLC-FLD detection limit was 1 μM CoM in buffered solution, which corresponded to 10 pmol injected CoM. Additional HPLC-FLD experiments aimed at improving yields for the XcbE1 incubated with L-cysteine and sulfolactate reaction did not generate any detectable levels of CoM (data not shown). Due to these results, sulfolactate was then eliminated from consideration as a cosubstrate for XcbE1.

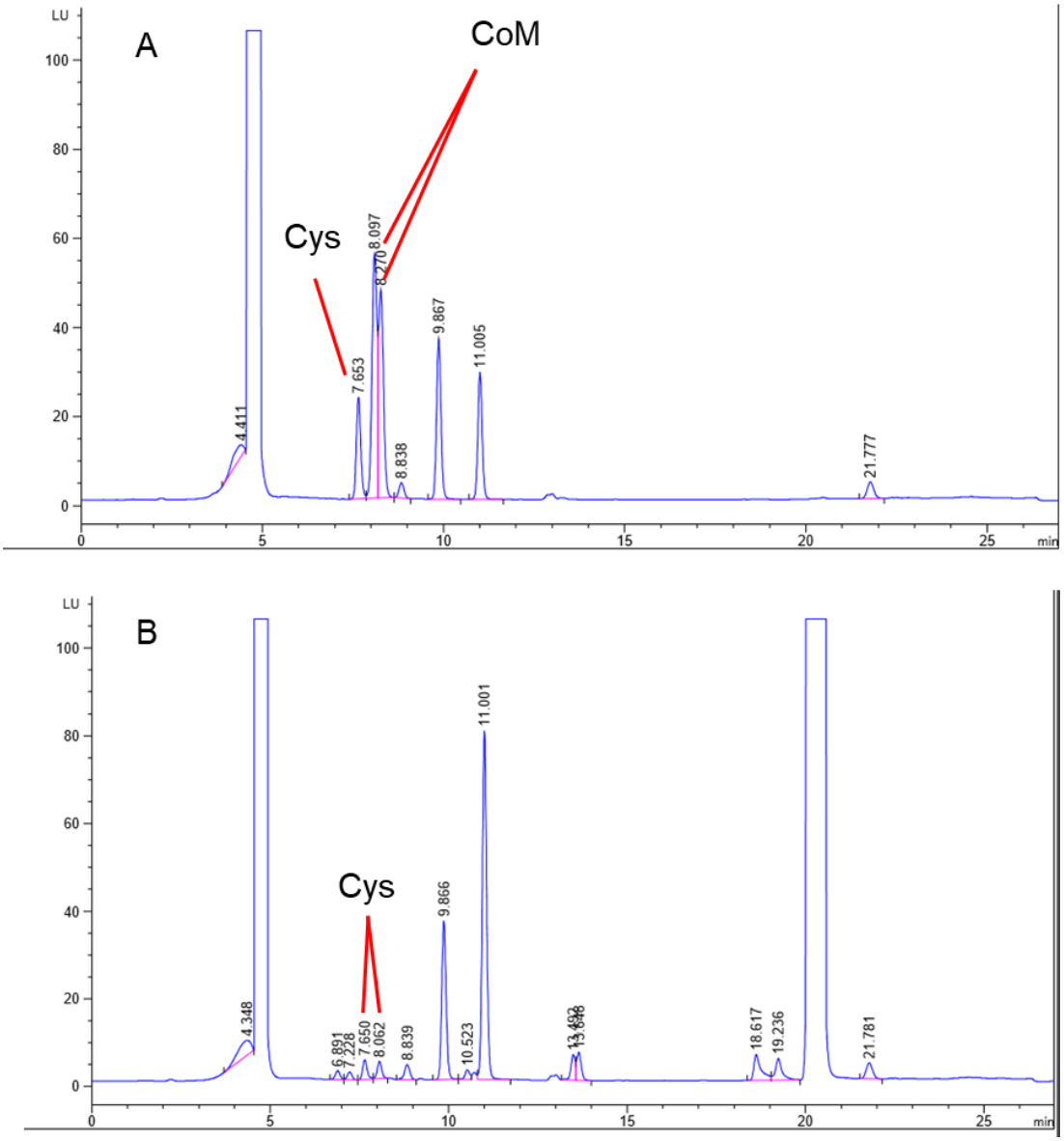

Figure 3.18. Standards of 1 mm L-cysteine, 20 µM CoM, and 2 mM sulfolactate were mixed and injected to determine retention times for more complex samples (A). CoM has two peaks at 8.0 and 8.2 mins that we attributed to a racemic mixture of the CoM-NPM adduct, where L-cysteine has two peaks at 7.6 and 8.0 min. The second peak is not visible due to co-elution with the CoM signal. Sulfolactate appears to not undergo significant derivatization, and is undetected. In enzymatic samples where XcbE1 was incubated with 1 mM L-cysteine and 2 mM sulfolactate, both peaks for L-cysteine were visible but CoM was undetected (B).

Sulfoacetaldehyde. Finally, sulfoacetaldehyde was synthesized for use as a co-substrate. This molecule was particularly intriguing due to the correlation with the final intermediate for both methanoarchaeal pathways. As in both methanoarchaeal pathways, we envisioned a similar reduction and thiol addition to yield CoM. Like the other proposed cosubstrates, sulfoacetaldehyde was incubated with XcbE1 and L-cysteine to compare against XcbE1 incubated with only L-cysteine (Fig 3.19). Of all cosubstrates tested, sulfoacetaldehyde appeared to reduce H_2S levels most substantially.

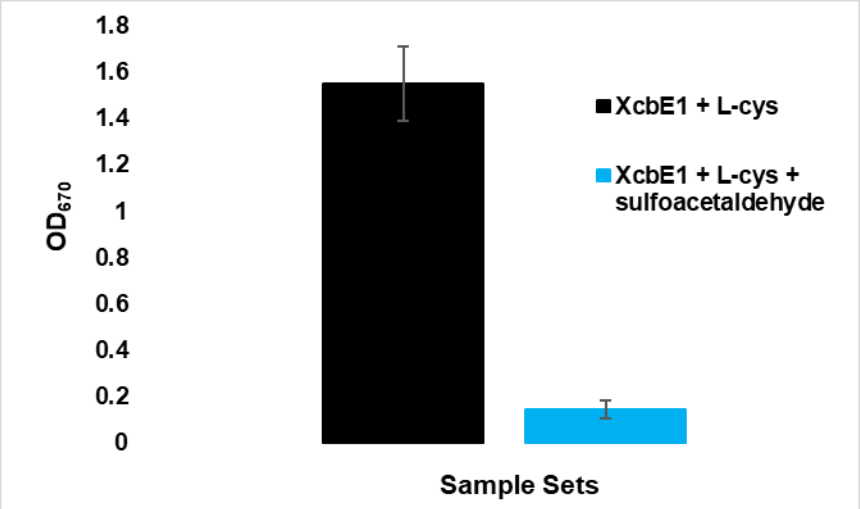

Figure 3.19. XcbE1 (0.1 mg) incubated with 2 mM L-cysteine was compared to samples of XcbE1 incubated with 2-mM L-cysteine and 2 mM sulfoacetaldehyde for 1 hr at pH 8.

Addition of sulfoacetaldehyde to enzymatic reactions reduced the pH to approximately 7.9. When XcbE1 H_2S formation was tested at pH 7.9, we observed approximately 10% reduction in H_2S levels, which is substantially less than the approximately 90% reduction of H_2S levels seen in the presence of sulfoacetaldehyde. Like sulfolactate, there are a few possibilities to explain the preliminary results for sulfoacetaldehyde; 1) a viable

cosubstrate for the XcbE1 reaction, 2) an XcbE1 inhibitor, or 3) a side reaction between sulfoacetaldehyde and cysteine/H2S that results in an unexpected product. When samples were tested for pyruvate production using the LDH coupled assay method, there appeared to be comparable levels of pyruvate production between sample sets with and without sulfoacetaldehyde, suggesting that sulfoacetaldehyde does not inhibit XcbE1 activity, and reacts with H_2S only (data not shown). Additionally, Purpald assays indicated a reduction in free aldehyde levels in the reaction.

In Ch. 1, it was mentioned that combining sulfoacetaldehyde, H_2S, and dithionite would spontaneously generate CoM (unpublished results from R. H. White). It is intriguing to propose that XcbE1 could carry out the necessary reduction and thiol addition steps on sulfoacetaldehyde, using released H_2S. However, the possibility of side reactions are high since previous studies have shown that nucleophilic H_2S can spontaneously react with aldehydes containing electron withdrawing groups to form dithioacetals or hemithioacetals[37,38].

To determine if the presence of sulfoacetaldehyde yielded CoM, we utilized NPM derivatization of thiols for HPLC-FLD (data not shown). Even with the addition of reducing agents such as sodium dithionite or TCEP to the enzymatic reaction, we were unable to detect any levels of CoM. Sulfoacetaldehyde was also removed from consideration as a co-substrate, and preliminary H_2S formation/pyruvate formation results were attributed to the formation of hemithioacetals or dithioacetals.

Future inquiries into the identity of the XcbE1 cosubstrate can utilize the methods described in this section, with the inclusion of Q-TOF MS and time-resolved NMR

described in Ch.2. Using a combination of methods can help rule out issues like enzymatic inhibition, unwanted side reactions, or lack of any activity. When 1-2 mM CoM was incubated with XcbE1, no H_2S formation was detected, indicating that basic PLP conventions (i.e. an amino group for Schiff base formation) must still be observed, or that the reaction does not proceed as predicted. Ideally, identification of the cosubstrate would be accompanied with the appropriate structural studies, including mutagenesis and X-ray crystallography.

Preliminary Crystallization Conditions. Towards elucidating the role of XcbE1 in CoM biosynthesis, initial crystallization conditions were established. Potential structural studies in the future would investigate the proposed cosubstrate interactions in XcbE1. Initial crystal screens yielded yellow crystal clusters within 3-4 weeks for two conditions in HR PEG-ion; (0.2 M potassium chloride, 0.01 M calcium chloride dihydrate, 0.05 M sodium cacodylate trihydrate, 10% w/v PEG4000, pH 6) (Fig 3.20A) and (0.01 M magnesium sulfate, 0.05 M Sodium cacodylate trihydrate, 1.8 M ithium sulfate monohydrate, pH 6). The secondary crystal screens were designed around varied %PEG and KCl conditions, which yielded multiple crystals in under two weeks. The largest yellow clusters were found at 100 mM KCl, 8% w/v PEG4000, pH 6 (Fig 3.20B), leading to a third crystal screen set up that varied %PEG (7% w/v – 10% w/v) and pH (pH 5, 5.5, 6, 6.5, 7, and 7.5). Multiple conditions yielded yellow crystals again within two weeks. The most well-formed crystals were found at 9% w/v PEG4000, pH 6.5 (Fig 3.20C). These preliminary conditions may be useful for future structural studies.

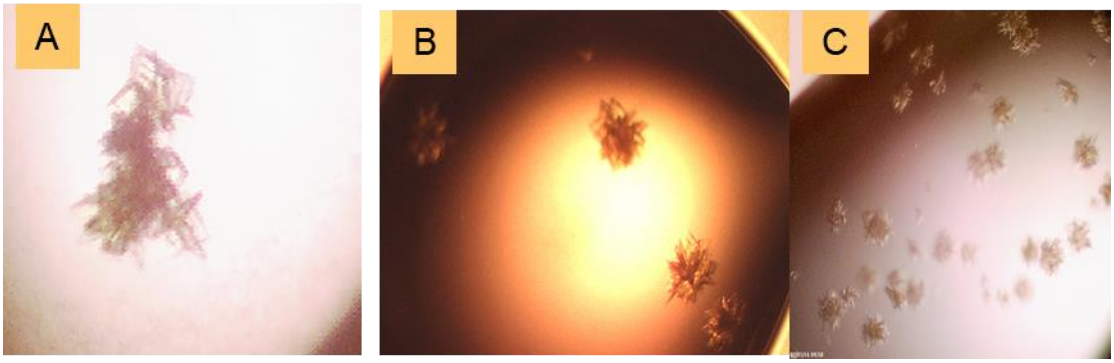

Figure 3.20. Example XcbE1 crystals from each of the three crystallization trials are shown; trial 1 (A), trial 2 (B), and trial 3 (C).

Determining if Thiol-Specific Alkylating Agent is an Effective XcbE1 Inhibitor

Since the alignment shown in Fig. 3.7 indicated that XcbE1 contains a cysteine residue in the same location as the active site cysteine in NifS, we conducted a preliminary experiment to determine if the thiol-specific alkylating agent NEM would inhibit XcbE1 activity. This might be expected if the conserved cysteine formed a covalent disulfide adduct with H_2S evolved from a substrate cysteine molecule. XcbE1 samples were titrated using 0, 0.25x, 0.5x, 1x, and 2x equimolar quantities of NEM to determine if levels of H_2S formation would be impacted with increasing amounts of NEM (Fig 3.21). Error bars for the 0 nmol NEM sample seems to eclipse the levels of H_2S formed at all other molar quantities of NEM, suggesting that there is no real decrease in H_2S levels. Even if there were issues with consistency in sample replicates, there does not appear to be a discernable trend with increasing molar quantities of NEM.

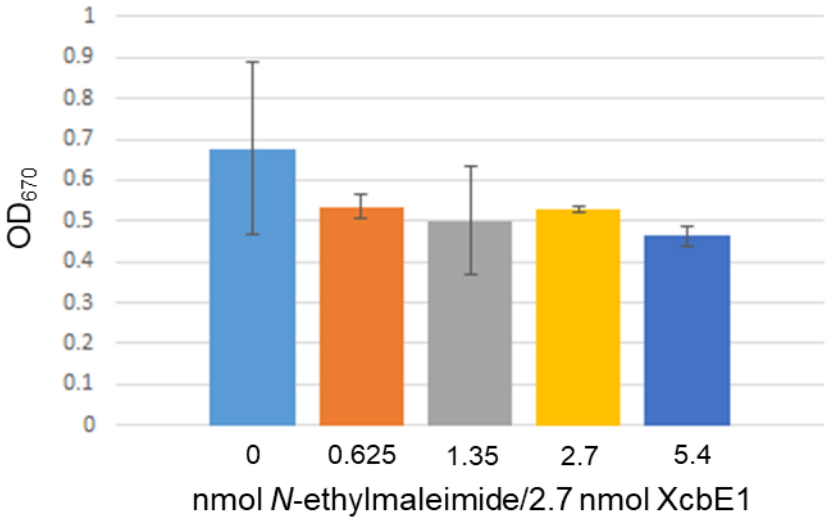

Figure 3.21. Levels of H_2S as detected by methylene blue assay are shown in the graph at each respective molar quantity of NEM used to titrate 2.7 nmol XcbE1.

Since this experiment has only been performed once, it may be another avenue worth examining to determine if the supposedly conserved cysteine residue in XcbE1 is purely coincidence or an actual indicator of activity. The conditions for NEM incubation could be altered by using 20 mM phosphate buffer as in Zheng et al, or other thiol-specific alkylating agents could be tested, such as *p*-chloromercuribenzoic acid, or iodoacetamide[14].

Proposed XcbE1 Scheme

A proposed scheme for XcbE1 entails the use of a cosubstrate putatively synthesized by XcbD1 in combination with cysteine to catalyze the final step of the reaction, yielding CoM (Fig 3.22).

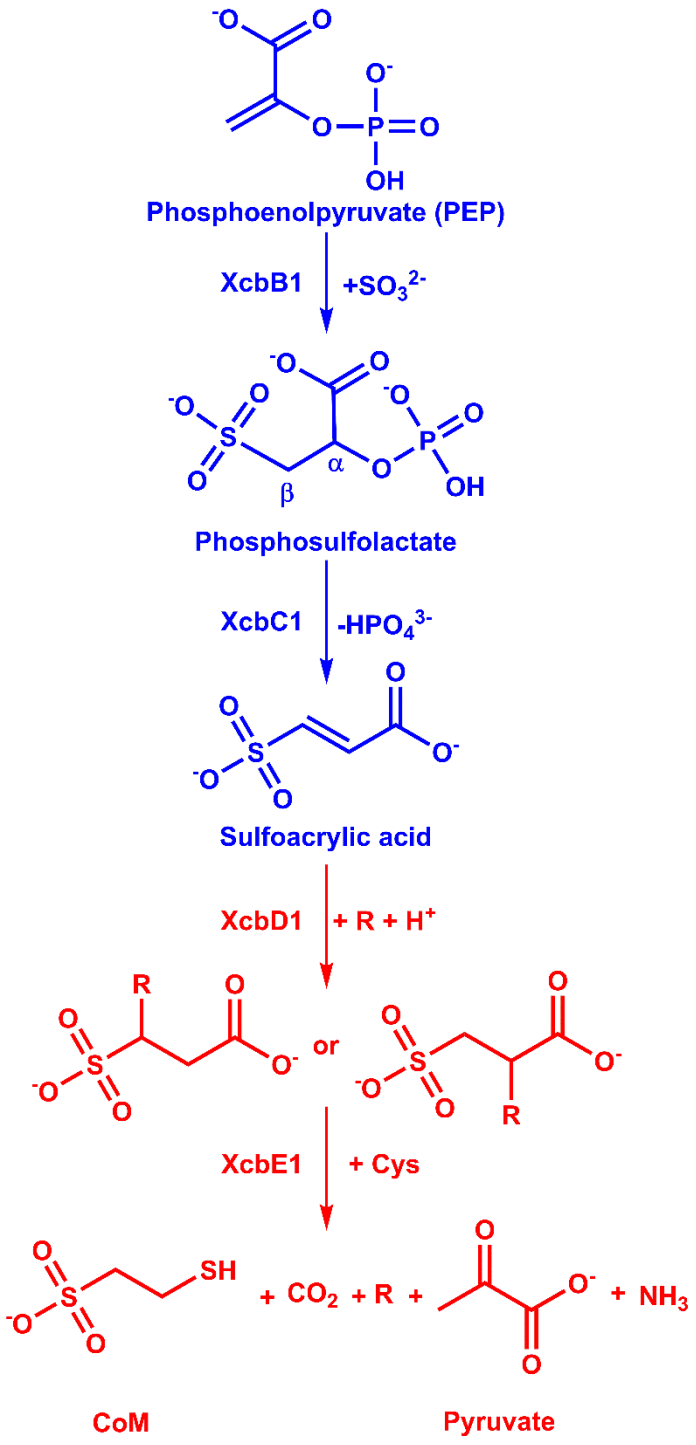

Figure 3.22. A proposed scheme for bacterial CoM biosynthesis is depicted with established steps in blue and hypothetical steps in red.

Conclusions and Future Directions

Bacterial CoM biosynthesis remained uncharacterized for several years prior to our work establishing the first two steps catalyzed by XcbB1 and XcbC1, and a framework for elucidating the role of XcbE1 in CoM biosynthesis has been discussed in this chapter. XcbE1 shares some sequence features with PLP-dependent D-cysteine desulfhydrases, and we have shown that it will catalyze D- and L-cysteine. Through bioinformatics, it appears that XcbE1 occupies a subclass of D-cysteine desulfhydrases implicated in CoM biosynthesis. Since many PLP-dependent enzymes can be multifunctional or catalyze basic PLP reaction combinations, it is attractive to propose that XcbE1 plays a bifunctional role in CoM biosynthesis with the addition of cysteine-derived thiol and possibly a decarboxylation reaction. We screened four proposed cosubstrates (isethionate, vinyl sulfonate, sulfolactate, and sulfoacetaldehyde) in the XcbE1 reaction with cysteine, and eventually eliminated them from consideration. The methods and analytical approaches described can be used to quickly screen potential cosubstrates and analyze how the additives affect the reaction. While ongoing studies continue to probe the XcbD1 reaction for activity (Ch.4), it may be worthwhile to obtain other commercially available 2-3 carbon sulfonated compounds (± carboxylic acid group) for additional cosubstrate screens. Future approaches to probing the potential cosubstrate reaction should always multi-faceted, with ways to detect substrate consumption and product formation, either directly or with general functional group probes (i.e. thiol reactive, aldehyde reactive, etc). As shown in the results, the H_2S methylene blue assay could be useful for rapid, initial cosubstrate screens, but is prone to false positives,

necessitating more targeted approaches. Spectroscopic approaches, including MS and NMR are also invaluable tools (refer to Ch. 2). Ideally, elucidating the XcbD1 reaction will provide the most direct route to solving the role of XcbE1, completing a pathway for bacterial CoM biosynthesis. Future studies will have the opportunity to not only solve the reaction, but to examine the intriguing structural basis for the reaction.

References

1 Toney, M. D. Reaction specificity in pyridoxal phosphate enzymes. *Arch Biochem Biophys* **433**, 279-287, doi:10.1016/j.abb.2004.09.037 (2005).

2 Eliot, A. C. & Kirsch, J. F. Pyridoxal phosphate enzymes: mechanistic, structural, and evolutionary considerations. *Annu Rev Biochem* **73**, 383-415, doi:10.1146/annurev.biochem.73.011303.074021 (2004).

3 Keller, J. W. *et al.* Pseudomonas cepacia 2,2-dialkylglycine decarboxylase. Sequence and expression in Escherichia coli of structural and repressor genes. *J Biol Chem* **265**, 5531-5539 (1990).

4 Watanabe, Y. & Shimura, K. BIOSYNTHESIS OF THREONINE FROM HOMOSERINE .5. NATURE OF AN INTERMEDIARY PRODUCT. *Journal of Biochemistry* **43**, 283-294 (1956).

5 Jansonius, J. N. Structure, evolution and action of vitamin B6-dependent enzymes. *Curr Opin Struct Biol* **8**, 759-769 (1998).

6 Schneider, G., Kack, H. & Lindqvist, Y. The manifold of vitamin B6 dependent enzymes. *Structure* **8**, R1-6 (2000).

7 Sugio, S., Petsko, G. A., Manning, J. M., Soda, K. & Ringe, D. Crystal structure of a D-amino acid aminotransferase: how the protein controls stereoselectivity. *Biochemistry* **34**, 9661-9669 (1995).

8 Alexander, F. W., Sandmeier, E., Mehta, P. K. & Christen, P. Evolutionary relationships among pyridoxal-5'-phosphate-dependent enzymes. Regio-specific alpha, beta and gamma families. *Eur J Biochem* **219**, 953-960 (1994).

9 Marchler-Bauer, A. *et al.* CDD/SPARCLE: functional classification of proteins via subfamily domain architectures. *Nucleic acids research* **45**, D200-D203, doi:10.1093/nar/gkw1129 (2017).

10 Singh, S. & Banerjee, R. PLP-dependent H2S biogenesis. *Biochimica et Biophysica Acta (BBA) - Proteins and Proteomics* **1814**, 1518-1527, doi:http://dx.doi.org/10.1016/j.bbapap.2011.02.004 (2011).

11 Guarneros, G. & Ortega, M. V. Cysteine desulfhydrase activities of Salmonella typhimurium and Escherichia coli. *Biochimica et Biophysica Acta (BBA) - Enzymology* **198**, 132-142, doi:https://doi.org/10.1016/0005-2744(70)90041-0 (1970).

12 Kumagai, H., Choi, Y.-J., Sejima, S. & Yamada, H. Synthesis of S-alkyl-L-cysteine from pyruvate, ammonia and alkyl-mercaptan by cysteine desulfhydrase of Aerobacter aerogenes. *Biochemical and biophysical research communications* **59**, 789-795, doi:https://doi.org/10.1016/S0006-291X(74)80049-5 (1974).

13 Tchong, S. I., Xu, H. & White, R. H. L-cysteine desulfidase: an [4Fe-4S] enzyme isolated from Methanocaldococcus jannaschii that catalyzes the breakdown of L-cysteine into pyruvate, ammonia, and sulfide. *Biochemistry* **44**, 1659-1670, doi:10.1021/bi0484769 (2005).

14 Zheng, L., White, R. H., Cash, V. L., Jack, R. F. & Dean, D. R. Cysteine desulfurase activity indicates a role for NIFS in metallocluster biosynthesis. *Proc Natl Acad Sci U S A* **90**, 2754-2758 (1993).

15 Zhang, W. *et al.* IscS Functions as a Primary Sulfur-donating Enzyme by Interacting Specifically with MoeB and MoaD in the Biosynthesis of Molybdopterin in Escherichia coli. *Journal of Biological Chemistry* **285**, 2302-2308, doi:10.1074/jbc.M109.082172 (2010).

16 Soutourina, J., Blanquet, S. & Plateau, P. Role of D-cysteine desulfhydrase in the adaptation of Escherichia coli to D-cysteine. *J Biol Chem* **276**, 40864-40872, doi:10.1074/jbc.M102375200 (2001).

17 Todorovic, B. & Glick, B. R. The interconversion of ACC deaminase and D-cysteine desulfhydrase by directed mutagenesis. *Planta* **229**, 193-205, doi:10.1007/s00425-008-0820-3 (2008).

18 Oguri, T., Schneider, B. & Reitzer, L. Cysteine catabolism and cysteine desulfhydrase (CdsH/STM0458) in Salmonella enterica serovar typhimurium. *J Bacteriol* **194**, 4366-4376, doi:10.1128/jb.00729-12 (2012).

19 Yao, M. *et al.* Crystal structure of 1-aminocyclopropane-1-carboxylate deaminase from Hansenula saturnus. *J Biol Chem* **275**, 34557-34565, doi:10.1074/jbc.M004681200 (2000).

20 Bharath, S. R., Bisht, S., Harijan, R. K., Savithri, H. S. & Murthy, M. R. Structural and mutational studies on substrate specificity and catalysis of Salmonella typhimurium D-cysteine desulfhydrase. *PLoS One* **7**, e36267, doi:10.1371/journal.pone.0036267 (2012).

21 Nagasawa, T., Ishii, T., Kumagai, H. & Yamada, H. d-Cysteine desulfhydrase of Escherichia coli. *European Journal of Biochemistry* **153**, 541-551, doi:10.1111/j.1432-1033.1985.tb09335.x (1985).

22 Nagasawa, T., Ishii, T. & Yamada, H. Physiological comparison of d-cysteine desulfhydrase of Escherichia coli with 3-chloro-d-alanine dehydrochlorinase of Pseudomonas putida CR 1-1. *Archives of Microbiology* **149**, 413-416, doi:10.1007/bf00425580 (1988).

23 Friedman, M. Chemistry, Nutrition, and Microbiology of d-Amino Acids. *Journal of Agricultural and Food Chemistry* **47**, 3457-3479, doi:10.1021/jf990080u (1999).

24 Abe, K. & Kimura, H. The possible role of hydrogen sulfide as an endogenous neuromodulator. *The Journal of neuroscience : the official journal of the Society for Neuroscience* **16**, 1066-1071 (1996).

25 Kimura, H. Hydrogen sulfide induces cyclic AMP and modulates the NMDA receptor. *Biochemical and biophysical research communications* **267**, 129-133, doi:10.1006/bbrc.1999.1915 (2000).

26 Vorobets, V. S., Kovach, S. K. & Kolbasov, G. Y. Distribution of Ion Species and Formation of Ion Pairs in Concentrated Polysulfide Solutions in Photoelectrochemical Transducers. *Russian Journal of Applied Chemistry* **75**, 229-234, doi:10.1023/a:1016152117662 (2002).

27 Kabil, O. & Banerjee, R. Redox Biochemistry of Hydrogen Sulfide. *The Journal of Biological Chemistry* **285**, 21903-21907, doi:10.1074/jbc.R110.128363 (2010).

28 Liu, Y., Sieprawska-Lupa, M., Whitman, W. B. & White, R. H. Cysteine Is Not the Sulfur Source for Iron-Sulfur Cluster and Methionine Biosynthesis in the Methanogenic Archaeon Methanococcus maripaludis. *The Journal of Biological Chemistry* **285**, 31923-31929, doi:10.1074/jbc.M110.152447 (2010).

29 Droux, M., Martin, J., Sajus, P. & Douce, R. Purification and characterization of O-acetylserine (thiol) lyase from spinach chloroplasts. *Arch Biochem Biophys* **295**, 379-390 (1992).

30 Hirase, K. & Molin, W. T. Effect of Inhibitors of Pyridoxal-5′-Phosphate-Dependent Enzymes on Cysteine Synthase in Echinochloa crus-galli L. *Pesticide Biochemistry and Physiology* **70**, 180-188, doi:https://doi.org/10.1006/pest.2001.2553 (2001).

31 White, R. H. Characterization of the enzymic conversion of sulfoacetaldehyde and L-cysteine into coenzyme M (2-mercaptoethanesulfonic acid). *Biochemistry* **27**, 7458-7462, doi:10.1021/bi00419a043 (1988).

32 Winters, R. A., Zukowski, J., Ercal, N., Matthews, R. H. & Spitz, D. R. Analysis of glutathione, glutathione disulfide, cysteine, homocysteine, and other biological thiols by high-performance liquid chromatography following derivatization by n-(1-pyrenyl)maleimide. *Anal Biochem* **227**, 14-21, doi:10.1006/abio.1995.1246 (1995).

33 Ghatge, M. S. *et al.* Pyridoxal 5′-Phosphate Is a Slow Tight Binding Inhibitor of E. coli Pyridoxal Kinase. *PLOS ONE* **7**, e41680, doi:10.1371/journal.pone.0041680 (2012).

34 Kolluru, G. K., Shen, X., Bir, S. C. & Kevil, C. G. Hydrogen sulfide chemical biology: Pathophysiological roles and detection. *Nitric Oxide* **35**, 5-20, doi:https://doi.org/10.1016/j.niox.2013.07.002 (2013).

35 Marbach, E. P. & Weil, M. H. Rapid enzymatic measurement of blood lactate and pyruvate. Use and significance of metaphosphoric acid as a common precipitant. *Clin Chem* **13**, 314-325 (1967).

36 Gloster, J. A. & Harris, P. Observations on an enzymic method for the estimation of pyruvate in blood. *Clinica Chimica Acta* **7**, 206-211, doi:http://dx.doi.org/10.1016/0009-8981(62)90011-6 (1962).

37 Lienhard, G. E. & Jencks, W. P. Thiol Addition to the Carbonyl Group. Equilibria and Kinetics1. *Journal of the American Chemical Society* **88**, 3982-3995, doi:10.1021/ja00969a017 (1966).

38 Harris, J. Communications: Hydrogen Sulfide Adducts of Halogenated Aldehydes and Ketones. *The Journal of Organic Chemistry* **25**, 2259-2259, doi:10.1021/jo01082a629 (1960).

CHAPTER FOUR

AN ASPARTASE/FUMARASE SUPERFAMILY ENZYME MAY CATALYZE A SECOND REACTION IN COM BIOSYNTHESIS

Introduction

Previously, Ch. 2 discussed the biochemical, spectroscopic, and informatics approach to elucidating the reactions catalyzed by XcbB1 and XcbC1, thereby elucidating the first two steps in the putative pathway for bacterial CoM biosynthesis (Fig 4.1).

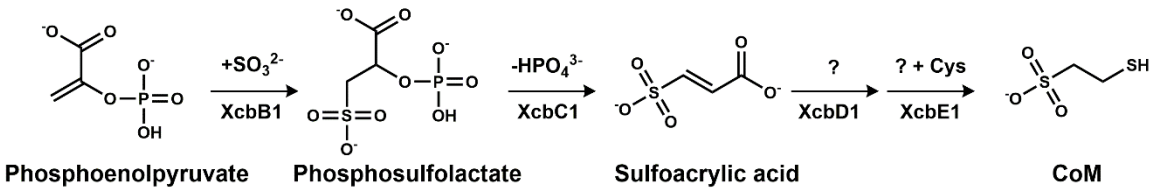

Figure 4.1 The first two solved steps for CoM biosynthesis in *X. autotrophicus* Py2 as detailed in Ch.2.

Ch. 3 provided rationale regarding a proposed bifunctional role for XcbE1 involving thiol addition and possibly decarboxylation in the final step of CoM biosynthesis and outlined the canonical cysteine desulfhydrase activity and attempts to screen for potential cosubstrates. The putative XcbD1 reaction that consumes the XcbC1 product and yields the cosubstrate for the proposed XcbE1 reaction is still part of ongoing studies. However, our work towards elucidating the XcbD1 reaction could possibly contribute to future studies aimed at completing the pathway.

XcbD1 is a member of the aspartase/fumarase superfamily (AFS) that also contains XcbC1. These enzymes are known for catalyzing reversible β-elimination reactions on various succinyl containing enzymes, culminating in the release of fumarate as a common product[1]. This family of enzymes includes; argininosuccinate lyases (ASL)/ δ2-crystallin**,** adenylosuccinate lyase (ADL), class II fumarase, and aspartases. Additionally, the 3-carboxy-*cis*,*cis*-muconate lactonizing enzyme (pCLME) is also a part of this family, but catalyzes the reversible conversion of 3-carboxy-*cis*,*cis*-muconate into a muconolactone, which is a departure from the typical AFS β-elimination reactions. In Ch. 2, XcbD1 was briefly introduced as an enzyme homologous to adenylosuccinate lyases (Fig 4.2).

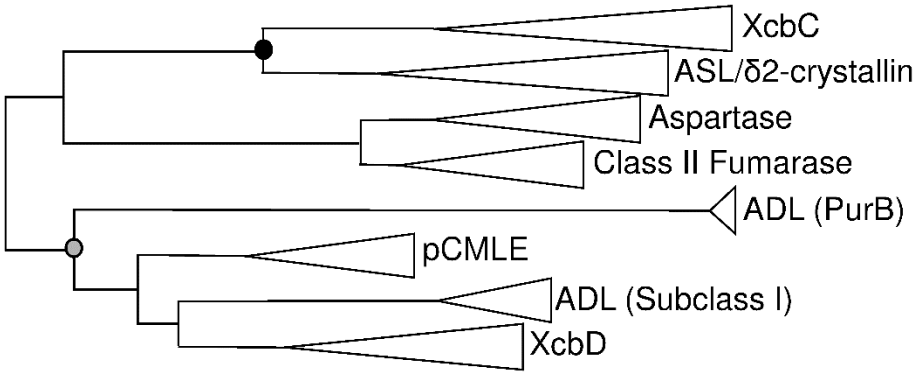

Figure 4.2. Bioinformatics analysis of XcbC1 and XcbD1 sequences identifies the AFS families to which each belongs. The maximum-likelihood tree (100 bootstrap reps) appears to show two sub-branches for argininosuccinate-lyase type enzymes. Bootstrap values are shown only for nodes of relevance to this work, as indicated by circles; ≥90 (black), 80-89 (grey). The canonical argininosuccinate lyase enzymes appear to occupy a separate clade from the XcbC-type enzymes that may be involved in a pathway for CoM biosynthesis, and XcbD appears to form an additional subgroup in the adenylosuccinate lyase clade.

ADL (EC 4.3.2.2) is a homotetramer that catalyzes two reactions in the *de novo* purine biosynthetic pathway; the reversible β-elimination of 5-aminoimidazole-(*N*-succinylcarboxamide) ribotide (SAICAR) to 5-aminoimidazole-4-carboxamide ribotide (AICAR) and fumarate, and the analogous reaction on adenylosuccinate to yield adenosine monophosphate (AMP) and fumarate[2-11] (Fig 4.3). Like the other AFS enzymes, these reactions proceed with a general acid-base catalytic mechanism that is initiated by catalytic base proton abstraction from the C_β of the substrate.

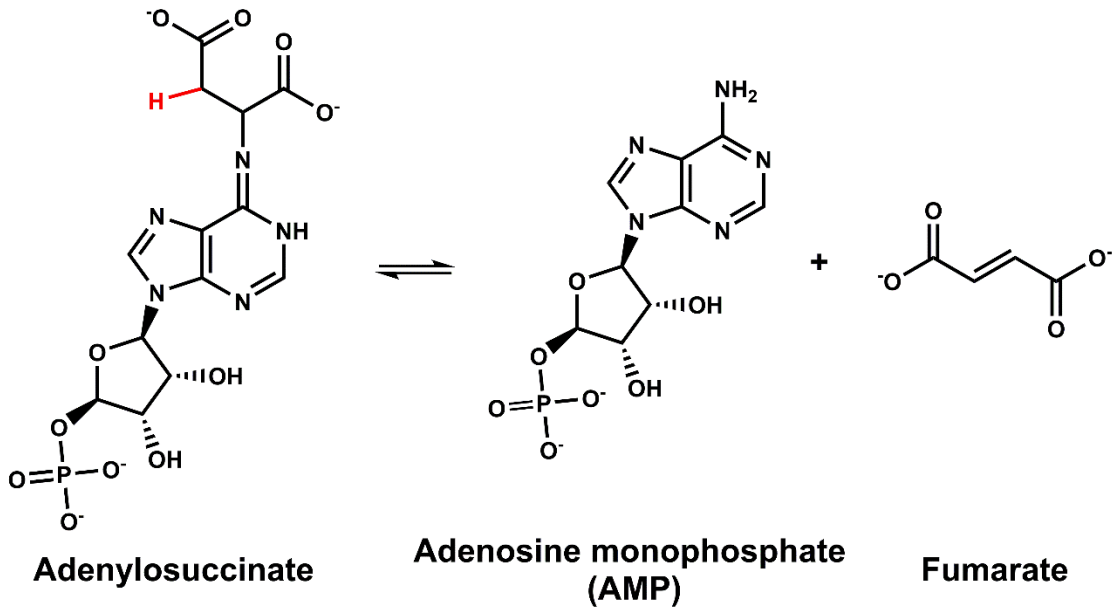

Figure 4.3. The β-elimination/conjugate addition of adenylosuccinate for ADL is depicted with the C_β proton highlighted in red.

The C_β proton abstraction results in the formation of a carbanion intermediate stabilized in the resonance form, followed by general acid protonation of an undetermined substrate nitrogen (N1 or N6), resulting in product release[2,6,8]. The National Center for

Biotechnology Information (NCBI) database provides a hierarchy for ADL in the Conserved Domain Database (CDD)[12] that indicates four ADL (cd01595) subclasses; ADL subgroup 1 (cd01360), pCMLE (cd01597), PurB (cd01598), and ADL subgroup 2 (cd03302). The ADL subgroup 1 contains bacterial and archaeal ADL enzymes while ADL subgroup 2 contains mostly eukaryotic ADL. The pCMLE catalyze the cyclization reaction described previously in this introduction, while PurB contains the *E. coli* ADL product of the *purB* gene.

We investigated the underlying chemical reaction of ADL and other AFS to develop a hypothesis for an XcbD1 reaction in the context of CoM biosynthesis. The XcbB1 reaction generates phosphosulfolactate, which undergoes β-elimination catalyzed by AFS enzyme XcbC1 to yield sulfoacrylic acid and phosphate (Fig 4.1). We proposed that the sulfoacrylic acid product of XcbC1 would be a substrate for XcbD1, indicating that XcbD1 catalyzes an analogous conjugate addition reaction to AFS in which an unspecified cosubstrate plus H^+ is added across the double bond. Our earliest proposal for XcbD1 suggested that water could be added across the double bond of sulfoacrylic acid in an analogous reaction to the class II fumarases to yield sulfolactate as the cosubstrate with cysteine in the XcbE1 reaction, but work described in Ch.3 suggested that this is likely not the case, since incubation of XcbE1 with sulfolactate and cysteine did not yield CoM. Since XcbD1 is more closely related to ADL in the AFS, we then proposed that AMP may be the cosubstrate added across the sulfoacrylic acid double bond, to yield the AMP conjugate of sulfoacrylic acid (AMP-SAA) (Fig. 4.4).

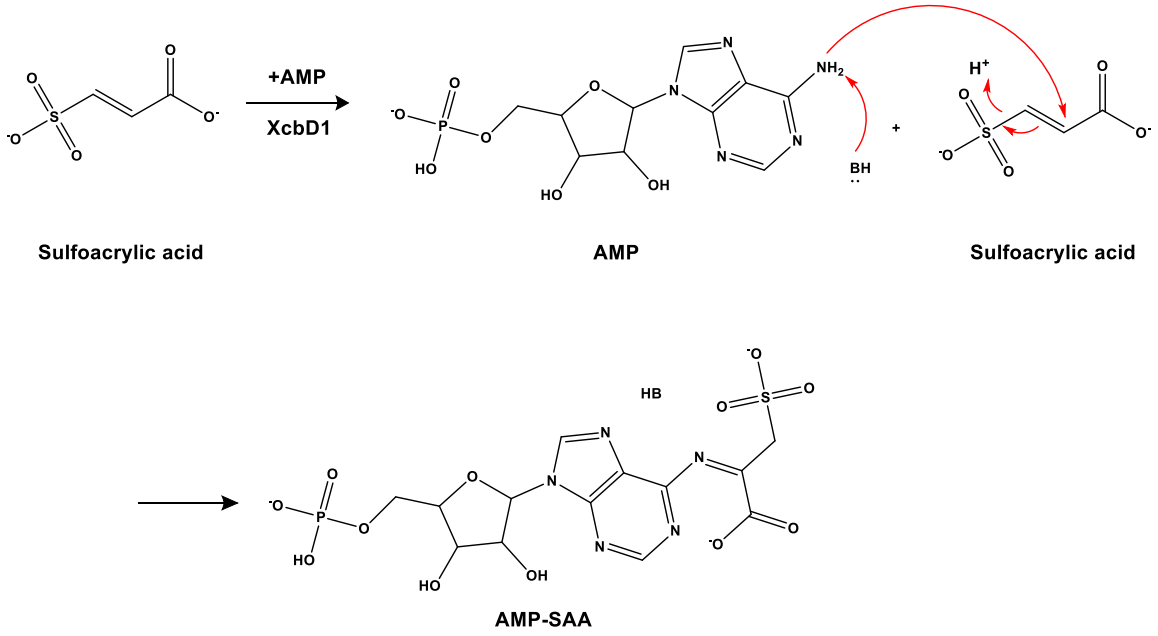

Figure 4.4. Using the analogous ADL reaction, a scheme for the XcbD1 catalyzed addition of AMP across the double bond of sulfoacrylic acid was proposed, yielding the AMP-SAA.

We then proposed that the product of XcbD1 would act as a cosubstrate for the XcbE1 plus cysteine reaction, although it was unclear how a compound such as AMP-SAA would undergo such a reaction. This proposal was examined using several methods, which could be useful in future studies.

Methods

Amplification of XcbD1

X. autotrophicus Py2 was grown as described in Ch. 2. Sequences for the putative biosynthetic operon were obtained from the NCBI database file for the pXAUT01 megaplasmid. Primers (Integrated DNA Technologies, San Diego, CA) were designed for *xcbD1* (XAUT_RS24690):

[Fwd: 5'- GTAAGATCTTATGACCGGCTGGTCCTTCGGC -3'] and

[Rev: 5'- ATAGATATCTCAGGCTGCTCCATCCCGCG - 3'].

Restriction sites were added to clone *xcbD1* (F: BglII/ R: EcoRV) without an added N-terminal His-tag into a Duet Expression System (Novagen). Amplicons were initially cloned into a pGEM-T vector and transformed into JM109 competent cells for propagation, before being cloned into a Duet vector. XcbD1 was inserted into multiple cloning site 2 (MCS2) of a pCDFDuet-1 ($Strep^R$) vector, and sequences were verified via Functional Biosciences (Functional Biosciences, Inc., Madison, WI).

Expression and Purification of XcbD1

The XcbD1-pCDFDuet-1 construct was transformed into BL21(DE3) competent cells and grown on streptomycin-supplemented (0.05 mg/mL) lysogeny broth (LB+Strep) agar plates. A single colony was used to inoculate an overnight culture in liquid LB+Strep medium. Expression was initiated with 10% volume of the overnight culture and incubated at 37°C with shaking at 250 rpm until the culture reached an OD_{600} of 0.6-0.8. Protein expression was induced with 1 mM IPTG and the cells moved to a 30°C incubator with shaking at 180 rpm. Protein expression proceeded for 3 h before the cells were harvested by centrifugation (7500 x *g* , 10 min) followed by flash freezing of the pellets in liquid nitrogen. For purification, frozen cell pellets were resuspended in buffer A (20 mM Tris, 10 mM NaCl, 20% glycerol pH 8) and homogenized with the addition of lysozyme, DNase, and PMSF. Cell pellets from cultures larger than 1 L were lysed using a microfluidizer (M-110L Microfluidics Corporation, Newton, MA). Lysates were

cleared by centrifugation at 105,000 x *g* for 1h prior to fast protein liquid chromatography (FPLC, Bio-Rad). Cleared lysate was loaded on a 75 mL Q-Sepharose Fast Flow resin (GE Healthcare Life Sciences, Pittsburgh, PA) equilibrated with sterile filtered buffer A. After the loaded lysate was washed with additonal buffer A, a 10-column volume gradient (750 mL) was programmed at 5 mL/min, and fraction collection was done manually, with 15x 50 mL fractions collected. Elution was achieved using buffer B (20 mM Tris, 1 M NaCl, 20% glycerol, pH 8, sterile filtered). The program was arranged as follows; 30 mL of 100% buffer A, followed by a 750 mL linear gradient from 0-80% buffer B with fractions collected every 50 mL, followed by a final 100 mL of 100 % buffer B. Fractions were run on SDS-PAGE gel to determine which ones contained XcbD1 (~49 kDa). Since we lacked a reliable activity assay, gels were taken to the MS facility for in-gel trypsin digests followed by MS confirmation of bands of interest. Once the Q-seph purification became more consistent, MS confirmation for each purifcation became unnecessary.

Fractions containing XcbD1 were pooled and concentrated down to 1-2% of the total column volume of a packed Sephacryl S-200 HR (GE Healthcare Life Sciences, Pittsburgh, PA) gel filtration column, typically 350-400 mL size. Column was equilibrated with gel filtration buffer (20 mM Tris, 100 mM NaCl, 10% glycerol), with void volume established using Dextran Blue (10 mg/mL) plus 1 M NaCl (1 mL total) at 1 mL/min flow rate. All material undergoing gel filtration was manually injected into the column flow adaptor with a syringe to reduce dilution of sample that can occur when using the BioRad pump, and a mark was made on the chromatogram when all material

was injected to establish start time. Gel filtration column was then calibrated at 1 mL/min using Gel Filtration Standards (BioRad, Hercules, CA) containing thyroglobulin (670,000 Da), γ-globulin (158,000 Da), ovalbumin (44,000 Da), myoglobin (17,000 Da) and vitamin B_{12} (1,350). V_E for each peak was divided by V_0 obtained from Dextran blue, and plotted against molecular weight for each calibrant. Concentrated XcbD1 samples were loaded on gel filtration via the direct inject method and eluted using an isocratic method at 1 mL/min with gel filtration buffer. Fractions were run on SDS-PAGE to determine location of XcbD1 and confirmed by in-gel trypsin digest for MS. All fractions containing XcbD1 were pooled, concentrated, and stored at -80°C for experimental use.

Detection of AMP and AMP Derivatives

To test canonical ADL and/or proposed activity in XcbD1, two methods were utilized.

UV-Vis. In canonical ADL reactions, the breakdown of adenylosuccinate to AMP and fumarate can be monitored by a decrease in absorbance at 290 nm[9] and the addition of AMP to fumarate can be monitored by an increase in absorbance at 290 nm[11]. XcbD1 (0.2 mg/mL) was incubated with either 1 mM adenylosuccinate or 1 mM each AMP and fumarate in buffer (50 mM Tris, 50 mM NaCl, 5 mM $MgCl_2$, pH 8) for 30 min at 30°C, then samples were arranged in a quartz 96-well plate for a BioTek plate reader (BioTek, Winooski, VT). Absorbance at 290 nm was measured and compared to an adenylosuccinate standard prepared under identical conditions (0-1 mM).

HPLC. AMP and its other derivatives are readily detected and separated by HPLC[13]. Enzymatic reactions were set up using buffer (50 mM Tris, 50 mM NaCl, pH 8) with XcbD1 (0.2 mg/mL) and varying concentrations of adenylosuccinate (0-0.5 mM), or AMP (0-0.5 mM) plus fumarate. Samples were incubated at 30°C for 30-45 mins and then filtered using molecular weight cutoff spin filters. HPLC analysis was performed on an Agilent 1100 series instrument, and a Luna 5u C18(2) column was used, with 100Å pore size, 150 x 4.6 mm dimensions (Phenomenex, Inc., Torrance, CA). Mobile phases were; A: 20 mM ammonium acetate, pH 4.5, and B: 100% acetonitrile. The gradient used for separation was; 0 min: 3%B to 10 min: 40% B, then back to 3% B for a total of 15 min, with DAD = 260 nm and a flow rate of 1 mL/min. Standard curves generated under the exact conditions used 0-0.8 mM AMP and 0-0.5 mM adenylosuccinate. Higher concentrations of either compound appeared to cause detection issues on the HPLC.

Q-TOF MS

Refer to Ch. 2 for general sample preparation and instrumentation methods.

Screening Proposed Cosubstrates Using Q-TOF MS. Stock sulfoacrylic acid was prepared for multiple experiments by incubating 5 mM PEP with 5 mM bisulfite with both XcbB1 and XcbC1 (500 µg) in minimal MS buffer (1 mM Tris,1 mM $MgCl_2$, pH 8) for 1 hr at 30°C. The reaction mixture was cleared of protein using molecular weight cutoff spin filtration, and aliquots of sulfoacrylic acid were stored at -20°C until used in assays. Cosubstrates for XcbD1 were screened by incubating 200 µL sulfoacrylic acid (indirect quantification; used an amount that was easily detectable when injected on Q-

TOF MS) with XcbD1 (0.2 mg/mL) and 2.5 or 5 mM AMP, ADP, ATP, GMP, or GTP, ± 2.5 mM L-cysteine in minimal MS buffer for 45 min at 30°C. Additional sample sets were tested, containing sulfoacrylic acid, XcbD1, XcbE1 (0.2 mg/mL), ± L-cysteine, ± AMP. To eliminate the possibility of XcbE1 consuming sulfoacrylic acid, XcbE1 ± L-cysteine was added to samples containing sulfoacrylic acid. In Ch.3, cysteine was found to be a substrate for XcbE1, and the tests done to find an XcbE1 cosubstrate were described. Synthetic CoM was used as a standard to determine if the combination of all enzyme reactions yielded any detectable levels of CoM.

Using *X. autotrophicus* Py2 Cell Lysates to Investigate XcbD1 Reaction. *X. autotrophicus* Py2 cells that were grown on propylene were pelleted and resuspended in minimal MS buffer using the general ratio; 500 µL of minimal MS buffer per 15 mL of cells at OD_{600} of 1-1.5. The resuspension was sonicated to lyse the cells, and the whole cell lysate was immediately used in assays. Assays were set up using 300 µL of whole cell lysate, plus 5 mM PEP/5 mM bisulfite or 200 µL prepared sulfoacrylic acid, with or without 5 mM L-cysteine. Some reactions also included 2 mM hydroxylamine to inhibit any XcbE reactions that could potentially consume any XcbD reaction products. Reactions were incubated at 30°C for 45 mins and filtered through 0.45 µm filters prior to Q-TOF MS analysis.

Time Resolved ^{1}H-NMR

Refer to Ch. 2 for general sample preparation and instrumentation methods. To sample tubes that contained the product of the XcbB1 and XcbC1 reactions (sulfoacrylic acid, respectively), XcbD1 (0.2 mg/mL) was added, ± 0.5 mM AMP, ± 1 mM L-cysteine, ± XcbE1 (0.2 mg/mL). The paired doublet peaks for sulfoacrylic acid were monitored for any change over a 30 min time course, i.e. a disappearance coupled with reappearance of another signal upfield or downfield. At the time of this thesis, other amines have not been tested.

Phylogeny and Homology Modeling

27 diverse members of the AFS including 6 argininosuccinate lyase family members were used to construct the maximum-likelihood tree on MEGA 6.06 with 100 bootstrap replications. The resulting tree was prepared for publication using FigTree v1.4.2.. SWISS-MODEL was used to generate a homology model for XcbD1 from the *Staphylococcus aureus* ADL crystal structure (2x75, 94% query coverage with 29% ID).

Results and Discussion

Purification of XcbD1

Lysis of cell pellet with expressed XcbD1 prior to purification seems to yield approximately 80-90% insoluble protein with only about 10-20% soluble material as observed in SDS-PAGE gel comparisons. Further expression or cell lysis optimization may be necessary in the future, but for this work, we opted to harvest larger cell pellets and purify the available soluble material. The decision to purify XcbD1 as an untagged

protein came after multiple failed attempts to express and purify the enzyme with a His-tag. XcbD1 eluted from the gel filtration column as a tetramer at ~200 kDa, as expected from ADL homology, but denatured XcbD1 runs slightly smaller (~ 44 kDa) than the predicted 49.9 kDa (Fig 4.5).

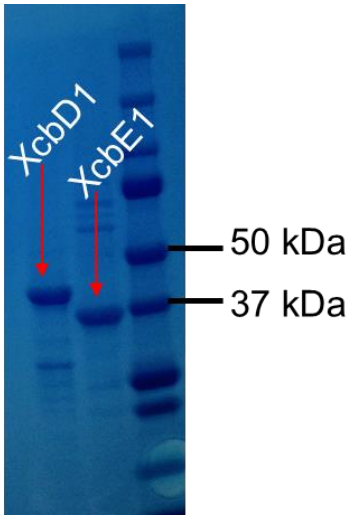

Figure 4.5. Example of purified XcbD1 on SDS-PAGE gel next to purified XcbE1 (predicted at ~34 kDa). The band for XcbD1 consistently runs smaller than the predicted 49.9 kDa.

While this could just be a result of inherent protein characteristics or normal discrepancies in predicted weight vs. SDS-PAGE migration, we wanted to confirm that the enzyme was not expressing or purifying as a truncated variant. Multiple in-gel trypsin digests with MS analysis have been performed, generally yielding 38-48% sequence coverage spanning the whole protein sequence, with approximately 13-18 peptide matches (Fig 4.6).

Figure 4.6. An example of one of the sequence coverage maps obtained from in-gel trypsin digest of XcbD1 appears to show peptides spanning the whole protein.

The peptide maps generated after in-gel trypsin digest indicate that purified XcbD1 is probably not missing significant portions of the enzyme. It may be useful to acquire MALDI-MS confirmation of the molecular weight in the future.

Testing XcbD1 for Canonical ADL Activity

Our proposal suggested that XcbD1 may add AMP across the double bond of sulfoacrylic acid to yield AMP-SAA, a possible cosubstrate with cysteine for the XcbE1 reaction. It was also pertinent to check XcbD1 for canonical ADL activity, to help differentiate if any lack of enzymatic activity towards sulfoacrylic acid is a result of the enzyme being strictly canonical or if the enzyme itself is inactive. XcbD1 was tested for both breakdown of adenylosuccinate and formation of adenylosuccinate through decrease and increase, respectively, in absorbance at 290 nm. Neither enzymatic assay yielded a change in aborbance at 290 nm. Similarly, HPLC analysis did not yield results towards breakdown or formation of adenylosuccinate. Based on these results, it might appear that XcbD1 does not retain canonical activity, or is simply inactive.

Investigating the XcbD1 Reaction with Q-TOF MS and Time Resolved ^{1}H-NMR

The Q-TOF MS method developed for investigating the XcbB1 and XcbC1 reactions was utilized while probing the next possible steps. These previous experiments clearly showed the course of the reaction, especially when paired with correlating time-

resolved ^{1}H-NMR data, to show consumption of PEP coupled with phosphosulfolactate production catalyzed by XcbB1, followed by consumption of phoshosulfolactate coupled with sulfoacrylic acid production catalyed by XcbC1. Logically, the next step of the reaction should clearly show the consumption of sulfoacrylic acid coupled with the appearance of "product X". We proposed that XcbD1 would catalyze this reaction by adding a molecule across the double bond of sulfoacrylic acid, so coupled with the disappearance of a sulfoacrylic acid signal, it would be possible to predict what species might occur based on the cosubstrates that were added to the reaction. We also explored the possibility that XcbE1 may need to be present for the reaction to proceed, by adding XcbD1 and XcbE1 to the same reactions with or without additonal additives like L-cysteine and AMP. XcbE1 ± L-cysteine was also added individually to reactions containing sulfoacrylic acid to eliminate the possibility of XcbE1 performing the next stage of the biosynthetic pathway through consumption of sulfoacrylic acid. XcbD1 was screened with sulfoacrylic acid with several nucleotides (AMP, ADP, ATP, GMP, GTP) in various combinations, with and without cysteine (Table 4.1). The table summarizes the Q-TOF MS trials, but for all conditions tested, there was no detectable consumption of sulfoacrylic acid, marked by a decrease in the signal at m/z 150.96.

Samples	**Q-TOF MS Results**
D1 + SAA	NC
D1 + SAA + Cys	NC
D1 + SAA + AMP	NC
D1 + SAA + AMP + Cys	NC
D1 + SAA + ADP	NC
D1 + SAA + ADP + Cys	NC
D1 + SAA + ATP	NC
D1 + SAA + ATP + Cys	NC
D1 + SAA + GMP	NC
D1 + SAA + GMP + Cys	NC
D1 + SAA + GTP	NC
D1 + SAA + GTP + Cys	NC
D1 + E1 + SAA + ADP + Cys	NC
D1 + E1 + SAA + ATP + Cys	NC
D1 + E1 + SAA + GMP + Cys	NC
D1 + E1 + SAA + GTP + Cys	NC
D1 + E1 + SAA	NC
D1 + E1 + SAA + AMP	NC
D1 + E1 + SAA + AMP + Cys	*NC
D1 + E1 + SAA + Cys	*NC
E1 + SAA	NC
E1 + SAA + Cys	*NC

Table 4.1. The summarized Q-TOF MS reaction sets testing purified XcbD1 (D1) and/or XcbE1 (E1) with different combinations of substrates including sulfoacrylic acid (SAA), L-cysteine (Cys), AMP, ADP, ATP, GMP, and GTP. For all samples listed, no change (NC) was observed in the sulfoacrylic acid signal.
Note* - The appearance of a new signal at m/z 199.96 was attributed to an unexpected side reaction that occurred through the addition of any remaining sulfite (from XcbB1 reaction) to XcbE1-activated cysteine, possibly forming sulfocysteine.

Since prior experiments testing the canonical ADL reaction in XcbD1 did not yield any consumption or formation of adenylosuccinate, it seemed possible for XcbD1 to instead catalyze the addition of AMP to sulfoacrylic acid. These results indicate that either the purified XcbD1 is inactive, or the added cosubstrates are incorrect for this particular reaction.

As in previous chapters, time-resolved ^{1}H-NMR was utilized to corroborate the Q-TOF MS data. Some additional benefits of using ^{1}H-NMR is the lack of ion suppression issues that can disrupt MS data collection, as well as the ability to observe the reaction in real time without undergoing additional filtration steps. In Ch. 2, sections of ^{1}H-NMR spectra were shown over multiple time points indicating clear consumption of respective substrates with concomittant production of respective products for both XcbB1 and XcbC1 catalyzed reactions. Under the sample run conditions, there is a possibility that if any peaks form within the 3.5-5.5 ppm region, they will either be hidden by Tris and glycerol peaks, or suppressed along with the water peak (Fig 4.7). However, sulfoacrylic acid is readily detected, and any consumption of this compound would be apparent over a time course method. Since the samples do not need to be quenched or filtered prior to ^{1}H-NMR analysis, additives like AMP or L-cysteine were added individually to the sample tubes containing sulfoacrylic acid, followed by approximately 15 mins of wait to determine if the most recent compound contributed to any changes in the sulfoacrylic acid pair of doublets (Table 4.2).

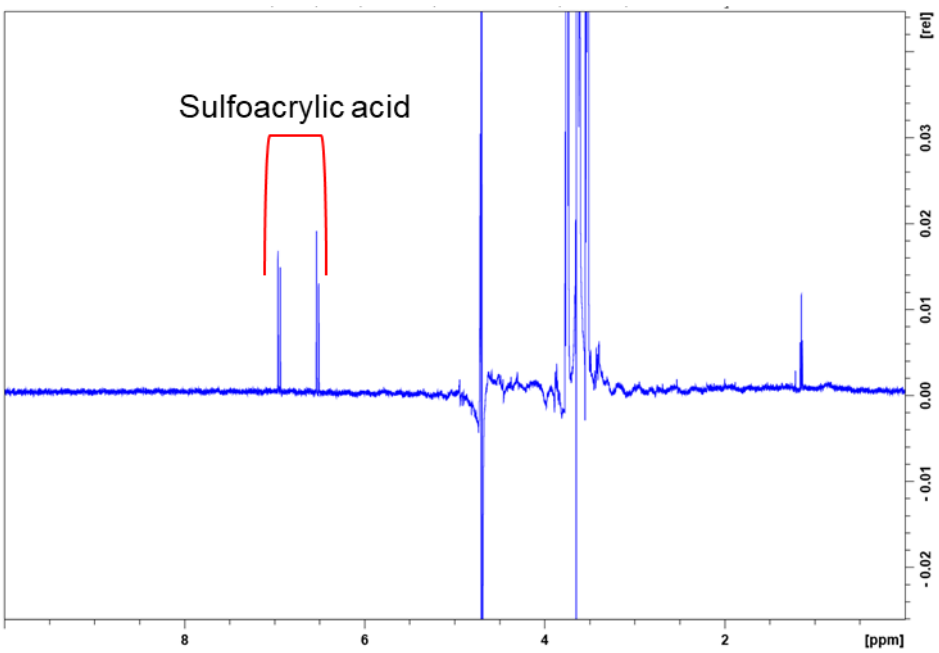

Figure 4.7 The ^{1}H-NMR spectrum showing sulfoacrylic acid pair of doublets in the context of the whole spectrum field. In the 3.5-5.5 ppm region resides Tris and glycerol peaks, with the water peak suppressed at approximately 4.7 ppm. Refer to Ch. 2 for ^{1}H-NMR conditions.

Reaction order	**Sample added**	**Time-resolved ^{1}H-NMR results**
1	SAA + XcbD1	NC
2	+ AMP	NC
3	+ Cys	NC
4	+ XcbE1	NC

Table 4.2. A summarized example of the time-resolved ^{1}H-NMR experiments run to determine if sulfoacrylic acid is consumed at any point. Between addition of each sample, there was a 15 min wait period to determine if the addtion resulted in any change. For each added sample, there was no change (NC) in the sulfoacrylic acid doublets.

Samples were also left overnight and re-scanned on ^{1}H-NMR to check if any new peaks formed, but the scans looked virtually identical to scans from the day before. It is also important to note that XcbD1 did not convert sulfoacrylic acid to sulfolactate through the addition of water across the double bond, as suggested in our earliest proposal described

briefly in the introduction to this chapter (refer to Fig B.S.3B) for synthetic sulfolactate ^{1}H-NMR). Using ^{1}H-NMR to corroborate the XcbD1 reactions tested on Q-TOF MS was confirmed lack of activity toward sulfoacrylic acid with any of the tested compounds; L-cysteine, AMP, ADP, ATP, GMP, or GTP, and the addition of XcbE1 was similarly ineffectual.

X. autotrophicus Py2 Cell Lysates Could
Provide Alternative Route to Solving the Reaction

Purified XcbD1 was inactive when used in canonical ADL assays or in assays to determine the next stage of CoM biosynthesis after the production of sulfoacrylic acid. It was therefore impossible to discern whether the negative results were due to an intrinsically inactive (e.g., improperly folded) enzyme, to suboptimal conditions (e.g., in pH or buffer), or to the lack of the appropriate substrate. To troubleshoot these experimental issues, propylene-grown *X. autotrophicus* Py2 cell lysates were incorporated into experiments, since presumably, all the enzymes necessary for biosynthesis of CoM should be expressed and active under propylene-growth condtions. If any pathway intermediates are used to supplement the cell lysate, they would presumably get consumed and undergo transformation to generate CoM. Since CoM is used in propylene metabolism, the concentration of free CoM within the cell is probably not very high, but if the cells are harvested and no longer growing on propylene, then it may be possible to observe the course of the biosynthetic pathway without all the CoM being sequestered. *X. autotrophicus* Py2 cell lysates were supplemented with PEP and

sulfite ± L-cysteine, or with sulfoacrylic acid and analyzed on Q-TOF MS for consumption of either intermediate (Table 4.3).

#	Sample	Q-TOF MS Result
1	Lysate only	CoM detected (low level)
2	Lysate + PEP + Sulfite	CoM detected (low level)
3	Lysate + PEP + Sulfite + Cys	CoM detected (low level)
4	Lysate + SAA	SAA undetected, appearance of large peak at m/z 271.99, and CoM undetected
5	Lysate + SAA + HA	SAA undetected, peak at m/z 271.99 undetected, and CoM undetected
6	Lysate + PEP + Sulfite + HA	CoM undetected
7	Lysate + PEP + Sulfite + HA + Cys	CoM undetected

Table 4.3. The preliminary results are summarized where *X. autotrophicus* Py2 whole cell lysates were incubated with pathway intermediates ± the PLP-enzyme inhibitor hydroxylamine (HA). Samples supplemented with sulfoacrylic acid (SAA) did not retain detectable levels of SAA, nor did they have detectable levels of CoM.

Additionally, the PLP-enzyme inhibitor hyroxylamine was added to some samples (#5-7) If the supplemented intermediate was transformed to CoM as proposed, any product formed by XcbD1 would likely undergo immediate catalysis by PLP-dependent XcbE1 with no accumulation for any detection methods. Thus, inhibiting the proposed final reaction of the pathway could possibly cause accumulation of XcbD1 product. In Table 3, inconsistent results when sulfoacrylic acid was present (#4 and 5) indicate that the experiments must be further optimized. The sample with lysate and sulfoacrylic acid (#4) seemed to generate a large signal at m/z 271.99, which might correspond to the predicted m/z for a cysteine-sulfoacrylic acid conjugate (thiolene) (Fig 4.8).

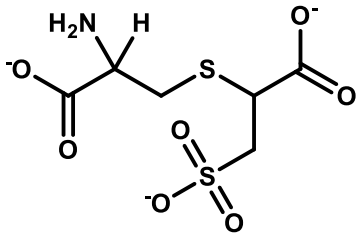

Cysteine-sulfoacrylic acid conjugate

Figure 4.8. A conjugated cysteine and sulfoacrylic acid, what is otherwise known as a thiolene adduct.

However, it is unclear why this particular signal was not present when hydroxylamine was added to the reaction (#5). Additionally, it is unclear why sulfoacrylic acid would form a cysteine conjugate instead of undergoing complete conversion to CoM. CoM was undetected in the last two samples (#6 and 7), which may be an artifact of inconsistent sample set up or actual interference from hydroxylamine interference of the XcbE1 reaction. Some inconsistencies may arise from using whole cell lysate rather than cleared lysate, and the fact that starting CoM levels are so low that minor differences between samples could obliterate the CoM signal. Optimization aimed at obtaining consistent results with *X. autotrphicus* Py2 cell lysates could develop a useful tool towards identifying the product formed after sulfoacrylic acid consumption. Whether that reaction is actually catalyzed by XcbD1 would likely require different approaches.

Phylogeny and Homology Modeling of XcbD1

XcbD1 has been shown to group as a separate subclass of ADL within the AFS phylogenetic tree (introduction to this chapter). When XcbD1 is subjected to pBLAST searches within the PDB, two of the top three hits include the crystal structure of ADL

from *S. aureus* (2x75[8], 94% query coverage with 29% ID) and the crystal structure of pCMLE from *Pseudomonas putida* (1RE5[14], p. putida 97% query coverage 35% ID). Although pCMLE is grouped as an ADL subclass, the lactonizing reaction catalyzed by canonical pCMLE seems inappropriate for CoM biosynthesis. Structural studies on ADL implicate an invariantly conserved serine residue as a catalytic base and a well conserved histidine residue as the catalytic acid that forms a charge relay pair with glutamate, and an invariantly conserved lysine residue present in all known AFS (Ser262, His141, Glu275, and Lys268, *S. aureus* numbering)[2,3,6,8]. The charge relay pair is disrupted in pCMLE, where the His/Glu pair is replaced by Trp/Ala[14]. Alignment of XcbD1 with canonical ADL and pCMLE indicate that XcbD1 retains all four catalytically important conserved residues present in ADL (Fig 4.9). Because XcbD1 retains these conserved residues, it makes the supposed inactivity towards adenylosuccinate or AMP and fumarate (or its structural analog, sulfoacrylic acid) somewhat puzzling, and investigation of the active site through homolgy modeling offers little insight.

```
                                  190          320         330
XcbD1                   VGRTHGQQGL SITMPHKRNP EIAEHLGTLS
ADL_Nocadioides         CGRTHGQAGL SITMPHKVNP EISEHLVTLA
ADL_B.subtilis          MGRTHGVHAE SSAMPHKRNP IGSENMTGMA
ADL_E.coli              LSRTHGQPAT SSTMPHKVNP IDFENSEGNL
ADL_S.typhimurium       LSRTHGQPAT SSTMPHKVNP IDFENSEGNL
ADL_S.aureus            MGRTHGVHAE SSAMPHKRNP IGSENITGIS
pCMLE_A.calcoaceticus   MGRTWLQQAL SSTMPHKRNP VAAASVLAAA
pCMLE_P.putida          VGRTWLQHAT SSTMPHKRNP VGAAVLIGAA
```

Figure 4.9. Two sections from an alignment of XcbD1 with canonical ADL and canonical pCMLE indicate that XcbD1 retains all four conserved catalytic residues from ADL. Charge relay pair (yellow), catalytic base (green), and conserved lysine (blue) are all highlighted with respective colors.

The XcbD1 homology model was superimposed over adenylosuccinate-bound 2x75 (Fig 4.10) and residues in the active site pocket were compared (Table 4.4). While XcbD1 residues around the 2x75 substrate adenine and ribose moiety could conceivabely behave as general hydrogen bond donors and acceptors, there are multiple tryptophan residues in XcbD1 that appear to occlude the active site pocket when compared to the 2x75 crystal structure. It is unclear whether these changes in the active site are indicative of CoM-related activity in XcbD1 or simply inherent variabilty amongst ADL homologs.

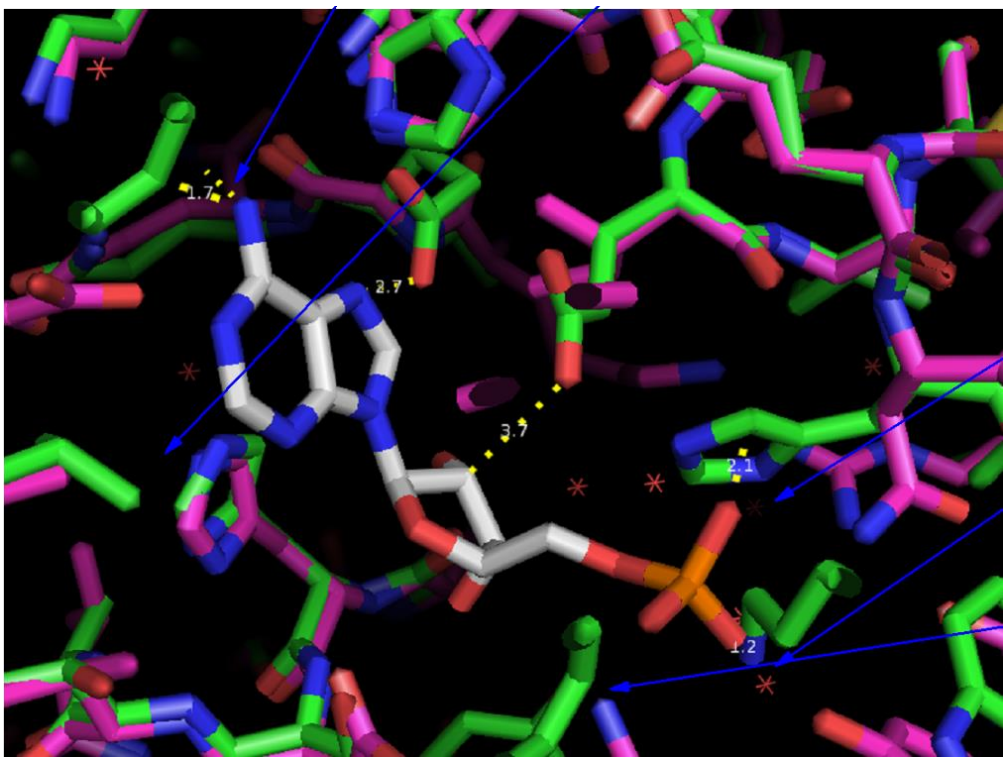

Figure 4.10. The XcbD1 homology model (green) was superimposed over AMP-bound 2x75 (magenta). Blue arrows were added to draw attention to abberant residues from XcbD1 that appear to form unfavorable interactions around the 2x75 substrate. Most notably, the residues by the phosphate group of adenylosuccinate are ≤2Å apart. Yellow lines indicate spacing (Å) between residues and various components of the AMP substrate.

Position	**XcbD1 model**	**2x75**
Phosphate	Trp 15	Arg4
	Trp 15	Tyr 5
	His 295	Asn 276
	Trp 325	Ser 306
	Trp 329	Arg 310
Ribose	Gly 322	Ile 303
	Glu 291	Ile 272
Adenosine	Gln 112	Thr 95
	His 84	His 68
	His 158	His 141
	Lys 287	Lys 268
	Trp 231	Gln 212

Table 4.4. The active site residues of 2x75 in each of the respective positions around the adenylosuccinate substrate were compared to the corresponding residues in the superimposed XcbD1 model.

Conclusions and Future Directions

Regarding these preliminary experiments on XcbD1, it is clear that there are issues to be resolved. Based on these results, XcbD1 was inactive when tested for canonical ADL actvitity, and also seemingly inactive in the series of experiments testing activity in the CoM biosynthetic pathway. There are some possibilities that can explain these results, including; 1) purified XcbD1 is somehow inactive under the conditions used in these experiments, 2) the wrong cosubstrate is being tested, 3) XcbD1 does not catalyze the enzymatic step after XcbC1, 4) XcbD1 needs a cofactor for enzymatic activity, or 5) XcbD1 requires another enzyme for activity. The last two possibilities are probably the least likely explanations for the observed XcbD1 issues, because AFS enzymes do not typically contain cofactors or prosthetic groups, and do not typically

form protein-protein interactions. Following up on the state of the purifed XcbD1 enzyme either through MALDI-MS confirmation of the molecular weight or other means might be a useful step to confirm that there are no drastic discrepancies between the amino acid sequence and the heterologously expressed enzyme.

Using propylene-grown *X. autotrophicus* Py2 cell lysates seems like a promising method to circumvent the issues we faced with purified XcbD1, but the preliminary results were inconsistent and need further optimization. Conclusively showing that adding sulfoacrylic acid to cell lysates results in consumption of sulfoacrylic acid and formation of CoM would be the first step towards unraveling the enzymatic reactions that catalyze this transformation. For consideration, a CoM analog, bromoethanesulfonate, has been shown to be an effective specific inhibitor of the enzymes involved in propylene metabolism, or more specifically, 2-KPCC[15]. Bromoethanesulfonate may be useful in future undetermined experiments if it is deemed necessary to attempt termination of propylene metabolism once the cells have been able to grow efficiently.

If the issues faced with purified XcbD1 were a result of supplying the incorrect cosubstrate, then the metabolite profile of propylene-grown *X. autotrophicus* Py2 would presumably contain the necessary cosubstrate for XcbD1 catalysis. One immediately obvious issue is that even if the XcbD1 reaction forms product X, it may be at concentrations too low for Q-TOF MS detection. Thus, designing methods to increase yields of respective intermediates and also inhibiting the next step of the reaction so that product X is not consumed would be necessary steps towards utilizing the cell lysates.

There is also the possibility that XcbD1 does not catalyze sulfoacrylic acid, and that role falls on another enzyme expressed under propylene-growth conditions (refer to Broberg et al., for the list of enzymes detected[16]).

Another experiment to try in the future would involve incubating purified XcbD1 with sulfoacrylic acid in a pH 7 ± 1 buffer containing high concentrations (approximately 400 mM) ammonium chloride or other ammonium salt, to determine if XcbD1 could catalyze the addition of ammonium across the double bond of sulfoacrylic acid. This reaction could be readily monitored on ^{1}H-NMR through a distinctive resonance peak shift if the sulfoacryic acid is transformed into an alkane, rather than containing olefinic hydrogens. One of the possible isomers for this reaction is L-cysteate (the other being an aminosulfopropionic acid), which happens to be an intermediate in the L-phosphoserine-dependent pathway in methanoarchaeal CoM biosynthesis, and serves as a substrate for the PLP-dependent canonical aspartate aminotransferase. This would be an intriguing development, particularly because the putative next enzyme in the pathway, XcbE1, is a PLP-dependent enzyme. These enzymes are known for catalyzing reactions on predominantly amino acid substrates by forming PLP-substrate adducts through Schiff base formation between the PLP cofactor and the amino group of the respective substrate. Testing the XcbD1 reaction for formation of L-cysteate and also possibly screening the XcbE1 reaction with cysteine and L-cysteate (as described by methods in Ch. 3) could either provide more clues, or effectively rule out another potential intermediate. If L-cysteate appears to be an unviable intermediate, we predict that a primary amine would be the most likely candidate for addition to sulfoacrylic acid, by virtue of the proposed

subsequent PLP-dependent step. At the time of this thesis, other amines have not been screened in this reaction other than the adenylated/guanylated compounds listed throughout this chapter, meaning that there are many potential compounds left to be screened, like ammonium salts, amino acids, and simple organic alkyl amines.

Based on our studies done on XcbD1 and XcbE1, it is apparent that the final stages of bacterial CoM biosynthesis are not as clear cut as the first two steps catalyzed by XcbB1 and XcbC1. Future studies contain the potential exciting opportunity to uncover yet another unique AFS enzyme, like XcbC1, that catalyzes an unprecedented reaction.

References

1 Puthan Veetil, V., Fibriansah, G., Raj, H., Thunnissen, A. M. & Poelarends, G. J. Aspartase/fumarase superfamily: a common catalytic strategy involving general base-catalyzed formation of a highly stabilized aci-carboxylate intermediate. *Biochemistry* **51**, 4237-4243, doi:10.1021/bi300430j (2012).

2 Tsai, M. *et al.* Substrate and product complexes of Escherichia coli adenylosuccinate lyase provide new insights into the enzymatic mechanism. *J Mol Biol* **370**, 541-554, doi:10.1016/j.jmb.2007.04.052 (2007).

3 Toth, E. A. & Yeates, T. O. The structure of adenylosuccinate lyase, an enzyme with dual activity in the de novo purine biosynthetic pathway. *Structure* **8**, 163-174, doi:https://doi.org/10.1016/S0969-2126(00)00092-7 (2000).

4 Porter, D. J., Rudie, N. G. & Bright, H. J. Nitro analogs of substrates for adenylosuccinate synthetase and adenylosuccinate lyase. *Arch Biochem Biophys* **225**, 157-163 (1983).

5 Lee, T. T., Worby, C., Bao, Z. Q., Dixon, J. E. & Colman, R. F. His68 and His141 are critical contributors to the intersubunit catalytic site of adenylosuccinate lyase of Bacillus subtilis. *Biochemistry* **38**, 22-32, doi:10.1021/bi982299s (1999).

6 Kozlov, G., Nguyen, L., Pearsall, J. & Gehring, K. The structure of phosphate-bound Escherichia coli adenylosuccinate lyase identifies His171 as a catalytic acid. *Acta Crystallographica Section F: Structural Biology and Crystallization Communications* **65**, 857-861, doi:10.1107/S1744309109029674 (2009).

7 He, B., Smith, J. M. & Zalkin, H. Escherichia coli purB gene: cloning, nucleotide sequence, and regulation by purR. *J Bacteriol* **174**, 130-136 (1992).

8 Fyfe, P. K., Dawson, A., Hutchison, M. T., Cameron, S. & Hunter, W. N. Structure of Staphylococcus aureus adenylosuccinate lyase (PurB) and assessment of its potential as a target for structure-based inhibitor discovery. *Acta Crystallogr D Biol Crystallogr* **66**, 881-888, doi:10.1107/s0907444910020081 (2010).

9 Bulusu, V., Srinivasan, B., Bopanna, M. P. & Balaram, H. Elucidation of the substrate specificity, kinetic and catalytic mechanism of adenylosuccinate lyase from Plasmodium falciparum. *Biochim Biophys Acta* **1794**, 642-654, doi:10.1016/j.bbapap.2008.11.021 (2009).

10 Brosius, J. L. & Colman, R. F. Three Subunits Contribute Amino Acids to the Active Site of Tetrameric Adenylosuccinate Lyase: Lys268 and Glu275 Are Required†. *Biochemistry* **41**, 2217-2226, doi:10.1021/bi011998t (2002).

11 Banerjee, S. *et al.* Structural and kinetic studies on adenylosuccinate lyase from Mycobacterium smegmatis and Mycobacterium tuberculosis provide new insights on the catalytic residues of the enzyme. *The FEBS journal* **281**, 1642-1658, doi:10.1111/febs.12730 (2014).

12 Marchler-Bauer, A. *et al.* CDD/SPARCLE: functional classification of proteins via subfamily domain architectures. *Nucleic acids research* **45**, D200-D203, doi:10.1093/nar/gkw1129 (2017).

13 Bartolini, M., Wainer, I. W., Bertucci, C. & Andrisano, V. The rapid and direct determination of ATP-ase activity by ion exchange chromatography and the application to the activity of heat shock protein-90. *Journal of pharmaceutical and biomedical analysis* **73**, 77-81, doi:10.1016/j.jpba.2012.03.021 (2013).

14 Yang, J. *et al.* Crystal structure of 3-carboxy-cis,cis-muconate lactonizing enzyme from Pseudomonas putida, a fumarase class II type cycloisomerase: enzyme evolution in parallel pathways. *Biochemistry* **43**, 10424-10434, doi:10.1021/bi036205c (2004).

15 Boyd, J. M., Ellsworth, A. & Ensign, S. A. Characterization of 2-Bromoethanesulfonate as a Selective Inhibitor of the Coenzyme M-Dependent Pathway and Enzymes of Bacterial Aliphatic Epoxide Metabolism. *Journal of Bacteriology* **188**, 8062-8069, doi:10.1128/JB.00947-06 (2006).

16 Broberg, C. A. & Clark, D. D. Shotgun proteomics of Xanthobacter autotrophicus Py2 reveals proteins specific to growth on propylene. *Arch Microbiol* **192**, 945-957, doi:10.1007/s00203-010-0623-3 (2010).

CHAPTER FIVE

CONCLUDING REMARKS

Bacterial CoM biosynthesis has remained uncharacterized since the discovery of CoM in a bacterial pathway for alkene metabolism in proteobacterium *Xanthobacter autotrophicus* Py2 in the late nineties[1,2]. This thesis focuses on gene products putatively involved in CoM biosynthesis encoded by *xcbB1, xcbC1, xcbD1,* and *xcbE1,* that are located directly downstream from genes for alkene monooxygenase and epoxide carboxylation on the *X. autotrophicus* Py2 plasmid. Multiple copies of these genes also exist on the plasmid. These gene products as well as the enzymes responsible for alkene monooxygenase and epoxide carboxylation have been shown to express under conditions where *X. autotrophicus* Py2 is grown with propylene as the sole supplemented carbon source, indicating a common regulatory element[3].

Investigating the putative gene products of *xcbB1* and *xcbC1* by informatics, biochemical, and spectroscopic means revealed a PEP-dependent pathway for bacterial CoM biosynthesis that is distinct from the PEP-dependent pathway in methanogens (Fig 5.1). Out of the four enzymes possibly involved in CoM biosynthesis, only XcbB1 is homologous to the pathway enzyme ComA, which is known to encode the first step in the PEP-dependent CoM biosynthesis in methanogens. XcbB1 catalyzes the addition of sulfite to PEP to yield phosphosulfolactate, which is delivered as the substrate for the subsequent XcbC1 reaction. The resulting reaction involves the β-elimination of phosphate, yielding sulfoacrylic acid and inorganic phosphate.

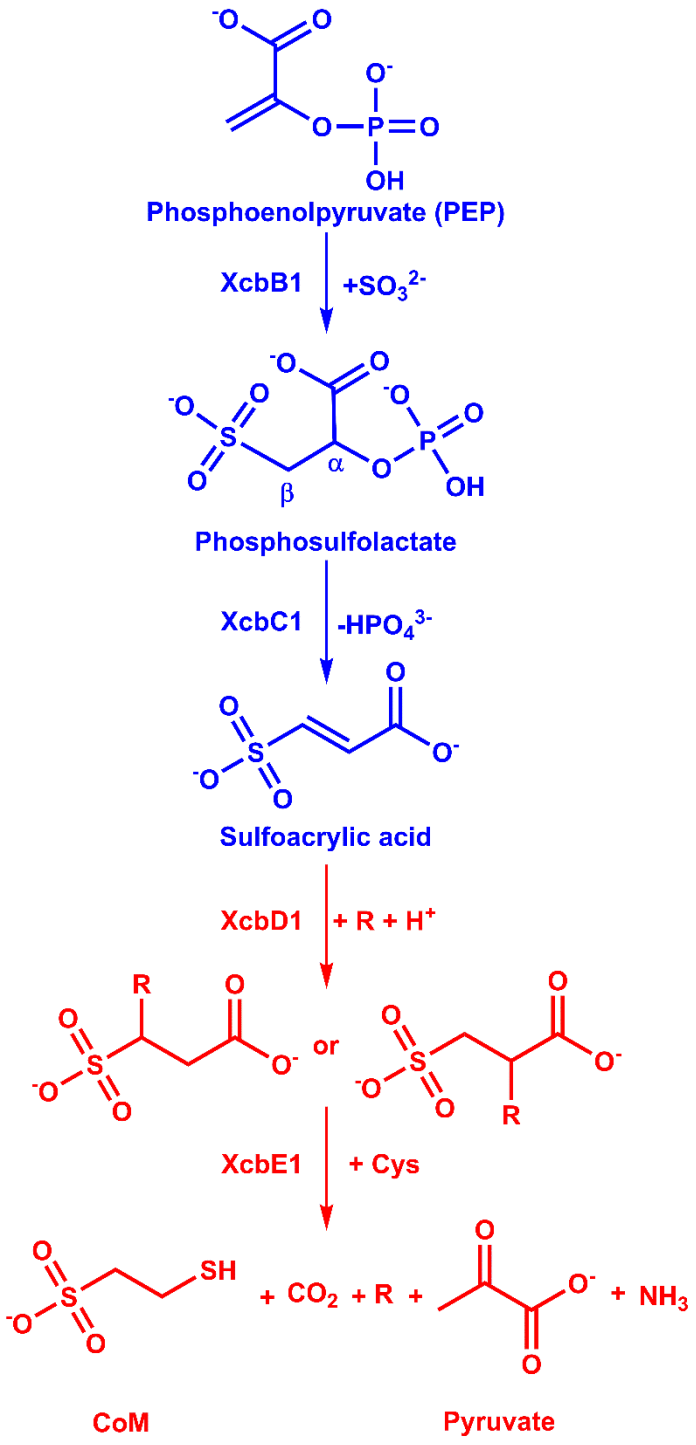

Figure 5.1. The PEP-dependent pathway for bacterial CoM biosynthesis is depicted. Steps supported by biochemical and spectroscopic data are shown in blue while hypothetical steps are shown in red.

Though the activity of XcbD1 remains unidentified, we proposed that XcbD1 catalyzes a conjugate addition reaction homologous to that of AFS enzymes. We also implicated an important role for PLP-dependent XcbE1 in providing the source of the CoM thiol derived from cysteine. This work will serve as the framework for future studies aimed at uncovering the final stages of the biosynthetic pathway. The reactions elucidated for XcbB1 and XcbC1 place firm restrictions on the subsequent steps required to complete CoM biosynthesis.

XcbD1 is homologous to adenylosuccinate lyases (ADL) that catalyze the reversible β-elimination of adenylosuccinate to AMP and fumarate[4]. Bioinformatics provided clues about the trajectory of the pathway after the XcbC1 reaction, and we proposed that XcbD1 may catalyze an analogous ADL-type reaction through the addition of an unidentified cosubstrate across the double bond of sulfoacrylic acid. Attempts to screen this reaction with multiple proposed cosubstrates including; AMP, ADP, ATP, GMP, and GTP ± cysteine, or with cysteine alone did not yield an adenylated or guanylated product, or some other cysteinyl-adduct. Additionally, XcbD1 incubated with sulfoacrylic acid individually did not seem to initiate any other sort of reaction when the reaction was observed in real time through time-resolved ^{1}H-NMR. Efforts to unravel XcbD1 activity are still ongoing, but we proposed that the XcbD1 product would be the substrate for XcbE1 (Fig 5.1).

XcbE1 is a pyridoxal 5’-phosphate (PLP)-dependent enzyme homologous to D-cysteine desulfhydrases, that catalyze the α,β-elimination of D-cysteine to H_2S, pyruvate, and ammonia[5]. We have shown that XcbE1 can catalyze both D-and L-cysteine, making

it an attractive candidate for supplying cysteine-derived sulfur towards the formation of the CoM thiol moiety. However, without knowing the product of the XcbD1 reaction, the cosubstrate for XcbE1 the mechanism of thiolation cannot be determined. In addition, the substrate of XbcE1 will also require decarboxylation to arrive at the CoM product. Because several PLP-dependent enzymes have been shown to be bifunctional, catalyzing combination reactions of the basic PLP-chemistry types[6], it was conceivable that XcbE1 could catalyze a more complicated reaction that couples thiolation with possibly decarboxylation. We attempted to screen several possible cosubstrates with XcbE1 plus D- or L-cysteine, including; isethionate, vinyl sulfonate, sulfolactate, and sulfoacetaldehyde, and were unable to detect CoM. Elucidating the XcbD1 reaction could possibly directly contribute to elucidating the role of XcbE1 in CoM biosynthesis. As discussed in Ch. 4, optimizing assay conditions when using *X. autotrophicus* Py2 cell lysates to determine if supplemented sulfoacrylic acid is transformed to CoM may also be a useful step towards elucidating the rest of the pathway.

Future work towards solving the rest of the pathway may involve examining other enzymes expressed under propylene-growth conditions in *X. autotrophicus* Py2. For example, the open reading frame directly previous to *xcbB1* (labeled *xcbA1*) appears to contain a stop codon in the middle of the sequence, encoding an incomplete protein that does not express during propylene-growth conditions. However, the downstream copy of this gene (*xcbA2*) appears to encode a complete protein that was expressed during propylene-growth condtions[3]. XcbA2 is not homologous to any known enzymes, and pBLAST results indicate homology with other hypothetical/conserved proteins. Several

of these hypothetical/conserved proteins are found in organisms that utilize CoM-dependent alkene metabolism (i.e. *Nocardioidies, Mycobacterium,* etc). Ni-NTA purification of His-tagged XcbA2 (refer to Appendix A for list of plasmids, and Ch. 2 for general expression and purification methods for His-tagged enzymes) followed by Q-sepharose purification (refer to Ch. 4 for general Q-sepharose purification methods) yields a pinkish or when more concentrated, a reddish-brown enzyme (Fig 5.2) at ~35 kDa when run on SDS-PAGE.

Figure 5.2. Ni-NTA and Q-sepharose purification of XcbA2 yields pinkish or when more concentrated, a reddish-brown enzyme. The picture depicts a 30 kDa molecular weight cutoff filter that appears to have concentrated XcbA2 towards the bottom of the cone, indicating that the color is a feature of the protein and not an artifact of the cell lysate.

Uv-Vis scans of purified XcbA2 at pH 8 indicate peaks at 340 and 440 nm, hinting at the existence of a cofactor or prosthetic group. For example, some purified quinoproteins containing pyrroloquinoline quinone (PQQ) prosthetic groups exhibit absorption at 350 and 440 nm[7], and free PQQ solutions can appear pink at neutral pH[8]. Additionally, some pink copper proteins can exhibit dual absorption peaks in the 350-500 nm visible range at neutral pH[9]. Setting up preliminary experiments with XcbA2 and the

other purified enzymes (B1, C1, D1, and E1) may be a possible avenue towards solving the pathway. Besides XcbA2, there are other enzymes on the *X. autotrophicus* Py2 plasmid that also express under propylene growth conditions[3], and it may be worthwhile to utilize some additional bioinformatics gain clues into the potential activity of these enzymes.

Even without working directly towards elucidating CoM biosynthesis, XcbC1 could benefit from additional kinetics and structural studies to further examine this unique AFS enzyme. Obtaining crystal structures of phosphosulfolactate-bound XcbC1 would establish the mechanism proposed with the assistance of a homology model in Ch. 2. Once the trajectory of bacterial CoM biosynthesis is established, structural studies would be informative for all presumably unique enzymes. Currently, the enzyme(s) that catalyze the final stages of both PEP- and L-phosphoserine-dependent pathways of methanoarchaeal CoM biosynthesis remain unidentified. Solving the bacterial pathway for CoM biosynthesis in *X. autotrophicus* Py2 could not only contribute to the general field of knowledge surrounding CoM biosynthesis, but could potentially be the first complete pathway for CoM biosynthesis, while also being the first pathway solved in bacteria. The opportunities for future studies with the goal of characterizing the enzymes involved in the pathway may also contribute to the elucidation of other pathways for CoM biosynthesis in bacteria like *Nocardioides* sp. JS614 or *Mycobacterium* species that utilize CoM-dependent alkene metabolism. Though the path to completion after the steps catalyzed by XcbB1 and XcbC1 is subject to some speculation, the potential opportunities are numerous and exciting.

To conclude, we verified that XcbB1 catalyzes the addition of sulfite to PEP, initiating the first step of the bacterial CoM biosynthetic pathway in *X. autotrophicus* Py2. We also demonstrate herein that XcbC1 catalyzes a β-elimination reaction on the substrate phosphosulfolactate to yield sulfoacrylic acid and inorganic phosphate. To our knowledge, β-elimination reactions releasing phosphate is unprecedented among the AFS, indicating XcbC1 is a unique phosphatase. We have also suggested methods towards identifying the last stages of bacterial CoM biosynthesis, and thus this work will serve as the framework for future studies aimed at uncovering the final stages of the biosynthetic pathway. We have demonstrated that bacterial CoM biosynthesis in *X. autotrophicus* Py2 is a PEP-dependent pathway that differs from that of the methanogens, and by elucidating the XcbB1 and XcbC1 reactions, we have made significant strides towards understanding bacterial CoM biosynthesis which evaded characterization in previous years.

References

1 Krishnakumar, A. M. *et al.* Getting a Handle on the Role of Coenzyme M in Alkene Metabolism. *Microbiology and Molecular Biology Reviews : MMBR* **72**, 445-456, doi:10.1128/MMBR.00005-08 (2008).

2 Allen, J. R., Clark, D. D., Krum, J. G. & Ensign, S. A. A role for coenzyme M (2-mercaptoethanesulfonic acid) in a bacterial pathway of aliphatic epoxide carboxylation. *Proc Natl Acad Sci U S A* **96**, 8432-8437 (1999).

3 Broberg, C. A. & Clark, D. D. Shotgun proteomics of Xanthobacter autotrophicus Py2 reveals proteins specific to growth on propylene. *Arch Microbiol* **192**, 945-957, doi:10.1007/s00203-010-0623-3 (2010).

4 Toth, E. A. & Yeates, T. O. The structure of adenylosuccinate lyase, an enzyme with dual activity in the de novo purine biosynthetic pathway. *Structure* **8**, 163-174, doi:https://doi.org/10.1016/S0969-2126(00)00092-7 (2000).

5 Soutourina, J., Blanquet, S. & Plateau, P. Role of D-cysteine desulfhydrase in the adaptation of Escherichia coli to D-cysteine. *J Biol Chem* **276**, 40864-40872, doi:10.1074/jbc.M102375200 (2001).

6 Eliot, A. C. & Kirsch, J. F. Pyridoxal phosphate enzymes: mechanistic, structural, and evolutionary considerations. *Annu Rev Biochem* **73**, 383-415, doi:10.1146/annurev.biochem.73.011303.074021 (2004).

7 Kawai, F. *et al. Identification of the prosthetic group and further characterization of a novel enzyme, polyethylene glycol dehydrogenase*. Vol. 49 (1985).

8 Ameyama, M., Hayashi, M., Matsushita, K., Shinagawa, E. & Adachi, O. Microbial Production of Pyrroloquinoline Quinone. *Agricultural and Biological Chemistry* **48**, 561-565, doi:10.1271/bbb1961.48.561 (1984).

9 Reed, D. W., Passon, P. G. & Hultquist, D. E. Purification and Properties of a Pink Copper Protein from Human Erythrocytes. *Journal of Biological Chemistry* **245**, 2954-2961 (1970).

APPENDICES

APPENDIX A

SUPPLEMENTARY INFORMATION TO CHAPTER 1

Old locus tag	New locus tag	Gene	Annotation	Enzyme accession
NA	XAUT_RS24675	*xcbA1*	Hypothetical protein – (pseudo)	N/A
xaut_4872	XAUT_RS24680	*xcbB1*	Phosphosulfolactate synthase	WP_011992985
xaut_4873	XAUT_RS24685	*xcbC1*	Argininosuccinate lyase	WP_049776202
xaut_4874	XAUT_RS24690	*xcbD1*	adenylosuccinate lyase family protein	WP_011992987
xaut_4875	XAUT_RS24695	*xcbE1*	1-Aminocyclopropane-1-carboxylate deaminase	WP_041578134
xaut_5051	XAUT_RS25610	*xcbA2*	Hypothetical protein	WP_011993152
xaut_5052	XAUT_RS25615	*xcbB2*	Phosphosulfolactate synthase	WP_011993153
xaut_5053	XAUT_RS25620	*xcbC2*	Argininosuccinate lyase	WP_011993154
xaut_5054	XAUT_RS25625	*xcbD2*	Adenylosuccinate lyase family protein	WP_011993155
xaut_5055	XAUT_RS25630	*xcbE2*	1-aminocyclopropane-1-carboxylate deaminase	WP_011993156
xaut_5070	XAUT_RS25710	*xcbA3*	Hypothetical protein	WP_011993171
xaut_5069	XAUT_RS25705	*xcbB3*	Phosphosulfolactate synthase	WP_011993170
xaut_5068	XAUT_RS25700	*xcbC3*	Argininosuccinate lyase	WP_011993169
xaut_5067	XAUT_RS25695	*xcbD3*	Adenylosuccinate lyase family protein	WP_011993168

Table S1. The gene and all known copies that putatively encode the enzymes responsible for CoM biosynthesis are listed with old and current locus tags, annotations, and enzyme accession numbers. Plasmid: pXAUT01, accession number: NC_009717.

Insert	**Vector**	**MCS1**	**MCS2**	**N-term His**	**ABX^{R}**	**F Site**	**R-site**
xcbB1	pETDUET-1	✓	-	✓	Amp	SacI	NdeI
xcbC1	pACYCDuet-1	✓	-	✓	Cm	BamHI	BglII
xcbD1	pCDFDuet-1	-	✓	-	Strep	BglII	EcoRV
xcbE1	pETDuet-1	✓	-	✓	Amp	PstI	EcoRV
xcbA2	pETDuet-1	✓	-	✓	Amp	BamHI	NdeI

Table S2. The expression vectors discussed throughout the thesis are summarized here for convenience.

Locus Tag	Gene	NCBI Annotation	Old locus tag
XAUT_RS24575		polyphosphate kinase 2	
XAUT_RS27075		toll/interleukin-1 receptor domain-containing protein	
XAUT_RS24585		IS3 family transposase	
XAUT_RS24590		ATP-binding protein	
XAUT_RS24595		hypothetical protein	
XAUT_RS27080		hypothetical protein	
XAUT_RS27085		DUF3363 domain-containing protein	
XAUT_RS24610	*xamoA*	methane/phenol/toluene hydroxylase	Xaut_4857
XAUT_RS24615	*xamoB*	toluene-4-monooxygenase system B	Xaut_4858
XAUT_RS24620	*xamoC*	(2Fe-2S)-binding protein	Xaut_4859
XAUT_RS24625	*xamoE*	monooxygenase	Xaut_4860
XAUT_RS24630	*xamoF*	toluene hydroxylase	Xaut_4861
XAUT_RS24635		oxidoreductase FAD-binding subunit	Xaut_4862
XAUT_RS24640		aldehyde dehydrogenase	Xaut_4863
XAUT_RS24645		transcriptional regulator	Xaut_4864
XAUT_RS24650	*xecA1*	2-hydroxypropyl-CoM lyase	Xaut_4865
XAUT_RS24655	*xecB1*	hypothetical protein	Xaut_4866
XAUT_RS24660	*xecC1*	2-oxopropyl-CoM reductase (carboxylating)	Xaut_4867
XAUT_RS24665	*xecD1*	2-(R)-hydroxypropyl-CoM dehydrogenase	Xaut_4868
XAUT_RS24670	*xecE1*	2-(S)-hydroxypropyl-CoM dehydrogenase	Xaut_4869
XAUT_RS24675	*xcbA1*	hypothetical protein	
XAUT_RS24680	*xcbB1*	phosphosulfolactate synthase	xaut_4872
XAUT_RS24685	*xcbC1*	argininosuccinate lyase	xaut_4873
XAUT_RS24690	*xcbD1*	adenylosuccinate lyase family protein	xaut_4874
XAUT_RS24695	*xcbE1*	1-aminocyclopropane-1-carboxylate deaminase	xaut_4875
XAUT_RS24700		LysR family transcriptional regulator	
XAUT_RS24705		OmpW family protein	
XAUT_RS24710		IS1380 family transposase	
XAUT_RS24715		copper oxidase	xaut_4880
XAUT_RS24720		DUF302 domain-containing protein	xaut_4881
XAUT_RS24725		rhodanese-like domain-containing protein	
XAUT_RS24730		NADH-quinone oxidoreductase subunit I	
XAUT_RS24735		Ni Fe-hydrogenase III large subunit	
XAUT_RS27090		hypothetical protein	
XAUT_RS24745		hypothetical protein	
XAUT_RS24750		DUF2933 domain-containing protein	
XAUT_RS24755		isoprenylcysteine carboxylmethyltransferase family protein	
XAUT_RS24760		hypothetical protein	

XAUT_RS24765		autoinducer-binding protein	
XAUT_RS24770		hypothetical protein	
XAUT_RS24775		DUF1419 domain-containing protein	
XAUT_RS24780		DUF3085 domain-containing protein	
XAUT_RS24785		lactate dehydrogenase	
XAUT_RS24790		DDE transposase	
XAUT_RS24795		hypothetical protein	

Table S3. The gene loci for 20 genes upstream and downstream from the putative CoM biosynthetic genes are listed. Genes that putatively encode CoM biosynthetic genes are pink, expoxide carboxylase are green, and alkene monooxygenase are yellow.

Locus tag	Gene	Product	Enzyme accession
MJ_0255	*comA*	phosphosulfolactate synthase	AAB98242
MJ_1140	*comB*	2-Phosphosulfolactate phosphatase	AAB99140
MJ_1425	*comC*	Sulfolactate dehydrogenase	AAB99436
MJ_0255.1	*comD*	Sulfopyruvate decarboxylase subunit alpha	P58415
MJ_0256	*comE*	Sulfopyruvate decarboxylase subunit beta	P58416
MA3297	*thrC*	Cysteate synthase	AAM06667
MA3298	*comDE*	sulfopyruvate decarboxylase	AAM06668

Table S4. The genes and respective encoded products for both PEP and L-phosphoserine-dependent pathways in methanogenic archaea. Enzymes from the PEP-dependent pathway in Methanocaldococcus jannaschii DSM 2661 are highlighted in yellow and enzymes from the L-phosphoserine dependent Methanosarcina acetivorans C2A are highlighted in blue.

APPENDIX B

SUPPLEMENTARY INFORMATION FOR CHAPTER TWO

Gene	**Primer Sequence**	**Restriction Sites**
xcbB1	Fwd: 5'- AAAGAGCTCGATGCAAGCTAGATCGGACCGC–3'	SacI
	Rev: 5'- TTACATATGCTAGACATGGCGCAGCTCTTG -3'	NdeI
xcbC1	Fwd: 5'- ATTGGATCCTATGACTAGGCTTTCCGACCGG -3'	BamHI
	Rev: 5'- AACAGATCTTCATGGCGCCCTCCCC -3'	BglII
xcbE1	Fwd: 5'- ACACTGCAGATGGAGCAGCCTGACATGCGG-3'	PstI
	Rev: 5'- AGCGATATCTCACGCGGTTCCATCGACGAAC -3'	EcoRV

Table S1**.** The primers used for amplifying *xcbB1* and *xcbC1* sequences from the *X. autotrophicus* Py2 linear megaplasmid. Highlighted regions indicate restriction sites.

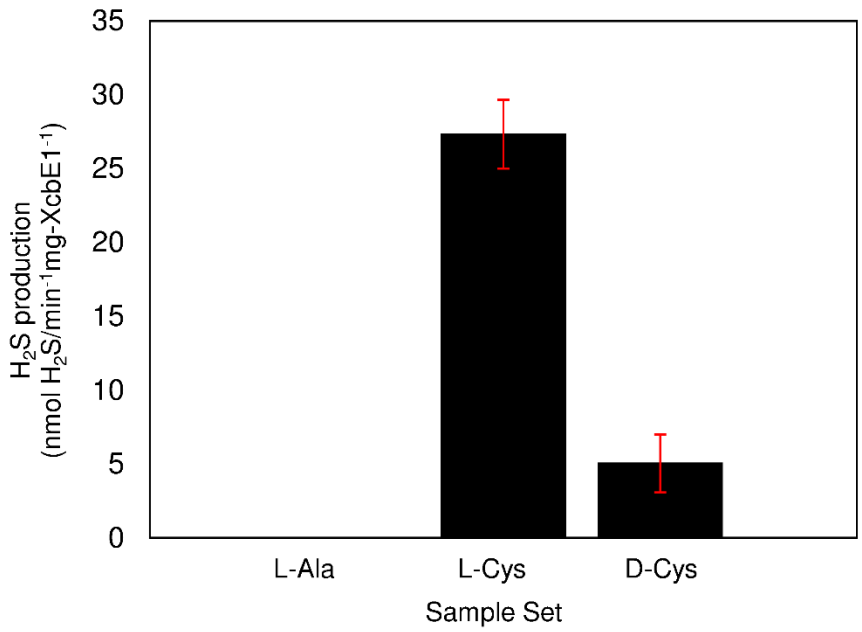

Figure S1**.** A methylene blue activity assay measuring levels of H_2S gas was used to determine relative activity of XcbE1 when supplemented with D- or L-Cys, with L-Ala used as a control. Specific activity was 27.31 ± 2.31 nmol $H_2S/min^{-1}mg\text{-}XcbE1^{-1}$ for L-Cys and 5.04 ± 1.95 nmol $H_2S/min^{-1}mg\text{-}XcbE1^{-1}$for D-cys.

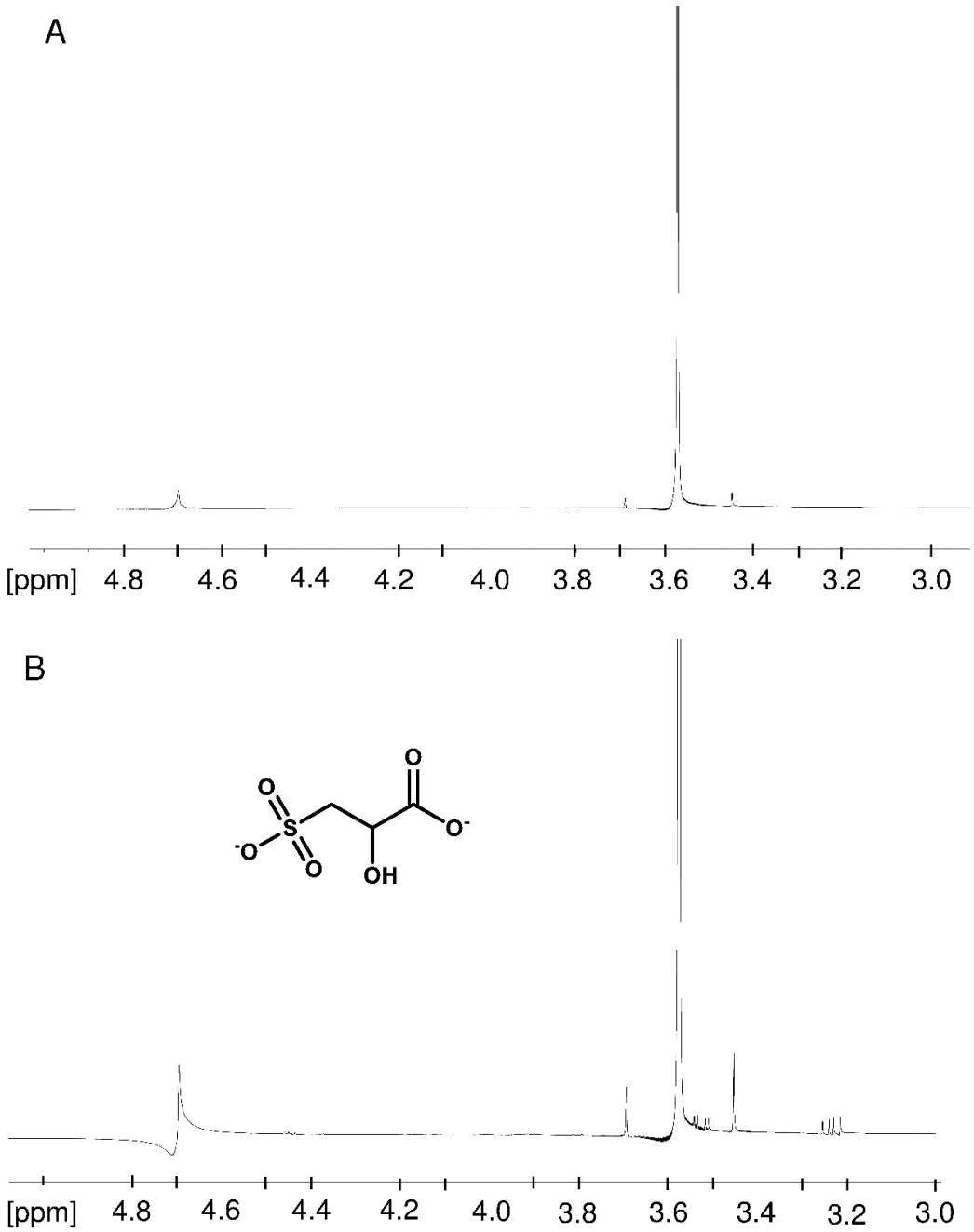
A
[ppm] 4.8 4.6 4.4 4.2 4.0 3.8 3.6 3.4 3.2 3.0
B
O
O
S
-O
O
OH
O
O-
[ppm] 4.8 4.6 4.4 4.2 4.0 3.8 3.6 3.4 3.2 3.0

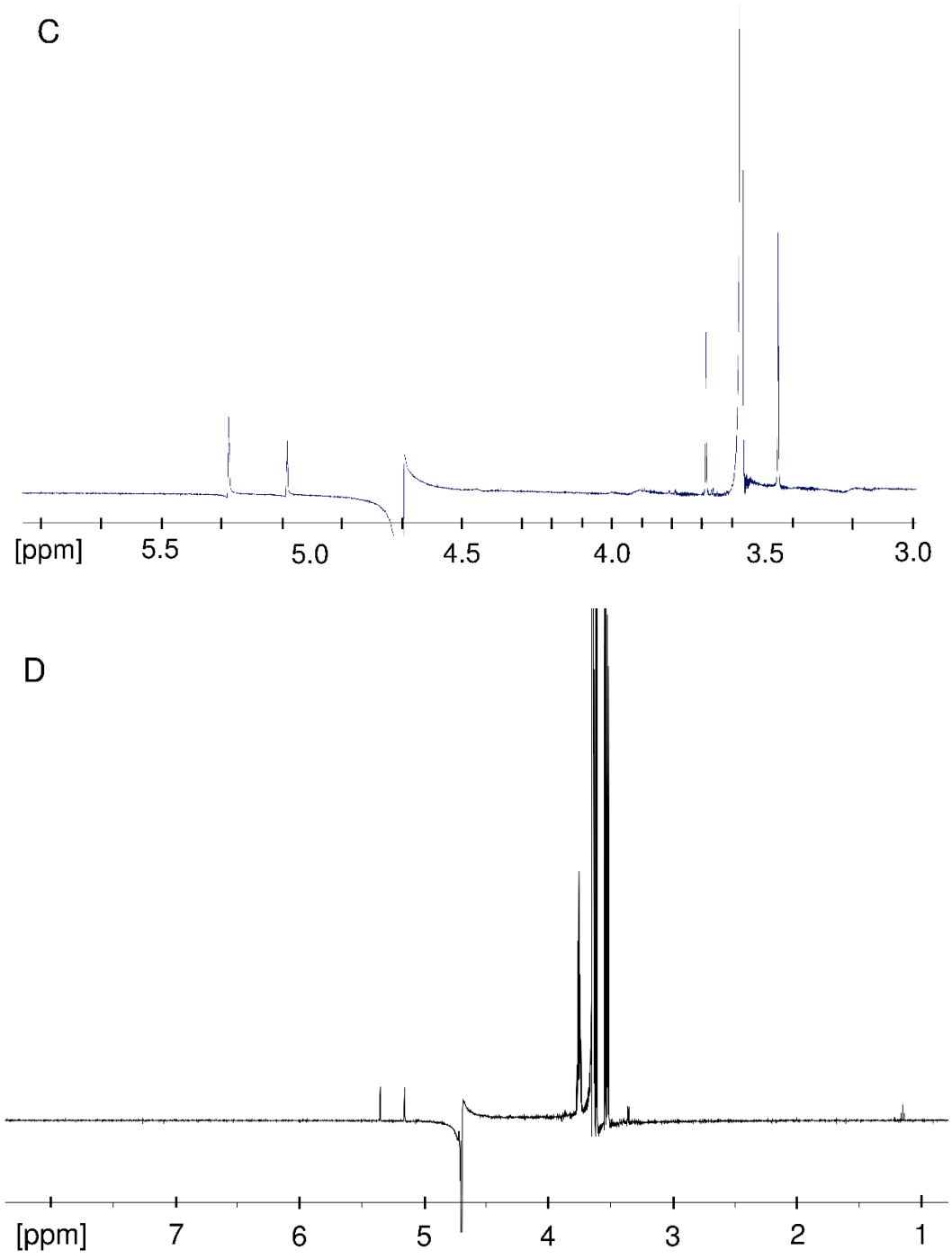

Figure S2. Controls for time-resolved ^{1}H-NMR experiments are shown; 50 mM Tris, 50 mM NaCl, 5 mM $MgCl_2$, pH 8 reaction buffer only (A), 1 mM sulfolactate in reaction buffer (B), 1 mM PEP in reaction buffer (C), 2 mM PEP + XcbB1 in reaction buffer at t=0 min (D).

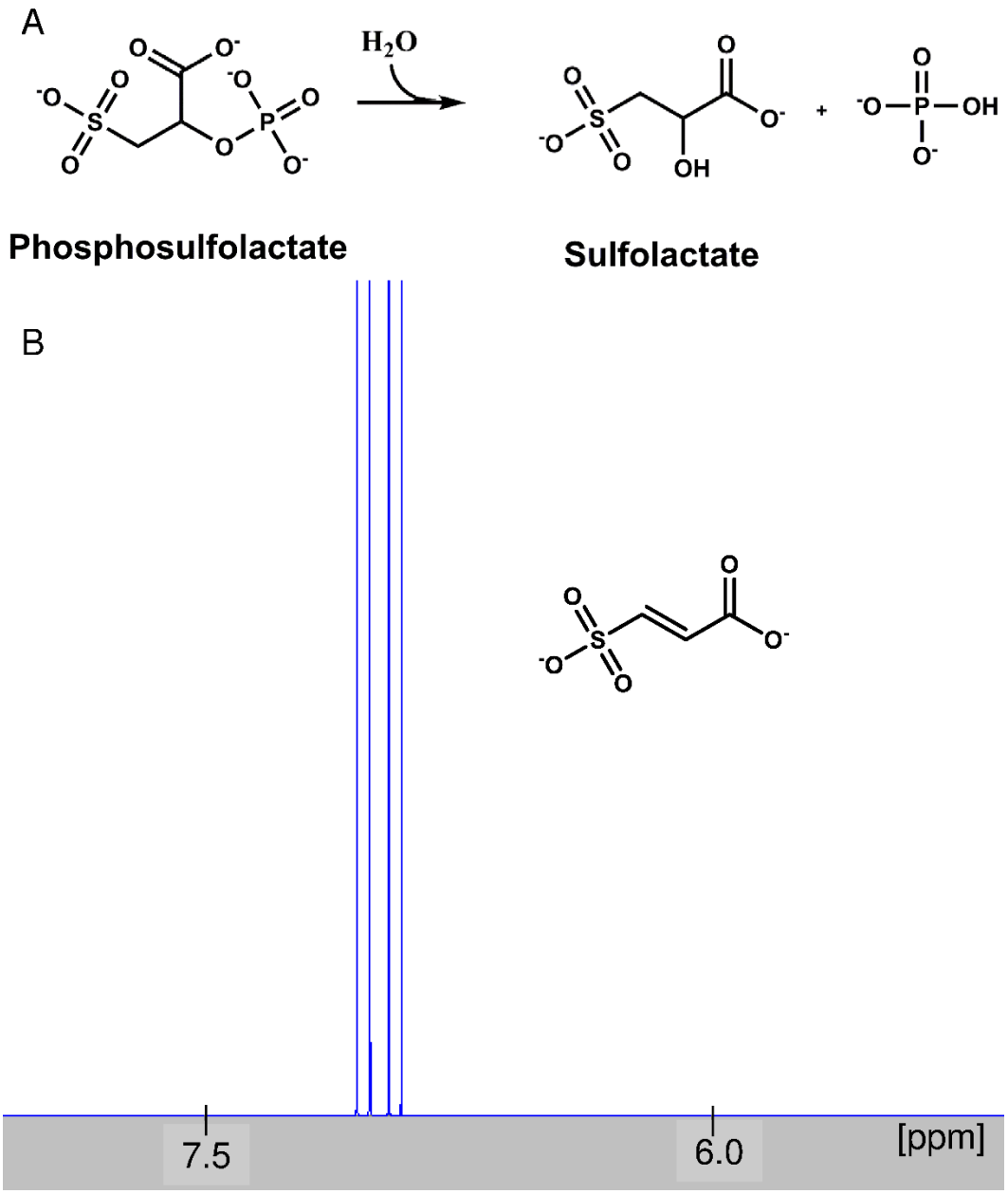

Figure S3. A scheme for a canonical phosphatase reaction for XcbC1 is shown (A), where cleavage of the phosphosulfolactate phosphomonoester is followed by production of an alcohol product (sulfolactate) and inorganic phosphate. The ^{1}H-NMR predicted spectrum for sulfoacrylic acid (B) was obtained for experimental comparison purposes, in lieu of a synthetic standard. The enlarged view of the spectrum shows a pair of doublets between 6-7.5 ppm. Predicted ^{1}H-NMR data calculated using Advanced Chemistry Development, Inc. (ACD/Labs) Software V11.01 (© 1994-2017 ACD/Labs).

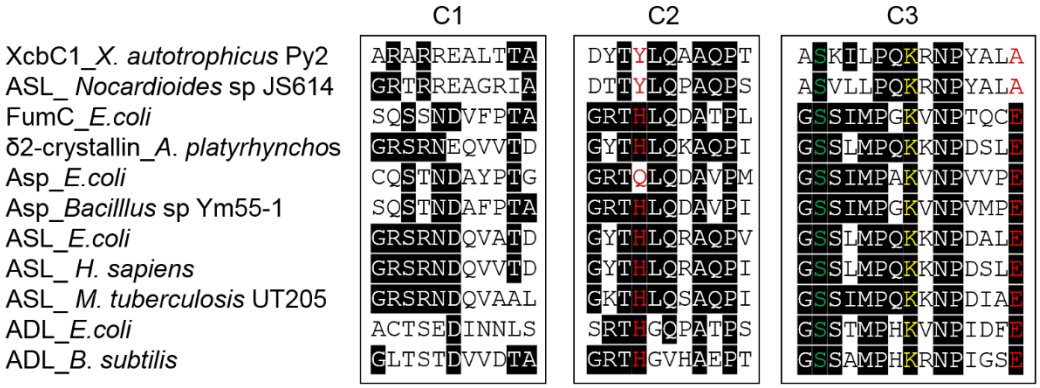

Figure S4. The conserved regions C1-C3 for AFS memebers are shown at 50% identity. The other argininosuccinate lyase-like enzyme that may be involved in a pathway for CoM biosynthesis is labeled as 'ASL_Nocardioides sp. JS614' (NocARL). The catalytic base serine (green), the position of the variable catalytic acid histidine/glutamate charge relay pair (red) and the conserved Lys that interacts with the substrate α-carboxylate (yellow) are all marked. Abbreviations for enzymes are; ASL – argininosuccinate lyase, ADL – adenylosuccinate lyase, Asp – aspartase, FumC – class II fumarase, and the unabbreviated δ2-crystallin.

CUMULATIVE REFERENCES CITED

Chapter one

1 McBride, B. C. & Wolfe, R. S. A new coenzyme of methyl transfer, Coenzyme M. *Biochemistry* **10**, 2317-2324 (1971).

2 Taylor, C. D. & Wolfe, R. S. Structure and Methylation of Coenzyme M ($HSCH_2CH_2SO_3$). *Journal of Biological Chemistry* **15**, 4879-4885 (1974).

3 Taylor, C. D. & Wolfe, R. S. A Simplified Assay for Coenzyme M ($HSCH_2CH_2SO_3$). *Journal of Biological Chemistry* **15**, 4886-4890 (1974).

4 Balch, W. E. & Wolfe, R. S. New Approach to the Cultivation of Methanogenic Bacteria: 2-Mercaptoethanesulfonic Acid (HS-CoM)-Dependent Growth of *Methanobacterium ruminantium* in a Pressurized Atmosphere. *Applied and Environmental Microbiology* **32**, 781-791 (1976).

5 Taylor, C. D., McBride, B. C., Wolfe, R. S. & Bryant, M. P. Coenzyme M, Essential for Growth of a Rumen Strain of *Methanobacterium ruminantium*. *Journal of Bacteriology* **120**, 974-975 (1974).

6 Balch, W. E. & Wolfe, R. S. Specificity and biological distribution of coenzyme M (2-mercaptoethanesulfonic acid). *J Bacteriol* **137**, 256-263 (1979).

7 Shima, S., Warkentin, E., Thauer, R. K. & Ermler, U. Structure and function of enzymes involved in the methanogenic pathway utilizing carbon dioxide and molecular hydrogen. *Journal of bioscience and bioengineering* **93**, 519-530 (2002).

8 Neue, H.-U. Methane Emission from Rice Fields. *BioScience* **43**, 466-474, doi:10.2307/1311906 (1993).

9 Rouviere, P. E. & Wolfe, R. S. Novel biochemistry of methanogenesis. *J Biol Chem* **263**, 7913-7916 (1988).

10 Ermler, U., Grabarse, W., Shima, S., Goubeaud, M. & Thauer, R. K. Crystal structure of methyl-coenzyme M reductase: the key enzyme of biological methane formation. *Science* **278**, 1457-1462 (1997).

11 Olson, K. D., Chmurkowska-Cichowlas, L., McMahon, C. W. & Wolfe, R. S. Structural modifications and kinetic studies of the substrates involved in the final step of methane formation in Methanobacterium thermoautotrophicum. *J Bacteriol* **174**, 1007-1012 (1992).

12 Krishnakumar, A. M. *et al.* Getting a Handle on the Role of Coenzyme M in Alkene Metabolism. *Microbiology and Molecular Biology Reviews : MMBR* **72**, 445-456, doi:10.1128/MMBR.00005-08 (2008).

13 Scheller, S., Goenrich, M., Boecher, R., Thauer, R. K. & Jaun, B. The key nickel enzyme of methanogenesis catalyses the anaerobic oxidation of methane. *Nature* **465**, 606-608, doi:10.1038/nature09015 (2010).

14 Chen, S. L., Blomberg, M. R. & Siegbahn, P. E. How is methane formed and oxidized reversibly when catalyzed by Ni-containing methyl-coenzyme M reductase? *Chemistry* **18**, 6309-6315, doi:10.1002/chem.201200274 (2012).

15 Sluis, M. K. & Ensign, S. A. Purification and characterization of acetone carboxylase from Xanthobacter strain Py2. *Proceedings of the National Academy of Sciences* **94**, 8456-8461 (1997).

16 Boyd, J. M., Ellsworth, H. & Ensign, S. A. Bacterial Acetone Carboxylase Is a Manganese-dependent Metalloenzyme. *Journal of Biological Chemistry* **279**, 46644-46651, doi:10.1074/jbc.M407177200 (2004).

17 Allen, J. R. & Ensign, S. A. Purification to homogeneity and reconstitution of the individual components of the epoxide carboxylase multiprotein enzyme complex from Xanthobacter strain Py2. *J Biol Chem* **272**, 32121-32128 (1997).

18 Clark, D. D., Allen, J. R. & Ensign, S. A. Characterization of five catalytic activities associated with the NADPH:2-ketopropyl-coenzyme M [2-(2-ketopropylthio)ethanesulfonate] oxidoreductase/carboxylase of the Xanthobacter strain Py2 epoxide carboxylase system. *Biochemistry* **39**, 1294-1304 (2000).

19 Swaving, J., de Bont, J. A., Westphal, A. & de Kok, A. A novel type of pyridine nucleotide-disulfide oxidoreductase is essential for NAD+- and NADPH-dependent degradation of epoxyalkanes by Xanthobacter strain Py2. *Journal of Bacteriology* **178**, 6644-6646 (1996).

20 Westphal, A. H., Swaving, J., Jacobs, L. & Kok, A. d. Purification and characterization of a flavoprotein involved in the degradation of epoxyalkanes by Xanthobacter Py2. *European Journal of Biochemistry* **257**, 160-168, doi:10.1046/j.1432-1327.1998.2570160.x (2013).

21 van Ginkel, C. G. & de Bont, J. A. M. Isolation and characterization of alkene-utilizing Xanthobacter spp. *Archives of Microbiology* **145**, 403-407, doi:10.1007/BF00470879 (1986).

22 Allen, J. R. & Ensign, S. A. Carboxylation of epoxides to beta-keto acids in cell extracts of Xanthobacter strain Py2. *Journal of Bacteriology* **178**, 1469-1472 (1996).

23 Ensign, S. A., Small, F. J., Allen, J. R. & Sluis, M. K. New roles for CO2 in the microbial metabolism of aliphatic epoxides and ketones. *Arch Microbiol* **169**, 179-187 (1998).

24 Small, F. J. & Ensign, S. A. Carbon dioxide fixation in the metabolism of propylene and propylene oxide by Xanthobacter strain Py2. *Journal of Bacteriology* **177**, 6170-6175 (1995).

25 Allen, J. R., Clark, D. D., Krum, J. G. & Ensign, S. A. A role for coenzyme M (2-mercaptoethanesulfonic acid) in a bacterial pathway of aliphatic epoxide carboxylation. *Proc Natl Acad Sci U S A* **96**, 8432-8437 (1999).

26 Wade, D. R., Airy, S. C. & Sinsheimer, J. E. Mutagenicity of aliphatic epoxides. *Mutat Res* **58**, 217-223 (1978).

27 Archelas, A. & Furstoss, R. Synthesis of enantiopure epoxides through biocatalytic approaches. *Annu Rev Microbiol* **51**, 491-525, doi:10.1146/annurev.micro.51.1.491 (1997).

28 Besse, P. & Veschambre, H. Chemical and biological synthesis of chiral epoxides. *Tetrahedron* **50**, 8885-8927, doi:http://dx.doi.org/10.1016/S0040-4020(01)85362-X (1994).

29 Small, F. J. & Ensign, S. A. Carbon dioxide fixation in the metabolism of propylene and propylene oxide by Xanthobacter strain Py2. *J Bacteriol* **177**, 6170-6175 (1995).

30 Allen, J. R. & Ensign, S. A. Characterization of three protein components required for functional reconstitution of the epoxide carboxylase multienzyme complex from Xanthobacter strain Py2. *Journal of Bacteriology* **179**, 3110-3115 (1997).

31 Ensign, S. A., Hyman, M. R. & Arp, D. J. Cometabolic degradation of chlorinated alkenes by alkene monooxygenase in a propylene-grown Xanthobacter strain. *Applied and Environmental Microbiology* **58**, 3038-3046 (1992).

32 Krum, J. G. & Ensign, S. A. Heterologous expression of bacterial Epoxyalkane:Coenzyme M transferase and inducible coenzyme M biosynthesis in Xanthobacter strain Py2 and Rhodococcus rhodochrous B276. *J Bacteriol* **182**, 2629-2634 (2000).

33 Coleman, N. V. & Spain, J. C. Distribution of the coenzyme M pathway of epoxide metabolism among ethene- and vinyl chloride-degrading Mycobacterium strains. *Appl Environ Microbiol* **69**, 6041-6046 (2003).

34 Liu, X. & Mattes, T. E. Epoxyalkane:Coenzyme M Transferase Gene Diversity and Distribution in Groundwater Samples from Chlorinated-Ethene-Contaminated Sites. *Applied and Environmental Microbiology* **82**, 3269-3279, doi:10.1128/AEM.00673-16 (2016).

35 Allen, J. R. & Ensign, S. A. Two short-chain dehydrogenases confer stereoselectivity for enantiomers of epoxypropane in the multiprotein epoxide carboxylating systems of Xanthobacter strain Py2 and Nocardia corallina B276. *Biochemistry* **38**, 247-256, doi:10.1021/bi982114h (1999).

36 Mattes, T. E., Coleman, N. V., Spain, J. C. & Gossett, J. M. Physiological and molecular genetic analyses of vinyl chloride and ethene biodegradation in Nocardioides sp. strain JS614. *Arch Microbiol* **183**, 95-106, doi:10.1007/s00203-004-0749-2 (2005).

37 Coleman, N. V., Mattes, T. E., Gossett, J. M. & Spain, J. C. Phylogenetic and kinetic diversity of aerobic vinyl chloride-assimilating bacteria from contaminated sites. *Appl Environ Microbiol* **68**, 6162-6171 (2002).

38 Coleman, N. V. & Spain, J. C. Epoxyalkane: coenzyme M transferase in the ethene and vinyl chloride biodegradation pathways of mycobacterium strain JS60. *J Bacteriol* **185**, 5536-5545 (2003).

39 Danko, A. S., Saski, C. A., Tomkins, J. P. & Freedman, D. L. Involvement of coenzyme M during aerobic biodegradation of vinyl chloride and ethene by Pseudomonas putida strain AJ and Ochrobactrum sp. strain TD. *Appl Environ Microbiol* **72**, 3756-3758, doi:10.1128/aem.72.5.3756-3758.2006 (2006).

40 Hartmans, S., de Bont, J. A. & Harder, W. Microbial metabolism of short-chain unsaturated hydrocarbons. *FEMS Microbiol Rev* **5**, 235-264 (1989).

41 van Ginkel, C. G., Welten, H. G. J. & de Bont, J. A. M. Oxidation of Gaseous and Volatile Hydrocarbons by Selected Alkene-Utilizing Bacteria. *Applied and Environmental Microbiology* **53**, 2903-2907 (1987).

42 Ensign, S. A. Microbial metabolism of aliphatic alkenes. *Biochemistry* **40**, 5845-5853 (2001).

43 Small, F. J. & Ensign, S. A. Alkene Monooxygenase from Xanthobacter Strain Py2: PURIFICATION AND CHARACTERIZATION OF A FOUR-COMPONENT SYSTEM CENTRAL TO THE BACTERIAL METABOLISM OF ALIPHATIC ALKENES. *Journal of Biological Chemistry* **272**, 24913-24920, doi:10.1074/jbc.272.40.24913 (1997).

44 Zhou, N.-Y., Jenkins, A., Chan Kwo Chion, C. K. N. & Leak, D. J. The Alkene Monooxygenase from Xanthobacter Strain Py2 Is Closely Related to Aromatic Monooxygenases and Catalyzes Aromatic Monohydroxylation of Benzene, Toluene, and Phenol. *Applied and Environmental Microbiology* **65**, 1589-1595 (1999).

45 Tallant, T. C., Paul, L. & Krzycki, J. A. The MtsA subunit of the methylthiol:coenzyme M methyltransferase of Methanosarcina barkeri catalyses both half-reactions of corrinoid-dependent dimethylsulfide: coenzyme M methyl transfer. *J Biol Chem* **276**, 4485-4493, doi:10.1074/jbc.M007514200 (2001).

46 Boyd, J. M. & Ensign, S. A. Evidence for a metal-thiolate intermediate in alkyl group transfer from epoxypropane to coenzyme M and cooperative metal ion binding in epoxyalkane:CoM transferase. *Biochemistry* **44**, 13151-13162, doi:10.1021/bi0505619 (2005).

47 Krum, J. G., Ellsworth, H., Sargeant, R. R., Rich, G. & Ensign, S. A. Kinetic and Microcalorimetric Analysis of Substrate and Cofactor Interactions in Epoxyalkane:CoM Transferase, a Zinc-Dependent Epoxidase. *Biochemistry* **41**, 5005-5014, doi:10.1021/bi0255221 (2002).

48 Jörnvall, H. *et al.* Short-chain dehydrogenases/reductases (SDR). *Biochemistry* **34**, 6003-6013, doi:10.1021/bi00018a001 (1995).

49 Kallberg, Y., Oppermann, U., Jornvall, H. & Persson, B. Short-chain dehydrogenases/reductases (SDRs). *Eur J Biochem* **269**, 4409-4417 (2002).

50 Krishnakumar, A. M., Nocek, B. P., Clark, D. D., Ensign, S. A. & Peters, J. W. Structural Basis for Stereoselectivity in the (R)- and (S)-Hydroxypropylthioethanesulfonate Dehydrogenases†,‡. *Biochemistry* **45**, 8831-8840, doi:10.1021/bi0603569 (2006).

51 Clark, D. D. & Ensign, S. A. Characterization of the 2-[(R)-2-Hydroxypropylthio]ethanesulfonate Dehydrogenase from Xanthobacter Strain Py2: Product Inhibition, pH Dependence of Kinetic Parameters, Site-Directed Mutagenesis, Rapid Equilibrium Inhibition, and Chemical Modification. *Biochemistry* **41**, 2727-2740, doi:10.1021/bi0118005 (2002).

52 Pai, E. F. Variations on a theme: the family of FAD-dependent NAD(P)H-(disulphide)-oxidoreductases. *Current Opinion in Structural Biology* **1**, 796-803, doi:http://dx.doi.org/10.1016/0959-440X(91)90181-R (1991).

53 Pandey, A. S., Mulder, D. W., Ensign, S. A. & Peters, J. W. Structural basis for carbon dioxide binding by 2-ketopropyl coenzyme M oxidoreductase/carboxylase. *FEBS Letters* **585**, 459-464, doi:10.1016/j.febslet.2010.12.035 (2011).

54 Nocek, B. *et al.* Structural Basis for CO2 Fixation by a Novel Member of the Disulfide Oxidoreductase Family of Enzymes, 2-Ketopropyl-Coenzyme M Oxidoreductase/Carboxylase. *Biochemistry* **41**, 12907-12913, doi:10.1021/bi026580p (2002).

55 Kofoed, M. A., Wampler, D. A., Pandey, A. S., Peters, J. W. & Ensign, S. A. Roles of the Redox-Active Disulfide and Histidine Residues Forming a Catalytic Dyad in Reactions Catalyzed by 2-Ketopropyl Coenzyme M Oxidoreductase/Carboxylase. *Journal of Bacteriology* **193**, 4904-4913, doi:10.1128/JB.05231-11 (2011).

56 Prussia, G. A. *et al.* Substitution of a conserved catalytic dyad into 2-KPCC causes loss of carboxylation activity. *FEBS Letters* **590**, 2991-2996, doi:10.1002/1873-3468.12325 (2016).

57 Argyrou, A. & Blanchard, J. S. Flavoprotein disulfide reductases: advances in chemistry and function. *Prog Nucleic Acid Res Mol Biol* **78**, 89-142, doi:10.1016/s0079-6603(04)78003-4 (2004).

58 Sauer, K. & Thauer, R. K. Methyl-coenzyme M formation in methanogenic archaea. *European Journal of Biochemistry* **267**, 2498-2504, doi:10.1046/j.1432-1327.2000.01245.x (2000).

59 Pandey, A. S., Nocek, B., Clark, D. D., Ensign, S. A. & Peters, J. W. Mechanistic Implications of the Structure of the Mixed-Disulfide Intermediate of the Disulfide Oxidoreductase, 2-Ketopropyl-Coenzyme M Oxidoreductase/Carboxylase. *Biochemistry* **45**, 113-120, doi:10.1021/bi051518o (2006).

60 Graham, D. E., Taylor, S. M., Wolf, R. Z. & Namboori, S. C. Convergent evolution of coenzyme M biosynthesis in the Methanosarcinales: cysteate synthase evolved from an ancestral threonine synthase. *Biochem J* **424**, 467-478, doi:10.1042/bj20090999 (2009).

61 Graham, D. E., Graupner, M., Xu, H. & White, R. H. Identification of coenzyme M biosynthetic 2-phosphosulfolactate phosphatase. A member of a new class of Mg(2+)-dependent acid phosphatases. *Eur J Biochem* **268**, 5176-5188 (2001).

62 Graham, D. E., Xu, H. & White, R. H. Identification of coenzyme M biosynthetic phosphosulfolactate synthase: a new family of sulfonate-biosynthesizing enzymes. *J Biol Chem* **277**, 13421-13429, doi:10.1074/jbc.M201011200 (2002).

63 Graupner, M., Xu, H. & White, R. H. Identification of an archaeal 2-hydroxy acid dehydrogenase catalyzing reactions involved in coenzyme biosynthesis in methanoarchaea. *J Bacteriol* **182**, 3688-3692 (2000).

64 Graupner, M., Xu, H. & White, R. H. Identification of the gene encoding sulfopyruvate decarboxylase, an enzyme involved in biosynthesis of coenzyme M. *J Bacteriol* **182**, 4862-4867 (2000).

65 White, R. H. Biosynthesis of coenzyme M (2-mercaptoethanesulfonic acid). *Biochemistry* **24**, 6487-6493, doi:10.1021/bi00344a027 (1985).

66 White, R. H. Characterization of the enzymic conversion of sulfoacetaldehyde and L-cysteine into coenzyme M (2-mercaptoethanesulfonic acid). *Biochemistry* **27**, 7458-7462, doi:10.1021/bi00419a043 (1988).

67 White, R. H. Intermediates in the biosynthesis of coenzyme M (2-mercaptoethanesulfonic acid). *Biochemistry* **25**, 5304-5308, doi:10.1021/bi00366a047 (1986).

68 Graham, D. E. & White, R. H. Elucidation of methanogenic coenzyme biosyntheses: from spectroscopy to genomics. *Nat Prod Rep* **19**, 133-147 (2002).

69 Wise, E. L., Graham, D. E., White, R. H. & Rayment, I. The structural determination of phosphosulfolactate synthase from Methanococcus jannaschii at 1.7-A resolution: an enolase that is not an enolase. *J Biol Chem* **278**, 45858-45863, doi:10.1074/jbc.M307486200 (2003).

70 Liu, Y., Sieprawska-Lupa, M., Whitman, W. B. & White, R. H. Cysteine Is Not the Sulfur Source for Iron-Sulfur Cluster and Methionine Biosynthesis in the Methanogenic Archaeon Methanococcus maripaludis. *The Journal of Biological Chemistry* **285**, 31923-31929, doi:10.1074/jbc.M110.152447 (2010).

71 Weinstein, C. L. & Griffith, O. W. Cysteinesulfonate and beta-sulfopyruvate metabolism. Partitioning between decarboxylation, transamination, and reduction pathways. *J Biol Chem* **263**, 3735-3743 (1988).

72 Helgadottir, S., Rosas-Sandoval, G., Soll, D. & Graham, D. E. Biosynthesis of phosphoserine in the Methanococcales. *J Bacteriol* **189**, 575-582, doi:10.1128/jb.01269-06 (2007).

73 Krum, J. G. & Ensign, S. A. Evidence that a linear megaplasmid encodes enzymes of aliphatic alkene and epoxide metabolism and coenzyme M (2-mercaptoethanesulfonate) biosynthesis in Xanthobacter strain Py2. *J Bacteriol* **183**, 2172-2177, doi:10.1128/jb.183.7.2172-2177.2001 (2001).

74 Broberg, C. A. & Clark, D. D. Shotgun proteomics of Xanthobacter autotrophicus Py2 reveals proteins specific to growth on propylene. *Arch Microbiol* **192**, 945-957, doi:10.1007/s00203-010-0623-3 (2010).

Chapter two

1 Balch, W. E. & Wolfe, R. S. New Approach to the Cultivation of Methanogenic Bacteria: 2-Mercaptoethanesulfonic Acid (HS-CoM)-Dependent Growth of *Methanobacterium ruminantium* in a Pressurized Atmosphere. *Applied and Environmental Microbiology* **32**, 781-791 (1976).

2 Balch, W. E. & Wolfe, R. S. Specificity and biological distribution of coenzyme M (2-mercaptoethanesulfonic acid). *J Bacteriol* **137**, 256-263 (1979).
3 McBride, B. C. & Wolfe, R. S. A new coenzyme of methyl transfer, Coenzyme M. *Biochemistry* **10**, 2317-2324 (1971).

4 Taylor, C. D., McBride, B. C., Wolfe, R. S. & Bryant, M. P. Coenzyme M, Essential for Growth of a Rumen Strain of *Methanobacterium ruminantium*. *Journal of Bacteriology* **120**, 974-975 (1974).

5 Wolfe, R. S. in *The Molecular Basis of Bacterial Metabolism* Vol. 41 *41. Colloquium der Gesellschaft für Biologische Chemie 5.–7. April 1990 in Mosbach/Baden* (eds Günter Hauska & RudolfK Thauer) Ch. 1, 1-12 (Springer Berlin Heidelberg, 1990).

6 Allen, J. R., Clark, D. D., Krum, J. G. & Ensign, S. A. A role for coenzyme M (2-mercaptoethanesulfonic acid) in a bacterial pathway of aliphatic epoxide carboxylation. *Proc Natl Acad Sci U S A* **96**, 8432-8437 (1999).

7 Coleman, N. V., Mattes, T. E., Gossett, J. M. & Spain, J. C. Phylogenetic and kinetic diversity of aerobic vinyl chloride-assimilating bacteria from contaminated sites. *Appl Environ Microbiol* **68**, 6162-6171 (2002).

8 Liu, X. & Mattes, T. E. Epoxyalkane:Coenzyme M Transferase Gene Diversity and Distribution in Groundwater Samples from Chlorinated-Ethene-Contaminated Sites. *Applied and Environmental Microbiology* **82**, 3269-3279, doi:10.1128/AEM.00673-16 (2016).

9 Mattes, T. E., Coleman, N. V., Spain, J. C. & Gossett, J. M. Physiological and molecular genetic analyses of vinyl chloride and ethene biodegradation in Nocardioides sp. strain JS614. *Arch Microbiol* **183**, 95-106, doi:10.1007/s00203-004-0749-2 (2005).

10 Small, F. J., Tilley, J. K. & Ensign, S. A. Characterization of a new pathway for epichlorohydrin degradation by whole cells of xanthobacter strain py2. *Appl Environ Microbiol* **61**, 1507-1513 (1995).

11 van Ginkel, C. G., Welten, H. G. J. & de Bont, J. A. M. Oxidation of Gaseous and Volatile Hydrocarbons by Selected Alkene-Utilizing Bacteria. *Applied and Environmental Microbiology* **53**, 2903-2907 (1987).

12 Ensign, S. A., Hyman, M. R. & Arp, D. J. Cometabolic degradation of chlorinated alkenes by alkene monooxygenase in a propylene-grown Xanthobacter strain. *Applied and Environmental Microbiology* **58**, 3038-3046 (1992).

13 Small, F. J. & Ensign, S. A. Alkene Monooxygenase from Xanthobacter Strain Py2: PURIFICATION AND CHARACTERIZATION OF A FOUR-COMPONENT SYSTEM CENTRAL TO THE BACTERIAL METABOLISM OF ALIPHATIC ALKENES. *Journal of Biological Chemistry* **272**, 24913-24920, doi:10.1074/jbc.272.40.24913 (1997).

14 Krum, J. G. & Ensign, S. A. Heterologous expression of bacterial Epoxyalkane:Coenzyme M transferase and inducible coenzyme M biosynthesis in Xanthobacter strain Py2 and Rhodococcus rhodochrous B276. *J Bacteriol* **182**, 2629-2634 (2000).

15 Krum, J. G., Ellsworth, H., Sargeant, R. R., Rich, G. & Ensign, S. A. Kinetic and Microcalorimetric Analysis of Substrate and Cofactor Interactions in Epoxyalkane:CoM Transferase, a Zinc-Dependent Epoxidase. *Biochemistry* **41**, 5005-5014, doi:10.1021/bi0255221 (2002).

16 Krishnakumar, A. M. *et al.* Getting a Handle on the Role of Coenzyme M in Alkene Metabolism. *Microbiology and Molecular Biology Reviews : MMBR* **72**, 445-456, doi:10.1128/MMBR.00005-08 (2008).

17 Ensign, S. A. Microbial metabolism of aliphatic alkenes. *Biochemistry* **40**, 5845-5853 (2001).

18 Allen, J. R. & Ensign, S. A. Two short-chain dehydrogenases confer stereoselectivity for enantiomers of epoxypropane in the multiprotein epoxide

carboxylating systems of Xanthobacter strain Py2 and Nocardia corallina B276. *Biochemistry* **38**, 247-256, doi:10.1021/bi982114h (1999).

19 Clark, D. D., Allen, J. R. & Ensign, S. A. Characterization of five catalytic activities associated with the NADPH:2-ketopropyl-coenzyme M [2-(2-ketopropylthio)ethanesulfonate] oxidoreductase/carboxylase of the Xanthobacter strain Py2 epoxide carboxylase system. *Biochemistry* **39**, 1294-1304 (2000).

20 Westphal, A. H., Swaving, J., Jacobs, L. & Kok, A. d. Purification and characterization of a flavoprotein involved in the degradation of epoxyalkanes by Xanthobacter Py2. *European Journal of Biochemistry* **257**, 160-168, doi:10.1046/j.1432-1327.1998.2570160.x (2013).

21 Kofoed, M. A., Wampler, D. A., Pandey, A. S., Peters, J. W. & Ensign, S. A. Roles of the Redox-Active Disulfide and Histidine Residues Forming a Catalytic Dyad in Reactions Catalyzed by 2-Ketopropyl Coenzyme M Oxidoreductase/Carboxylase. *Journal of Bacteriology* **193**, 4904-4913, doi:10.1128/JB.05231-11 (2011).

22 Pandey, A. S., Mulder, D. W., Ensign, S. A. & Peters, J. W. Structural basis for carbon dioxide binding by 2-ketopropyl coenzyme M oxidoreductase/carboxylase. *FEBS Letters* **585**, 459-464, doi:10.1016/j.febslet.2010.12.035 (2011).

23 Graham, D. E., Xu, H. & White, R. H. Identification of coenzyme M biosynthetic phosphosulfolactate synthase: a new family of sulfonate-biosynthesizing enzymes. *J Biol Chem* **277**, 13421-13429, doi:10.1074/jbc.M201011200 (2002).

24 Wise, E. L., Graham, D. E., White, R. H. & Rayment, I. The structural determination of phosphosulfolactate synthase from Methanococcus jannaschii at 1.7-A resolution: an enolase that is not an enolase. *J Biol Chem* **278**, 45858-45863, doi:10.1074/jbc.M307486200 (2003).

25 Graham, D. E., Graupner, M., Xu, H. & White, R. H. Identification of coenzyme M biosynthetic 2-phosphosulfolactate phosphatase. A member of a new class of Mg(2+)-dependent acid phosphatases. *Eur J Biochem* **268**, 5176-5188 (2001).

26 White, R. H. Biosynthesis of coenzyme M (2-mercaptoethanesulfonic acid). *Biochemistry* **24**, 6487-6493, doi:10.1021/bi00344a027 (1985).

27 White, R. H. Intermediates in the biosynthesis of coenzyme M (2-mercaptoethanesulfonic acid). *Biochemistry* **25**, 5304-5308, doi:10.1021/bi00366a047 (1986).

28 Graupner, M., Xu, H. & White, R. H. Identification of an archaeal 2-hydroxy acid dehydrogenase catalyzing reactions involved in coenzyme biosynthesis in methanoarchaea. *J Bacteriol* **182**, 3688-3692 (2000).

29 Graupner, M., Xu, H. & White, R. H. Identification of the gene encoding sulfopyruvate decarboxylase, an enzyme involved in biosynthesis of coenzyme M. *J Bacteriol* **182**, 4862-4867 (2000).

30 White, R. H. Characterization of the enzymic conversion of sulfoacetaldehyde and L-cysteine into coenzyme M (2-mercaptoethanesulfonic acid). *Biochemistry* **27**, 7458-7462, doi:10.1021/bi00419a043 (1988).

31 Graham, D. E., Taylor, S. M., Wolf, R. Z. & Namboori, S. C. Convergent evolution of coenzyme M biosynthesis in the Methanosarcinales: cysteate synthase evolved from an ancestral threonine synthase. *Biochem J* **424**, 467-478, doi:10.1042/bj20090999 (2009).

32 Broberg, C. A. & Clark, D. D. Shotgun proteomics of Xanthobacter autotrophicus Py2 reveals proteins specific to growth on propylene. *Arch Microbiol* **192**, 945-957, doi:10.1007/s00203-010-0623-3 (2010).

33 Krum, J. G. & Ensign, S. A. Evidence that a linear megaplasmid encodes enzymes of aliphatic alkene and epoxide metabolism and coenzyme M (2-mercaptoethanesulfonate) biosynthesis in Xanthobacter strain Py2. *J Bacteriol* **183**, 2172-2177, doi:10.1128/jb.183.7.2172-2177.2001 (2001).

34 Puthan Veetil, V., Fibriansah, G., Raj, H., Thunnissen, A. M. & Poelarends, G. J. Aspartase/fumarase superfamily: a common catalytic strategy involving general base-catalyzed formation of a highly stabilized aci-carboxylate intermediate. *Biochemistry* **51**, 4237-4243, doi:10.1021/bi300430j (2012).

35 Wiegant, W. M. & De Bont, J. A. M. A New Route for Ethylene Glycol Metabolism in *Mycobacterium* E44. *Journal of General Microbiology* **120**, 325-331 (1980).

36 Vishniac, W. & Santer, M. The Thiobacilli. *Bacteriol Rev* **21**, 195-213 (1957).

37 Bessey, O. A., Lowry, O. H. & Brock, M. J. A method for the rapid determination of alkaline phosphates with five cubic millimeters of serum. *J Biol Chem* **164**, 321-329 (1946).

38 Fiske, C. H. & Subbarow, Y. THE COLORIMETRIC DETERMINATION OF PHOSPHORUS. *Journal of Biological Chemistry* **66**, 375-400 (1925).

39 Palmer, R. E. An experiment to quantitate organically bound phosphate: With special emphasis on biochemical molecules. *Journal of Chemical Education* **62**, 898, doi:10.1021/ed062p898 (1985).

40 Todorovic, B. & Glick, B. R. The interconversion of ACC deaminase and D-cysteine desulfhydrase by directed mutagenesis. *Planta* **229**, 193-205, doi:10.1007/s00425-008-0820-3 (2008).

41 Bhaumik, P., Koski, M. K., Bergmann, U. & Wierenga, R. K. Structure determination and refinement at 2.44 A resolution of argininosuccinate lyase from Escherichia coli. *Acta Crystallogr D Biol Crystallogr* **60**, 1964-1970, doi:10.1107/s0907444904021912 (2004).

42 Farrell, K. & Overton, S. Characterization of argininosuccinate lyase (EC 4.3.2.1) from Chlamydomonas reinhardtii. *Biochem J* **242**, 261-266 (1987).

43 Garrard, L. J., Bui, Q. T., Nygaard, R. & Raushel, F. M. Acid-base catalysis in the argininosuccinate lyase reaction. *J Biol Chem* **260**, 5548-5553 (1985).

44 Patejunas, G., Barbosa, P., Lacombe, M. & O'Brien, W. E. Exploring the role of histidines in the catalytic activity of duck delta-crystallins using site-directed mutagenesis. *Exp Eye Res* **61**, 151-154 (1995).

45 Paul, A., Mishra, A., Surolia, A. & Vijayan, M. Cloning, expression, purification, crystallization and preliminary X-ray studies of argininosuccinate lyase (Rv1659) from Mycobacterium tuberculosis. *Acta Crystallographica Section F: Structural Biology and Crystallization Communications* **69**, 1422-1424, doi:10.1107/S1744309113031138 (2013).

46 Sampaleanu, L. M. *et al.* Structural studies of duck delta2 crystallin mutants provide insight into the role of Thr161 and the 280s loop in catalysis. *Biochem J* **384**, 437-447, doi:10.1042/bj20040656 (2004).

47 Tsai, M. *et al.* Substrate and product complexes of Escherichia coli adenylosuccinate lyase provide new insights into the enzymatic mechanism. *J Mol Biol* **370**, 541-554, doi:10.1016/j.jmb.2007.04.052 (2007).

48 Viola, R. E. L-aspartase: new tricks from an old enzyme. *Adv Enzymol Relat Areas Mol Biol* **74**, 295-341 (2000).

49 Puthan Veetil, V., Raj, H., Quax, W. J., Janssen, D. B. & Poelarends, G. J. Site-directed mutagenesis, kinetic and inhibition studies of aspartate ammonia lyase from Bacillus sp. YM55-1. *The FEBS journal* **276**, 2994-3007, doi:10.1111/j.1742-4658.2009.07015.x (2009).

50 Woods, S. A., Schwartzbach, S. D. & Guest, J. R. Two biochemically distinct classes of fumarase in Escherichia coli. *Biochim Biophys Acta* **954**, 14-26 (1988).

51 Yoon, M. Y. *et al.* Acid-base chemical mechanism of aspartase from Hafnia alvei. *Arch Biochem Biophys* **320**, 115-122 (1995).

52 Banerjee, S. *et al.* Structural and kinetic studies on adenylosuccinate lyase from Mycobacterium smegmatis and Mycobacterium tuberculosis provide new insights on the catalytic residues of the enzyme. *The FEBS journal* **281**, 1642-1658, doi:10.1111/febs.12730 (2014).

53 Brosius, J. L. & Colman, R. F. Three Subunits Contribute Amino Acids to the Active Site of Tetrameric Adenylosuccinate Lyase: Lys268 and Glu275 Are Required†. *Biochemistry* **41**, 2217-2226, doi:10.1021/bi011998t (2002).

54 Bulusu, V., Srinivasan, B., Bopanna, M. P. & Balaram, H. Elucidation of the substrate specificity, kinetic and catalytic mechanism of adenylosuccinate lyase from Plasmodium falciparum. *Biochim Biophys Acta* **1794**, 642-654, doi:10.1016/j.bbapap.2008.11.021 (2009).

55 Fyfe, P. K., Dawson, A., Hutchison, M. T., Cameron, S. & Hunter, W. N. Structure of Staphylococcus aureus adenylosuccinate lyase (PurB) and assessment of its potential as a target for structure-based inhibitor discovery. *Acta Crystallogr D Biol Crystallogr* **66**, 881-888, doi:10.1107/s0907444910020081 (2010).

56 Kozlov, G., Nguyen, L., Pearsall, J. & Gehring, K. The structure of phosphate-bound Escherichia coli adenylosuccinate lyase identifies His171 as a catalytic acid. *Acta Crystallographica Section F: Structural Biology and Crystallization Communications* **65**, 857-861, doi:10.1107/S1744309109029674 (2009).

57 Lee, T. T., Worby, C., Bao, Z. Q., Dixon, J. E. & Colman, R. F. His68 and His141 are critical contributors to the intersubunit catalytic site of adenylosuccinate lyase of Bacillus subtilis. *Biochemistry* **38**, 22-32, doi:10.1021/bi982299s (1999).

58 Toth, E. A. & Yeates, T. O. The structure of adenylosuccinate lyase, an enzyme with dual activity in the de novo purine biosynthetic pathway. *Structure* **8**, 163-174, doi:https://doi.org/10.1016/S0969-2126(00)00092-7 (2000).

59 Yang, J. *et al.* Crystal structure of 3-carboxy-cis,cis-muconate lactonizing enzyme from Pseudomonas putida, a fumarase class II type cycloisomerase: enzyme evolution in parallel pathways. *Biochemistry* **43**, 10424-10434, doi:10.1021/bi036205c (2004).

60 Soutourina, J., Blanquet, S. & Plateau, P. Role of D-cysteine desulfhydrase in the adaptation of Escherichia coli to D-cysteine. *J Biol Chem* **276**, 40864-40872, doi:10.1074/jbc.M102375200 (2001).

61 Eliot, A. C. & Kirsch, J. F. Pyridoxal phosphate enzymes: mechanistic, structural, and evolutionary considerations. *Annu Rev Biochem* **73**, 383-415, doi:10.1146/annurev.biochem.73.011303.074021 (2004).

62 Toney, M. D. Reaction specificity in pyridoxal phosphate enzymes. *Arch Biochem Biophys* **433**, 279-287, doi:10.1016/j.abb.2004.09.037 (2005).

63 Watanabe, Y. & Shimura, K. BIOSYNTHESIS OF THREONINE FROM HOMOSERINE .5. NATURE OF AN INTERMEDIARY PRODUCT. *Journal of Biochemistry* **43**, 283-294 (1956).

64 Keller, J. W. *et al.* Pseudomonas cepacia 2,2-dialkylglycine decarboxylase. Sequence and expression in Escherichia coli of structural and repressor genes. *J Biol Chem* **265**, 5531-5539 (1990).

65 Bull, H., Murray, P. G., Thomas, D., Fraser, A. M. & Nelson, P. N. Acid phosphatases. *Molecular Pathology* **55**, 65-72 (2002).

66 Kim, E. E. & Wyckoff, H. W. Reaction mechanism of alkaline phosphatase based on crystal structures. Two-metal ion catalysis. *J Mol Biol* **218**, 449-464 (1991).

67 Millán, J. L. Alkaline Phosphatases: Structure, substrate specificity and functional relatedness to other members of a large superfamily of enzymes. *Purinergic Signalling* **2**, 335-341, doi:10.1007/s11302-005-5435-6 (2006).

68 Sharma, U., Pal, D. & Prasad, R. Alkaline Phosphatase: An Overview. *Indian Journal of Clinical Biochemistry* **29**, 269-278, doi:10.1007/s12291-013-0408-y (2014).

69 Simopoulos, T. T. & Jencks, W. P. Alkaline phosphatase is an almost perfect enzyme. *Biochemistry* **33**, 10375-10380 (1994).

70 Stec, B., Holtz, K. M. & Kantrowitz, E. R. A revised mechanism for the alkaline phosphatase reaction involving three metal ions1. *Journal of Molecular Biology* **299**, 1303-1311, doi:https://doi.org/10.1006/jmbi.2000.3799 (2000).

71 Tabaldi, L. A. *et al.* Effects of metal elements on acid phosphatase activity in cucumber (Cucumis sativus L.) seedlings. *Environmental and Experimental Botany* **59**, 43-48, doi:https://doi.org/10.1016/j.envexpbot.2005.10.009 (2007).

72 Fibriansah, G., Veetil, V. P., Poelarends, G. J. & Thunnissen, A.-M. W. H. Structural Basis for the Catalytic Mechanism of Aspartate Ammonia Lyase. *Biochemistry* **50**, 6053-6062, doi:10.1021/bi200497y (2011).

73 Sampaleanu, L. M., Vallée, F., Slingsby, C. & Howell, P. L. Structural Studies of Duck δ1 and δ2 Crystallin Suggest Conformational Changes Occur during Catalysis. *Biochemistry* **40**, 2732-2742, doi:10.1021/bi002272k (2001).

Chapter three

1 Toney, M. D. Reaction specificity in pyridoxal phosphate enzymes. *Arch Biochem Biophys* **433**, 279-287, doi:10.1016/j.abb.2004.09.037 (2005).

2 Eliot, A. C. & Kirsch, J. F. Pyridoxal phosphate enzymes: mechanistic, structural, and evolutionary considerations. *Annu Rev Biochem* **73**, 383-415, doi:10.1146/annurev.biochem.73.011303.074021 (2004).

3 Keller, J. W. *et al.* Pseudomonas cepacia 2,2-dialkylglycine decarboxylase. Sequence and expression in Escherichia coli of structural and repressor genes. *J Biol Chem* **265**, 5531-5539 (1990).

4 Watanabe, Y. & Shimura, K. BIOSYNTHESIS OF THREONINE FROM HOMOSERINE .5. NATURE OF AN INTERMEDIARY PRODUCT. *Journal of Biochemistry* **43**, 283-294 (1956).

5 Jansonius, J. N. Structure, evolution and action of vitamin B6-dependent enzymes. *Curr Opin Struct Biol* **8**, 759-769 (1998).

6 Schneider, G., Kack, H. & Lindqvist, Y. The manifold of vitamin B6 dependent enzymes. *Structure* **8**, R1-6 (2000).

7 Sugio, S., Petsko, G. A., Manning, J. M., Soda, K. & Ringe, D. Crystal structure of a D-amino acid aminotransferase: how the protein controls stereoselectivity. *Biochemistry* **34**, 9661-9669 (1995).

8 Alexander, F. W., Sandmeier, E., Mehta, P. K. & Christen, P. Evolutionary relationships among pyridoxal-5'-phosphate-dependent enzymes. Regio-specific alpha, beta and gamma families. *Eur J Biochem* **219**, 953-960 (1994).

9 Marchler-Bauer, A. *et al.* CDD/SPARCLE: functional classification of proteins via subfamily domain architectures. *Nucleic acids research* **45**, D200-D203, doi:10.1093/nar/gkw1129 (2017).

10 Singh, S. & Banerjee, R. PLP-dependent H2S biogenesis. *Biochimica et Biophysica Acta (BBA) - Proteins and Proteomics* **1814**, 1518-1527, doi:http://dx.doi.org/10.1016/j.bbapap.2011.02.004 (2011).

11 Guarneros, G. & Ortega, M. V. Cysteine desulfhydrase activities of Salmonella typhimurium and Escherichia coli. *Biochimica et Biophysica Acta (BBA) - Enzymology* **198**, 132-142, doi:https://doi.org/10.1016/0005-2744(70)90041-0 (1970).

12 Kumagai, H., Choi, Y.-J., Sejima, S. & Yamada, H. Synthesis of S-alkyl-L-cysteine from pyruvate, ammonia and alkyl-mercaptan by cysteine desulfhydrase of Aerobacter aerogenes. *Biochemical and biophysical research communications* **59**, 789-795, doi:https://doi.org/10.1016/S0006-291X(74)80049-5 (1974).

13 Tchong, S. I., Xu, H. & White, R. H. L-cysteine desulfidase: an [4Fe-4S] enzyme isolated from Methanocaldococcus jannaschii that catalyzes the breakdown of L-cysteine into pyruvate, ammonia, and sulfide. *Biochemistry* **44**, 1659-1670, doi:10.1021/bi0484769 (2005).

14 Zheng, L., White, R. H., Cash, V. L., Jack, R. F. & Dean, D. R. Cysteine desulfurase activity indicates a role for NIFS in metallocluster biosynthesis. *Proc Natl Acad Sci U S A* **90**, 2754-2758 (1993).

15 Zhang, W. *et al.* IscS Functions as a Primary Sulfur-donating Enzyme by Interacting Specifically with MoeB and MoaD in the Biosynthesis of Molybdopterin in Escherichia coli. *Journal of Biological Chemistry* **285**, 2302-2308, doi:10.1074/jbc.M109.082172 (2010).

16 Soutourina, J., Blanquet, S. & Plateau, P. Role of D-cysteine desulfhydrase in the adaptation of Escherichia coli to D-cysteine. *J Biol Chem* **276**, 40864-40872, doi:10.1074/jbc.M102375200 (2001).

17 Todorovic, B. & Glick, B. R. The interconversion of ACC deaminase and D-cysteine desulfhydrase by directed mutagenesis. *Planta* **229**, 193-205, doi:10.1007/s00425-008-0820-3 (2008).

18 Oguri, T., Schneider, B. & Reitzer, L. Cysteine catabolism and cysteine desulfhydrase (CdsH/STM0458) in Salmonella enterica serovar typhimurium. *J Bacteriol* **194**, 4366-4376, doi:10.1128/jb.00729-12 (2012).

19 Yao, M. *et al.* Crystal structure of 1-aminocyclopropane-1-carboxylate deaminase from Hansenula saturnus. *J Biol Chem* **275**, 34557-34565, doi:10.1074/jbc.M004681200 (2000).

20 Bharath, S. R., Bisht, S., Harijan, R. K., Savithri, H. S. & Murthy, M. R. Structural and mutational studies on substrate specificity and catalysis of Salmonella typhimurium D-cysteine desulfhydrase. *PLoS One* **7**, e36267, doi:10.1371/journal.pone.0036267 (2012).

21 Nagasawa, T., Ishii, T., Kumagai, H. & Yamada, H. d-Cysteine desulfhydrase of Escherichia coli. *European Journal of Biochemistry* **153**, 541-551, doi:10.1111/j.1432-1033.1985.tb09335.x (1985).

22 Nagasawa, T., Ishii, T. & Yamada, H. Physiological comparison of d-cysteine desulfhydrase of Escherichia coli with 3-chloro-d-alanine dehydrochlorinase of Pseudomonas putida CR 1-1. *Archives of Microbiology* **149**, 413-416, doi:10.1007/bf00425580 (1988).

23 Friedman, M. Chemistry, Nutrition, and Microbiology of d-Amino Acids. *Journal of Agricultural and Food Chemistry* **47**, 3457-3479, doi:10.1021/jf990080u (1999).

24 Abe, K. & Kimura, H. The possible role of hydrogen sulfide as an endogenous neuromodulator. *The Journal of neuroscience : the official journal of the Society for Neuroscience* **16**, 1066-1071 (1996).

25 Kimura, H. Hydrogen sulfide induces cyclic AMP and modulates the NMDA receptor. *Biochemical and biophysical research communications* **267**, 129-133, doi:10.1006/bbrc.1999.1915 (2000).

26 Vorobets, V. S., Kovach, S. K. & Kolbasov, G. Y. Distribution of Ion Species and Formation of Ion Pairs in Concentrated Polysulfide Solutions in Photoelectrochemical Transducers. *Russian Journal of Applied Chemistry* **75**, 229-234, doi:10.1023/a:1016152117662 (2002).

27 Kabil, O. & Banerjee, R. Redox Biochemistry of Hydrogen Sulfide. *The Journal of Biological Chemistry* **285**, 21903-21907, doi:10.1074/jbc.R110.128363 (2010).

28 Liu, Y., Sieprawska-Lupa, M., Whitman, W. B. & White, R. H. Cysteine Is Not the Sulfur Source for Iron-Sulfur Cluster and Methionine Biosynthesis in the Methanogenic Archaeon Methanococcus maripaludis. *The Journal of Biological Chemistry* **285**, 31923-31929, doi:10.1074/jbc.M110.152447 (2010).

29 Droux, M., Martin, J., Sajus, P. & Douce, R. Purification and characterization of O-acetylserine (thiol) lyase from spinach chloroplasts. *Arch Biochem Biophys* **295**, 379-390 (1992).

30 Hirase, K. & Molin, W. T. Effect of Inhibitors of Pyridoxal-5′-Phosphate-Dependent Enzymes on Cysteine Synthase in Echinochloa crus-galli L. *Pesticide Biochemistry and Physiology* **70**, 180-188, doi:https://doi.org/10.1006/pest.2001.2553 (2001).

31 White, R. H. Characterization of the enzymic conversion of sulfoacetaldehyde and L-cysteine into coenzyme M (2-mercaptoethanesulfonic acid). *Biochemistry* **27**, 7458-7462, doi:10.1021/bi00419a043 (1988).

32 Winters, R. A., Zukowski, J., Ercal, N., Matthews, R. H. & Spitz, D. R. Analysis of glutathione, glutathione disulfide, cysteine, homocysteine, and other biological thiols by high-performance liquid chromatography following derivatization by n-(1-pyrenyl)maleimide. *Anal Biochem* **227**, 14-21, doi:10.1006/abio.1995.1246 (1995).

33 Ghatge, M. S. *et al.* Pyridoxal 5′-Phosphate Is a Slow Tight Binding Inhibitor of E. coli Pyridoxal Kinase. *PLOS ONE* **7**, e41680, doi:10.1371/journal.pone.0041680 (2012).

34 Kolluru, G. K., Shen, X., Bir, S. C. & Kevil, C. G. Hydrogen sulfide chemical biology: Pathophysiological roles and detection. *Nitric Oxide* **35**, 5-20, doi:https://doi.org/10.1016/j.niox.2013.07.002 (2013).

35 Marbach, E. P. & Weil, M. H. Rapid enzymatic measurement of blood lactate and pyruvate. Use and significance of metaphosphoric acid as a common precipitant. *Clin Chem* **13**, 314-325 (1967).

36 Gloster, J. A. & Harris, P. Observations on an enzymic method for the estimation of pyruvate in blood. *Clinica Chimica Acta* **7**, 206-211, doi:http://dx.doi.org/10.1016/0009-8981(62)90011-6 (1962).

37 Lienhard, G. E. & Jencks, W. P. Thiol Addition to the Carbonyl Group. Equilibria and Kinetics1. *Journal of the American Chemical Society* **88**, 3982-3995, doi:10.1021/ja00969a017 (1966).

38 Harris, J. Communications: Hydrogen Sulfide Adducts of Halogenated Aldehydes and Ketones. *The Journal of Organic Chemistry* **25**, 2259-2259, doi:10.1021/jo01082a629 (1960).

Chapter four

1 Puthan Veetil, V., Fibriansah, G., Raj, H., Thunnissen, A. M. & Poelarends, G. J. Aspartase/fumarase superfamily: a common catalytic strategy involving general base-catalyzed formation of a highly stabilized aci-carboxylate intermediate. *Biochemistry* **51**, 4237-4243, doi:10.1021/bi300430j (2012).

2 Tsai, M. *et al.* Substrate and product complexes of Escherichia coli adenylosuccinate lyase provide new insights into the enzymatic mechanism. *J Mol Biol* **370**, 541-554, doi:10.1016/j.jmb.2007.04.052 (2007).

3 Toth, E. A. & Yeates, T. O. The structure of adenylosuccinate lyase, an enzyme with dual activity in the de novo purine biosynthetic pathway. *Structure* **8**, 163-174, doi:https://doi.org/10.1016/S0969-2126(00)00092-7 (2000).

4 Porter, D. J., Rudie, N. G. & Bright, H. J. Nitro analogs of substrates for adenylosuccinate synthetase and adenylosuccinate lyase. *Arch Biochem Biophys* **225**, 157-163 (1983).

5 Lee, T. T., Worby, C., Bao, Z. Q., Dixon, J. E. & Colman, R. F. His68 and His141 are critical contributors to the intersubunit catalytic site of adenylosuccinate lyase of Bacillus subtilis. *Biochemistry* **38**, 22-32, doi:10.1021/bi982299s (1999).

6 Kozlov, G., Nguyen, L., Pearsall, J. & Gehring, K. The structure of phosphate-bound Escherichia coli adenylosuccinate lyase identifies His171 as a catalytic acid. *Acta Crystallographica Section F: Structural Biology and Crystallization Communications* **65**, 857-861, doi:10.1107/S1744309109029674 (2009).

7 He, B., Smith, J. M. & Zalkin, H. Escherichia coli purB gene: cloning, nucleotide sequence, and regulation by purR. *J Bacteriol* **174**, 130-136 (1992).

8 Fyfe, P. K., Dawson, A., Hutchison, M. T., Cameron, S. & Hunter, W. N. Structure of Staphylococcus aureus adenylosuccinate lyase (PurB) and assessment of its potential as a target for structure-based inhibitor discovery. *Acta Crystallogr D Biol Crystallogr* **66**, 881-888, doi:10.1107/s0907444910020081 (2010).

9 Bulusu, V., Srinivasan, B., Bopanna, M. P. & Balaram, H. Elucidation of the substrate specificity, kinetic and catalytic mechanism of adenylosuccinate lyase from Plasmodium falciparum. *Biochim Biophys Acta* **1794**, 642-654, doi:10.1016/j.bbapap.2008.11.021 (2009).

10 Brosius, J. L. & Colman, R. F. Three Subunits Contribute Amino Acids to the Active Site of Tetrameric Adenylosuccinate Lyase: Lys268 and Glu275 Are Required†. *Biochemistry* **41**, 2217-2226, doi:10.1021/bi011998t (2002).

11 Banerjee, S. *et al.* Structural and kinetic studies on adenylosuccinate lyase from Mycobacterium smegmatis and Mycobacterium tuberculosis provide new insights on the catalytic residues of the enzyme. *The FEBS journal* **281**, 1642-1658, doi:10.1111/febs.12730 (2014).

12 Marchler-Bauer, A. *et al.* CDD/SPARCLE: functional classification of proteins via subfamily domain architectures. *Nucleic acids research* **45**, D200-D203, doi:10.1093/nar/gkw1129 (2017).

13 Bartolini, M., Wainer, I. W., Bertucci, C. & Andrisano, V. The rapid and direct determination of ATP-ase activity by ion exchange chromatography and the application to the activity of heat shock protein-90. *Journal of pharmaceutical and biomedical analysis* **73**, 77-81, doi:10.1016/j.jpba.2012.03.021 (2013).

14 Yang, J. *et al.* Crystal structure of 3-carboxy-cis,cis-muconate lactonizing enzyme from Pseudomonas putida, a fumarase class II type cycloisomerase: enzyme evolution in parallel pathways. *Biochemistry* **43**, 10424-10434, doi:10.1021/bi036205c (2004).

15 Boyd, J. M., Ellsworth, A. & Ensign, S. A. Characterization of 2-Bromoethanesulfonate as a Selective Inhibitor of the Coenzyme M-Dependent Pathway and Enzymes of Bacterial Aliphatic Epoxide Metabolism. *Journal of Bacteriology* **188**, 8062-8069, doi:10.1128/JB.00947-06 (2006).

16 Broberg, C. A. & Clark, D. D. Shotgun proteomics of Xanthobacter autotrophicus Py2 reveals proteins specific to growth on propylene. *Arch Microbiol* **192**, 945-957, doi:10.1007/s00203-010-0623-3 (2010).

Chapter five

1 Krishnakumar, A. M. *et al.* Getting a Handle on the Role of Coenzyme M in Alkene Metabolism. *Microbiology and Molecular Biology Reviews : MMBR* **72**, 445-456, doi:10.1128/MMBR.00005-08 (2008).

2 Allen, J. R., Clark, D. D., Krum, J. G. & Ensign, S. A. A role for coenzyme M (2-mercaptoethanesulfonic acid) in a bacterial pathway of aliphatic epoxide carboxylation. *Proc Natl Acad Sci U S A* **96**, 8432-8437 (1999).

3 Broberg, C. A. & Clark, D. D. Shotgun proteomics of Xanthobacter autotrophicus Py2 reveals proteins specific to growth on propylene. *Arch Microbiol* **192**, 945-957, doi:10.1007/s00203-010-0623-3 (2010).

4 Toth, E. A. & Yeates, T. O. The structure of adenylosuccinate lyase, an enzyme with dual activity in the de novo purine biosynthetic pathway. *Structure* **8**, 163-174, doi:https://doi.org/10.1016/S0969-2126(00)00092-7 (2000).

5 Soutourina, J., Blanquet, S. & Plateau, P. Role of D-cysteine desulfhydrase in the adaptation of Escherichia coli to D-cysteine. *J Biol Chem* **276**, 40864-40872, doi:10.1074/jbc.M102375200 (2001).

6 Eliot, A. C. & Kirsch, J. F. Pyridoxal phosphate enzymes: mechanistic, structural, and evolutionary considerations. *Annu Rev Biochem* **73**, 383-415, doi:10.1146/annurev.biochem.73.011303.074021 (2004).

7 Kawai, F. *et al. Identification of the prosthetic group and further characterization of a novel enzyme, polyethylene glycol dehydrogenase*. Vol. 49 (1985).

8 Ameyama, M., Hayashi, M., Matsushita, K., Shinagawa, E. & Adachi, O. Microbial Production of Pyrroloquinoline Quinone. *Agricultural and Biological Chemistry* **48**, 561-565, doi:10.1271/bbb1961.48.561 (1984).

9 Reed, D. W., Passon, P. G. & Hultquist, D. E. Purification and Properties of a Pink Copper Protein from Human Erythrocytes. *Journal of Biological Chemistry* **245**, 2954-2961 (1970).